ENERGY EFFICIENCY OPTIMIZATION OF HYBRID SYSTEM MODEL FOR BEYOND 5G NETWORKS

Thesis Submitted For the Award of the Degree of

DOCTOR OF PHILOSOPHY

in

Electronics and Communication Engineering

By

Preksha Jain

41900121

Supervised By
Dr. Akhil Gupta Associate Professor, L.P.U

LOVELY PROFESSIONAL UNIVERSITY
PUNJAB
2022

DECLARATION

I, hereby declared that the presented work in the thesis entitled "ENERGY EFFICIENCY OPTIMIZATION OF HYBRID SYSTEM MODEL FOR BEYOND 5G NETWORKS" in fulfilment of degree of **Doctor of Philosophy (Ph. D.)** is outcome of research work carried out by me under the supervision Dr. Akhil Gupta working as Associate Professor in the School of Electronics and Electrical Engineering of Lovely Professional University, Punjab, India. In keeping with general practice of reporting scientific observations, due acknowledgements have been made whenever work described here has been based on findings of other investigator. This work has not been submitted in part or full to any other University or Institute for the award of any degree.

(Signature of Scholar)

Name of the scholar: Preksha Jain
Registration No.: 41900121
Department/school: School of Electronics and Electrical Engineering
Lovely Professional University
Punjab, India

CERTIFICATE

This is to certify that the work reported in the Ph. D. thesis entitled ENERGY EFFICIENCY OPTIMIZATION OF HYBRID SYSTEM MODEL FOR BEYOND 5G NETWORKS" submitted in fulfillment of the requirement for the reward of degree of **Doctor of Philosophy (Ph.D.)** in the School of Electronics and Electrical Engineering, is a research work carried out by Preksha Jain, 41900121, is bonafide record of her original work carried out under my supervision and that no part of thesis has been submitted for any other degree, diploma or equivalent course.

(Signature of Supervisor)

Name of the Supervisor: Dr. Akhil Gupta
UID No.: 20239
Department/school: School of Electronics and Electrical Engineering
Lovely Professional University
Punjab, India

ACKNOWLEDGEMENT

I wish to express my sincere gratitude to my guide Dr. Akhil Gupta for his whole-hearted and invaluable guidance, inspiring discussions, encouragement, and support throughout my work. I found him always sincere in helping me even during his busiest hours of the day. His ardor and earnestness for studies are respected and will never be forgotten. Without his sustained and sincere effort, this thesis would not have taken this shape.

I would like to thank the School of Electronics and Electrical Engineering, Lovely Professional University, not only for supporting me to undertake this research, but also for giving me the opportunity to attend conferences and meet so many interesting people.

I also thank my parents for the unceasing encouragement, support and attention. I am also grateful to my siblings who supported me through this venture & provided me sophisticated tools during my studies. Thank you for supporting me for everything, and especially I can’t thank you enough for encouraging me throughout this experience

I also place on record, my sense of gratitude to one and all, who directly or indirectly, have lent their hand in this venture.

Finally, I am also indebted to all authors of the research papers and books referred to, which have helped us in carrying out the research work.

Preksha Jain

Reg. No: 41900121

LIST OF FIGURES

LIST OF TABLES

LIST OF APPENDICES

Abb.	Full Form
3GPP	3th Generation Partnership Project
5GPP	5th Generation Partnership Project
A-GPS	Assisted Global Positioning System
AI	Artificial intelligence
AMPS	Advanced Mobile Phone System
ANN	Artificial Neural Network
AP	Access Point
API	Application Program Interface
AR	Augmented reality
ASK	Amplitude-shift key
AUV	Autonomous underwater vehicle
B5G	Beyond 5G
BAN	Body area network
BCI	Brain-computer interface
BER	Bit error rate
BS	Base Station
CDMA	Code division multiple access
CMOS	Complementary-metal-oxide-semiconductor
CoMP	Coordinated multipoint
CP	Cyclic prefix
CP-DSSS	Cyclic Prefix direct sequence spread spectrum
CPU	Central processing unit
CR	Cognitive Radio
C-RAN	Cloud-Random Access Network
CRAS	Connected robots and autonomous systems
CSI	Channel state information
D2D	Device-to-device
DARPA	Defence Advanced Research Projects Agency
DDoS	Distributed denial of service attack
DFT	Discrete Fourier Transform
DL	Deep Learning
DNN	Deep Neural Network
DoF	Degree of freedom
DSRC	Dedicated short range communications
DSS	Decision support system
ECMA	European Computer Manufacturers Association
EHF	Extremely high frequency
ELPC	Extremely low-power communications
ERLLC	Extremely reliable low latency communication
eMBB	Enhanced mobile broadband

ETSI	European Telecommunication Standards Institute
FCC	Federal Communication Commission
FDD	Frequency division duplex
FeMBB	Further-enhanced mobile broadband
FR	Frequency range
FSK	Frequency shift key
FSO	Free space optics
GEO	Geo-stationary Earth orbit
GFDM	Generalized Frequency Division Multiplexing
GPS	Global Positioning System
GPU	Generic User Profile
GS	Ground station
GSM	Global Systems for Mobile communications
HAPS	High-altitude platform
HBC	Human Bond Communication
HetNet	Heterogeneous Network
HMD	Head-Mounted Device
ICI	Inter-carrier interference
ICN	Information Centric Networking
ICPS	Industrial Cyber-Physical System
ICT	Information and communications technology
IEEE	Institute of Electrical and Electronics Engineers
IF	Intermediate frequency
IFT	Federal Telecommunications Institute
IoBNT	Internet of Bio-Nano-Things
IoE	Internet of Everything
IIoT	Industrial Internet of Things
IoNT	Internet of Nano-Things
IoT	Internet of Things
IoUT	Internet of Underwater Things
IoV	Internet of Vehicles
IP	Internet Protocol
IMT	International Mobile Telecommunications
IRS	Intelligent reflecting surface
ISI	Inter-symbol interference
ITS	Intelligent transportation system
ITU	International Telecommunication Union
IVHS	Intelligent vehicle highway system
KPI	Key performance indicators
LAP	Low-altitude platform
LDHMC	Long-distance and high-mobility communications
LED	Light emitting devices
LEO	Low-Earth Orbit

LiDAR	Light detection and ranging
LiFi	Light Fidelity
LOS	Line of sight
LPWAN	Low-power wide area networks
LTE	Long Term Evolution
M2M	Machine-to-machine
MAC	Medium Access Control
MCC	Mobile cloud computing
MEC	Mobile edge computation
MEO	Medium-Earth Orbit
MIMO	Multiple-input multiple-output
ML	Machine learning
mMIMO	Massive multiple-input multiple-output
MMS	Multimedia Messaging Service
MMSE	Minimum mean square error
mMTC	Massive machine type communication
mmWave	millimeter Wave
MNO	Mobile network operator
MR	Mixed reality
NFV	Network function virtualization
NLOS	Non-line of sight
NMT	Nordic Mobile Telephone
NOMA	Non-orthogonal multiple access
NR	New Radio
NSA	None standalone
OAM	Optical angular momentum
OFDMA	Orthogonal frequency division multiple access
OFS	Overlay File System
OMA	Orthogonal Multiple Access
OoB	Out-of-band
OoT	Ocean of Things
OSI	Open Systems Interconnection
PAPR	Peak to average power ratio
QoE	Quality of Experience
QoPE	Quality-of-physical-experience
QoS	Quality of Service
QPSK	Quadrature-phase-shift-keying
RAN	Radio Access Network
RF	Radio frequency
ROV	Remotely operated vehicles
SA	Standalone
SC-FDMA	single-carrier frequency-division multiple access
SDN	Software defined networking

SIC	Successive interference cancellation
SLAM	Simultaneous localization and mapping
SMS	Short message service
SNR	Signal to noise ratio
SOA	Service-oriented architecture
SOI	Silicon-on-Insulator
SR	Symbiotic Radio
SWIPT	Simultaneous Wireless Information and Power Transfer
TACS	Total Access Communication System
TCP	Transmission Control Protocol
TDMA	Time division multiple access
THz	Terahertz
TI	Tactile Internet
TIXT	Tactile Internet eXtensible Testbed
UAV	Unmanned aerial vehicle
UDN	Ultra-dense networking
UE	User equipment
umMTC	Ultra-massive machine type communication
UMTS	Universal Mobile Telecommunications Systems
URLLC	Ultra-reliable low latency communication
UTRA	Universal terrestrial radio access
V2V	Vehicle-to-vehicle
V2X	Vehicle-to-everything
VLC	Visible light communication
VNF	Virtual Network Functions
VR	Virtual reality
WCDMA	Wideband CDMA
WiFi	Wireless Fidelity
WIMAX	Worldwide Interoperability for Microwave Access
WLAN	Wireless local area network
XR	Extended reality
ZSM	Zero touch network and service management

TABLE OF CONTENTS

ABSTRACT

The previous generation networks cover smaller than six percent of the total surface of Earth. The original definition of 5G also describes it as a terrestrial mobile communication network therefore, it has a radio coverage limitation. However, to make a global cellular connection the entire surface area of the earth should be interconnected. While the 5G implementations have high promises, the envisioned results from commercial deployments have just commenced and will take some time. In the industrial developments of 5G, the scenario of Enhanced mobile broadband (eMBB) is highly prioritized and has developed at a much higher pace than ultra-reliable low latency communications (URLLC) and massive machine-type-communications (mMTC). The reasons are the struggles occurring in advancing the diversified, fragmented, and unclear requirements of these IoT-related scenarios. Therefore, the researchers have gained interest in Beyond 5G (B5G)/ sixth generation (6G) networks that will intend to eliminate the variance between definition and realization. It will aim to cover the entire surface of the earth for interconnection and transcend the existing vision and requirements. The B5G/6G is envisioned as a platform for connecting everything; people, things, and even intelligence. The first source of induction for the need for the development of B5G/6G is to keep addressing the world's insatiable demands and insistence on better service experiences. Moreover, a unified platform needs to be designed to enable new industries and new services that 5G will be unable to achieve. The prime engine of continuous research is envisioning to raise the bars to attain, ultra-fast wireless speed, high mobility, full coverage, increased bandwidth, connectivity, and greater security while reducing the energy consumption and achieving ultra-low round-trip latency, to such a level that is unachievable with 5G.

The number of wireless communication devices boomed with the evolution of wireless communication generations. Moreover, the development of technologies such as the Internet of things (IoT) and massive machine-type communications (mMTC) are also fueling the rapid rise in the number of communication devices. It is anticipated that through B5G, the wireless communication networks will move in the direction of ultra-dense distribution of enormous devices with assorted service and rate requirements. This demands huge network data rate and energy. Efficient utilization of system energy in a hybrid system is prime requirement. It is anticipated that through 6G, the wireless communication networks will move in the direction of ultra-dense distribution of enormous devices with assorted service and rate requirements. This demands huge network energy, capacity, and efficient deployment of the spectrum. Employment of non-orthogonal multiple access (NOMA) technology helps in enhancing the energy efficiency of a network. Efficient implementation of NOMA operation can further improve the systems energy efficiency. However, complete exploration of NOMA and D2D networks for enhancing energy efficiency of in a hybrid THz, millimeter-wave, massive-MIMO and NOMA D2D enabled communication system remain unknown. The massive multi-input multi-output (mMIMO) and NOMA techniques which help in increasing the multiplexing gain and network capacity. We intend to utilize the benefit of millimeter Wave (mmWave) and Terahertz (THz) channels, as theses frequencies have massive bandwidths and can aid in delivering high data rates in Gbps and

Tbps range. Our first objective is to design a hybrid beyond 5G system model using THz, millimeter-wave, massive-MIMO and NOMA with D2D enabled small-cell communication network, for a static user system.

As THz and mmWave channels are highly complex. To diminish this problem, we use BS caching. Also, diverse applications in 6G will have varied rate requirements. To fulfill these requirements effectively, this we propose an application-specific channel selection (ASCS) scheme with a cache-enabled two-tier 6G Heterogeneous Network (HetNet). In the proposed scheme, bestowing to the application requirement of the small cell users the small cell base station (SBS) switches downlink channels dynamically. From the simulations it can be seen the proposed method of ASCS can perform better in terms of sum rate, energy efficiency, for the cache-enabled two-tier 6G HetNet.

Nevertheless, the higher frequencies such as THz cannot penetrate buildings, this can become a major problem in designing B5G/6G of mobile communication networks. Moreover, with rise in communication devices and new applications, there will explosion in the system's energy consumption. With the intention to unravel these issues, next we propose a hybrid green 6G HetNet with THz blockage alleviation (TBA) and modified cooperative NOMA (MCN) methods. The TBA method employs D2D communication where the devices redirect the propagating signal to evade the obstructions in the communication path and clinch the communication. The MCN integrates the benefits of the NOMA technology and cooperative communication. The procedures designed in MCN to forward signal to the end-user via cooperative NOMA communication are based on the power levels of the users, aiming efficient use of user power levels and interference mitigation. The total energy efficiency is defined as ratio of the archived data rate of the signal and the energy consumed in transmitting the signal. The reduction in interferences in MCN have positive impact on the signal-to-noise interference ratio (SINR) and data rate of the system and the cooperative communication aids in saving the transmission power at the BS. Therefore, the MCN enhances the energy efficiency. The results of the simulations validate that the efficiency of the proposes system regarding the sum rate, power consumption and energy efficiency than the conventional systems.

Efficient NOMA clustering can help in efficient system implementation. Antenna parameters consideration is important for reducing system interference and efficient clustering in a hybrid millimeter-wave, massive-MIMO and NOMA D2D enabled communication system. However, it remains unanalyzed. Further, we design a 6G hybrid system model employing THz communication, mMIMO, cooperative NOMA, and D2D communication with macrocells and small cells. Additionally, we propose Antenna Angle Bound (AAB) clustering technique to enhance the sum rate of the proposed B5G/6G hybrid system model. The proposed ABB clustering technique employs antenna parameters such as beam angle and beamwidth to form clusters and mitigate interference. The simulation results are provided to validate the better performance of the proposed B5G/6G hybrid system model in assessment with the traditional models. Moreover, the employment of the proposed ABB clustering technique in the proposed 6G system model is observed to attain an improved sum rate, significant power saving, and enhanced energy efficiency.

The wireless communication traffic is expected to explode in the coming years. As the number of users is expected to increase in B5G/6G wireless networks, installation of additional base stations (BS)s will be required for signal transmission. Deployment of the flying base station (BS)s as mobile small cells is a promising solution to offload such traffic and deliver high rate, cost-effective, energy-efficient, flexible, and reliable services B5G/6G systems. Moreover, the deployment of flying BSs can effectively cover remote areas that terrestrial BSs are unable to cover. These attractive benefits have recently urged increasing enthusiasm in both the academic world and industry escalating an explosion of new mobile BS applications, such as unmanned aerial vehicles (UAVs)-enabled data harvesting, UAV-enabled wireless power, UAV-enabled relaying and dissemination, etc. Reducing the global communication energy consumption is a prime objective in B5G/6G wireless communication system design. Energy optimization of NOMA enabled mobile small-cell systems remains unexplored. Therefore, in this research we have focused in designing a hybrid beyond 5G communication system model depending on the user mobility. Moreover, for designing an energy-efficient B5G/6G system, path optimization of flying BS is vital. Therefore, we propose a track selection scheme (TSS) for flying BS. The proposed TSS dynamically selects the finest flying BS path to decrease the flight time, and expand the energy efficiency of the two-tier B5G/6G HetNet. The simulations inspect the performance of TSS and compare it with traditional approaches with respect to flying latency, energy efficiency, and power saving.

Further, investigation of mobile small-cell systems for serving high mobility users and efficiently utilizing system's energy is critical. Moreover, with an upsurge in the number of users, the power allocation and clustering will get enormously complex. As the system topology becomes dynamic with mobile small cell BS, this issue escalates. The employment of machine learning (ML) tools enables systems to learn and adapt without direct human control and pull-out inferences from data patterns even in dynamic environments. Therefore, ML-based systems can support addressing this problem via the learning-based mechanism for making near-optimal decisions. In this paper, we combine mobile BS, THz communication, mMIMO, NOMA, and D2D technologies in a B5G/6G HetNet environment. We propose a power allocation and clustering scheme to enhance the sum rate of the proposed B5G/6G mobile small cell system. First, we propose a green 6G mobile small cell model with help of THz, NOMA, and D2D. Then, a novel fuzzy logic system that exploits channel gains to design optimum power allocation in NOMA is proposed. Further, we propose a clustering scheme that effectively integrates user device antenna parameters, NOMA, and D2D communication to reduce interference and enhance the energy efficiency of MSBS. The results of simulations demonstrate that the proposed schemes for mobile small cell-based B5G/6G HetNet can realize enhanced system performance, compared with the traditional methods with respect to sum rate, power saving, and energy efficiency.

CHAPTER 1
INTRODUCTION

This chapter describes the background of the research work carried out in the thesis. It commences with the overview showing 5G trends and B5G/6G driving force, following motivation behind picking the topic of research challenges to be faced while transitioning from 5G to B5G/6G, research gaps in the current works and culminates with the objectives and organization of thesis.

1.1Overview

5G New Radio (NR) is the global standard and is seen as a combining connectivity material that will effectively interconnect everything and its scale of impact is predicted to be staggering. For instance, healthcare services are expected to advance with Telemedicine and remote monitoring, self-computing wearable smartwatches, advancements in rescue and surveillance systems with drones, autonomous vehicle amenities, etc. Diverse deployment scenarios and a spectrum is incorporated in 5G design, like high millimeter wave (mmWave) bands like 28 GHz, 39 GHz, and 60 GHz, mid 2-7 GHz, and low sub 1 GHz, even higher frequencies beyond 100 GHz [1]. The fundamental difference in 5G and other previous generations is its flexible architectural framework. The previous generations focused on connecting people, whereas 5G also targets to connect all types of things which may enhance human's lives, this differentiates 5G from other previous generations. The introduction of 5G is targeted to achieve three major scenarios; enhanced mobile broadband (eMBB) with Gbps rates, massive machine type communication (mMTC) connecting about a million devices per square kilometer, and ultra-reliable low latency communication (URLLC) with air interface latency in millisecond (ms). To realize these scenarios new enabling technologies like software defined network (SDN), ultra-dense networking (UDN), network function virtualization (NFV), mobile edge computation (MEC), massive MIMO (mMIMO), millimeter-wave (mmWave) communication, non-orthogonal multiple access (NOMA), flexible frame structure, automated driving, network slicing, etc. are defined. Another key technology of 5G is artificial intelligence (AI) [1]. AI is a cloud-centric technology with capabilities like on-device learning, personalization benefits, and improved security, and is predicted to progressively spread in the future.

However, the current trends show a leap in the number of connections and global IP traffic. The development of IoT is affecting the way devices, processes, data, and people are connected with the Internet and each other. By 2022, M2M connections are predicted to be more than 50% of the total connections [2]. By 2023, the number of IP-connected devices will be three times the global population, and half of the global connections will be M2M connections [3]. Particularly, internet traffic caused by VR and AR applications will increase twelve times by 2022 [2]. Although, 3GPP 5G NR does not constantly meet the targeted URLLC demands as the short-packet and the sensing-based functions of 5G URLLC limit the high reliability low latency in such applications [4]. The evolution of the previous generations has directed ground-breaking goals of the Internet of Everything (IoE) in the 5G. However, addressing all IoE associated problems in this stage of 5G is difficult and a long-term process. Therefore, 5G may be viewed as merely the foundation phase of IoE. The set of the key performance indicators (KPIs) of the oncoming advanced 5G services, is highly diverse. Therefore, is an intimidating task to develop a single platform enabling all KPIs. The previous generation networks cover lower than six percent of total surface of the Earth. The original definition of 5G also describes it as a terrestrial mobile communication network therefore, it has a radio coverage limitation. However, to make a global cellular connection the entire surface area of the earth should be interconnected. While the 5G implementations have high promises, the envisioned results from commercial deployments have just commenced and will take some time. In the industrial developments of 5G, the eMBB is highly prioritized and has advanced at higher pace than URLLC and mMTC [4]. The motives behind the struggles in advancing the diversified, fragmented, and unclear requirements of these IoT-related scenarios. The research on B5G/6G will intend to eliminate the variance between definition and realization.

1.2.Research Challenges

Over the past few years, wireless communication networks have experienced ground-breaking progress. The 5G of mobile communication networks supports many growing verticals including enhanced mobile broadband, machine-to-machine (M2M) communications, e-commerce, contactless payment, virtual and augmented reality (VAR), and many other applications. Yet, year on year, a massive number of additional users and communication devices will be connected to the network. Leads to high latency, signal interference, low data rates, and mammoth data traffic demanding ultra-high-definition data services at hot-spot areas such as stadiums, disaster areas, concerts, movie theatres, and offices. The main reason behind this is a shift in user demands from connection-centric communications, for example, text messages and phone calls, to data-streaming communication, for example, connected cars, high-definition video streaming, and smart gaming. Nevertheless, with the evolution of the needs of society, there has been a noticeable escalation in a surfeit of emerging use cases that 5G cannot assist satisfactorily. For example, even the millimeter wave (mmWave) frequency bands within 5G cannot support microsecond (μs)-level latency and Tera-bits per second (Tbps)-level rates required in the next generation of VAR [5]. Moreover, a rise in the connection density will also upshoot the demands for enhanced energy efficiency, to a level that 5G cannot fulfill [5]. Additionally, with the development of industrial automation Industry 4.0 will be preceded by Industry X.0. The 5G is designed for 106 square km connectivity density metric and the connectivity density of upcoming Industry X.0 will surpass these set parameters. Subsequently, these challenges together with societal needs has driven the need for a generational leap beyond 5G wireless systems towards B5G/6G systems. The 6G is envisioned as a platform for connecting everything; people, things, and even intelligence [6]. The prime engine of continuous research is envisioning to raise the bars to attain, ultra-fast wireless speed, high mobility, full coverage, increased bandwidth, connectivity, and greater security while reducing the energy consumption and achieving ultra-low round-trip latency, to such a level that is unachievable with 5G. Prime visions and motivations of 6G systems are identified as:

- 1~10 Tbps Data rates in real-world
- Tremendous number of connected devices
- Every time everywhere services
- 10~100μs round trip Latency
- High bandwidth in the unit area
- Safety and Security of the Information
- Shrinking the Energy usage

To offer a mutual coupled stage for a diversity of B5G/6G needs and application, we will research the following technology components:

- Spectrum utilization, comprising working on current spectrum bands and exploring new spectrum bands for enlarging the communication bandwidth.
- Network topologies, embraced by considering the data requirements, intelligence and user mobility and new methods for efficient energy utilization in B5G/6G HetNets.
- New multiplexing techniques and resource management for realizing robust communication links.

The subjects that will combine a subsection of the aforementioned technology components to offers the solution of few aforementioned aims are:

- Further-enhanced Mobile Broadband (FeMBB): B5G/6G targets peak data rate as a minimum of 1Tbps and user experience data rate of a minimum of 1Gbps through FeMBB.
- Extremely Reliable Low Latency Communication (ERLLC): This will introduce new solutions capable of fulfilling the large diverse range of future reliability and latency requirements. The future B5G/6G communication networks are foreseeing ERLLC with a round trip latency of about 10-100 μs and 99.999% success probability.
- Long-distance and high-mobility communications (LDHMC): High latency is intolerable for some services, for time-critical applications that are specifically latency-sensitive. For supporting applications such as high availability seamless redundancy scenarios, deep-sea sighting, space travel, B5G/6G aims to achieve mobility greater than or equal to 1000 km/hr.
- Ultra-massive machine type communication (umMTC) In the future, machines will substitute humans on many platforms, and the world will move towards a machine-centric instead of a human-centric society. Therefore, B5G/6G targets to enhance machine connectivity, through umMTC
- Extremely low-power communications (ELPC): As cellular communications are required to operate through long distances, the power of the handset becomes the main constraint. Therefore, the 6G

system models intend to accomplish the maximum possible power efficiency, through ELPC.

Among the different technology components, I am choosing efficient spectrum utilization with THz communication technology, massive MIMO antenna technology, NOMA, mmWave and artificial intellegence for achieving enhanced energy efficiency.

1.2.1. Terahertz Communications

There are many merits of using THz communications. First, the THz communication system has the potential to provide about 100 Gbps rates. Second, with wider bandwidth of the order of tens to hundred GHz, the THz spectrum can resolve the problem of spectrum scarcity and immensely boost the system capacity. Third, characteristics like pico-second level symbol duration and narrow beam help in secured communication and considerably reducing the probability of eavesdropping. Forth, it can integrate thousands of sub-millimeter-long antennas and suffer low interference without regulatory barriers. Fifth, it can penetrate some materials with minor attenuation, which is fit for some special applications like medical or industrial inspections. Global standard agencies and regulatory bodies and such as the FCC [7], ETSI [8], and the ITU [9], are in quest of remarks to allot frequency bands above 95 GHz use cases [10]-[13], and some works have been carried out in the same direction: The FCC voted to permit experimental licensing up to 3 THz and unlicensed applications within the spectrum of 116 GHz and 246 GHz, in March 2019. Further, to fast-track the THz technologies' development, it launched Spectrum Horizons License [14]. Europe Horizon 2020, has funded ICT-09-2017 cluster and numerous projects, mostly directing for THz technologies. Aiming towards THz communication standardization, IEEE formed the IEEE 802.15.3d Task Group, the first world-wide wireless communication standard in the frequency range of 250-350 GHz. It channelizes the band into 32 channels of 2.16 GHz and provides data rate up to 100 Gb/s. ITU has classified 0.12THz and 0.2THz into communication. THz communication displays different attributes depending on many factors such as channel, antenna technology, and device technology. According to Friis free space shows that higher frequency links are realizable with the low loss [15], [16] with directional antennas at transmitter and receiver ends. Various losses ensue during THz wave communication, which is enlisted as:

Spreading Loss: The free space path loss intensifies quadratically with frequency, if A_e at both link ends reduces with an increase in frequency, while G_T and G_R are frequency-independent. Conversely, this free space path loss decreases quadratically with frequency, if A_e at both link ends is kept over frequency [17]-[19].

Atmospheric Loss: At frequencies below 6 GHz, molecular absorption is the reason of the atmospheric attenuation owing to polar gas molecules, which is minimal [21] however, the upshot of Mie scattering become acute at high frequencies as the wavelength falls to the dimensions of the dust particles, hail particles, snow particles, or rain particles [22]. Work in [23] showed that rain attenuation is significant at frequencies above 10 GHz and flattens out on frequencies from 100 GHz to 500 GHz [24]-[26]. This connotes that, the frequencies above 100 GHz are better immune atmospheric attenuation, and THz waves can propagate through minute aerial particulates. Due to atmospheric absorption, few frequency bands (183 GHz, 325 GHz, 380 GHz, 450 GHz, 550 GHz, and 760 GHz) suffer higher attenuation additional to Friis free space loss. These absorption peaks, due to the effects of atmospheric vapor and oxygen molecules, create spectral windows in the band. However, this peculiarity makes these bands suitable for short-distance secure communication applications like 'whisper radio' [24]. These bands can even aid achieving high targeted 6G speeds and coverage up to 10 km or beyond in some applications. the characteristics of THz frequencies area as below:

- *Scattering:* The electro-magnetic waves at THz frequencies, scatter when the fall on rough surfaces. This is due to the face that the wavelengths at these frequencies are small and are comparable with the particle size of the surface they fall on.
- *Diffraction and Shadowing:* The diffraction effect reduces with an increase in frequencies, as the sharp shadows are created by obstacles in the path of propagation and waves are unable to bend. Therefore, diffraction effects are not as prominent at THz frequencies. Moreover, shadow fading variance becomes stronger at higher frequencies, as a result of greater diffraction loss.
- *Scintillation Effects:* Rapid modifications of radio waves caused by variations in atmospheric temperature and pressure is called scintillation. It affects the power and phase of the beams. As a consequence, free-space optical communication is greatly affected by scintillation, whereas THz frequencies are less susceptible to it.

With High gain steered directional antennas, the effects of atmospheric attenuation in THz frequencies can be alleviated as gain and directivity intensifies quadratically with the frequency for a fixed antenna gain. Therefore, future networks can work fine up to 800 GHz using the small cell or with LOS propagation or with support of strong reflectors. These highly directional antennas transmit a "pencil" beam which makes interception difficult hence, aids in providing secure communication. The consumption factor (CF) theory in the communication system, provides analysis tools and method to plan the investigations of the power trade-offs. The CF theory proves that with fixed antenna aperture, mmWave and THz frequencies harvests enhanced energy efficiency and much wider bandwidth on (bps/W) basis, in comparison with network working at sub-6 GHz [25], [26]. The absence of compact high-power transmitters and high-sensitivity receivers, working at ambient temperatures is a challenge for THz communications. Many recent developments are cooperatively serving to overcome this challenge. For example, the BiCMOS circuit integration, DARPA T-MUSIC program is exploring CMOS/SOI, SiGe HBT, and, to realize power amplifier with and commercial transceivers at threshold frequencies of 500-750 GHz [27]. The small wavelength of THz frequencies offers small antennas sizes. Although, the challenges posed in encapsulating a vast number of antennas in a small area and improving power efficiency for network operations above 100 GHz frequency bands may need new approaches of transceiver designs. The physical area of RF amplifiers may not be comparable with THz antenna sizes for physical positionings. Hybrid beamforming approaches can overcome this challenge [28], [29]. In design developments of THz transceivers, graphene, and new nanomaterials can be employed to yield plasmonic nano-antennas [30]. Compared to conventional metallic antennas, these nano-antennas are two-fold smaller. This supports their integration virtually with anything moreover, it is possible to electronically tune their frequency response. Fig. 1.1 shows merits of THz communications

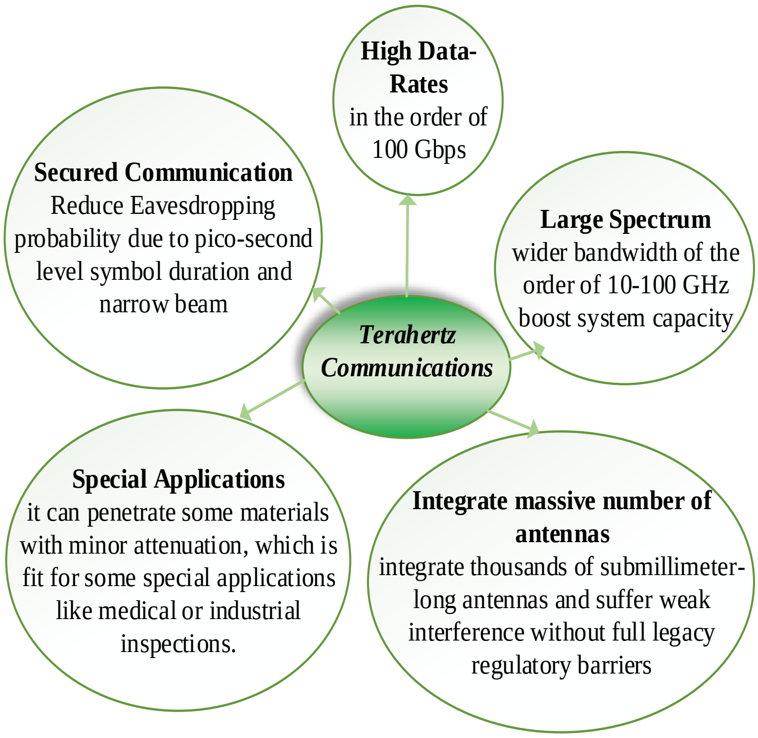

Fig. 1.1. Merits of THz communications

1.2.2. Massive MIMO

Most researches lately have been carried out to take full advantage of mMIMO scheme in the wireless communication networks. Massive MIMO technology employs SDMA scheme to accomplish realization of multiplexing gains through communicating to numerous users on the same frequency-time resource. SDMA is a method to access channel by using the same radio resource again and again in a considered area. Narrow beam transmission of SDMA aids improvement in the gain and capacity of the system. As the beams in SDMA are directive, this attribute helps in increasing the range of the BS. As the beams are more focused, the radio frequency (RF) can have enlarged range of the base station with reduced energy utilization. The fundamental way of implementing massive MIMO is to equip BS with more antennas than number of users in the cell, for efficient reduction in the interference. If there is growth in expected number of cellular users, then the BS unit should be upgraded to facilitate proportional increase in number of the antennas [30].

MIMO technology uses few antennas, nearly ten antennas at the BS in a uniform linear array. Therefore, through up scaling the network by employing a greater number of antennas have the potential to immensely improve the system's spectral efficiency. The ideology behind the mMIMO technology is, when the number of antennas at the BS approaches infinity, the interference due to multiple access scheme and simultaneous user scheduling, in uplink and downlink communication respectively, tends to approach zero. Another benefit of Massive MIMO technology is, tremendous improvements in the systems energy efficiency due to concentrated directed radiations. The operation of mMIMO in time division duplexing (TDD) helps in decreasing the overheads of channel state information (CSI), as because of multiple antennas dependency on the channel parameters reduces. Moreover, the hardware limitations, pitfalls due to thermal noise effects and fading can possibly be mitigated through deployment of enormous antennas.

When the BS is equipped with a large number of multiple antennas in a typical ULA, then the carrier frequency and BS form factor can pose a challenge. Current MIMO networks functions in only azimuth plane therefore, mostly works on the Massive MIMO system explores the beamforming and channel models in horizontal domain alone. However, in real scenarios, the Massive MIMO models significantly depends on the elevation plane as well. Researches has shown that, huge amount of energy, utmost ninety percent is concentrated in elevation plane of the Massive MIMO models. Therefore, azimuth plane beamforming models are not suitable for fully exploiting the advantages of Massive MIMO systems. The three-dimensional (3D) antennas have the capability of radiating in horizontal as well as vertical plane. The introduction of 3D antennas provides complete exploitation of all degree of freedom. Therefore, it can aid beamforming optimization even in vertical plane. BS form factor depends on the existing physical space at the BS for array antenna deployment. For example, when the BS is employing 64 antennas at the top in ULA, with 2.5GHz frequency of operation, at λ carrier wavelength and ${}^{\lambda}/_{2}$ antenna spacing. The required physical space for deployment of such antenna array, at the top of the BS is 4m. Clearly, such a linear antenna deployment is impractical.

1.2.3. Non-Orthogonal Multiple Access (NOMA)

NOMA scheme is seen as a capable technology for B5G wireless communication networks. The issue with the conventionally used multiple access techniques is inability to efficiently utilize the natural radio resources. The traditional Orthogonal Multiple Access (OMA) scheme, has many advantages like reducing inter-symbol interference (ISI) through introducing orthogonality between the carriers, inter-carrier interference (ICI) through overlapping of the orthogonal carriers and moderate improvements in the spectral efficiency. For example; in a system scenario, a user has is not been served on priority basis, since it has not been attended for a long time or has poor channel condition. In order to maintain fairness this user has high priority. However, as the radio resources are limited, OMA scheme is incapable of serving this user, as it exclusively allocates a single resource to a single user. Therefore, the spectral efficiency of OMA systems is incapable to meet the high capacity demands of B5G systems. NOMA on the other hand, deploys single radio resource for the purpose of serving multiple users. Therefore, as the limited radio resources are efficiently utilized, it helps in significantly increasing the spectral efficiency. Moreover, for such a case of priority serving, NOMA can ensure simultaneous communication for both the users with poor and good channel conditions. This helps in enhancing the fairness of the system. The fairness is defined as fair allocation of resources, which can be efficiently achieved with

NOMA scheme. Improvements in the system throughput can also be achieved due to employment of NOMA scheme. The prime benefits of NOMA over OMA are massive connectivity, high spectral efficiency and enhanced capacity due to the effective utilization of the radio resources, reduced latency due to simultaneous communication with multiple users, improved fairness through efficient resource allocation. Fig. 1.2. shows two-user downlink NOMA network.

The two key fundamentals of NOMA are superposition coding and successive interference cancellation (SIC). The principal of NOMA eliminates the orthogonality between the carriers. In NOMA scheme, first a bunch of users are grouped together for simultaneous communication over a single resource. The at the transmitter, the signals of all the users in this group are added together into one signal, through superposition coding. For aiding the reception, these signals are allocated either different power levels or codes, before super-positioning. Then this single signal is sent over a single resource to all the users in the group. All the users in the group receives this super-imposed signal. Each user receipts signal of the other users, in the super-imposed signal, as interference. For decoding their own signal, users use SIC scheme. SIC is also referred as dirty paper coding scheme. The principal of this scheme is eliminating the interference one by one, from the super-positioned data. In SIC scheme, for decoding its signal the user foremost decodes the strongest signal and further eliminates it from the super-positioned signal. This process is carried out multiple times until the user gets its signal, the weaker signals in the super-positioned signal is considered as interference by that user.

NOMA has many challenges such as high complexity of hardware, processing complexity and computation complexity of the SIC scheme limits NOMA scheme. Moreover, due to the possible allied error propagation in coding and decoding techniques, the performance of the whole system can deteriorate. Optimized non-linear NOMA detection algorithm can cope with this limitation. Moreover, inter-cell interference can also pose a problem in NOMA systems, since more power is allocated to the user with poor channels, these are generally located at the cell edge. Therefore, the signals for the users at the edge of the cell can interfere with the users in adjacent cells. To overcome this limitation, improvement in the interference cancellation schemes is required.

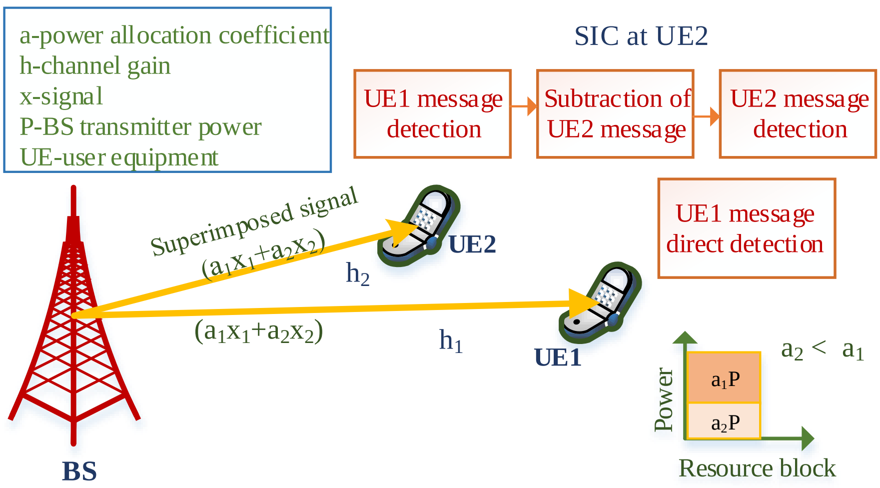

Fig. 1.2. Two-user downlink NOMA network.

The basis of user signature of NOMA is power allocation. The power allocation is mostly based on the user channel conditions, in NOMA, to guarantee fairness. The transmitter allocates the power after sorting the users in descending channel conditions. The highest and the lowest power coefficient is allotted to the users with worst and best channel conditions respectively. For example; consider a case of two users u_1 and u_2. The signals to be transmitted by the transmitter for u_1 and u_2 is s_1 and s_2, and the channel gains of the users are given as h_1 and h_2, with $|h_1| > |h_2|$. Therefore, to assurance fair allocation of resources, the transmitter allocates power allocation coefficients w_1 and w_2, such that $w_1 < w_2$. The signals of the two users are superimposed making one signal, given as $w_1 s_1 + w_2 s_2$. Both the users receive this superimposed signal. The user u_1, use SIC and first decodes s_2, then subtracts it from the superimposed signal to extract s_1. While at u_2, the first signal extracted is s_2 considering s_1 as interference.

1.2.4. Millimetre Wave Technology

Wireless communication systems and industries are developing day by day to reach new standards. With advancement the mobile communication generations the demands of higher cellular capacity have also increased. The bandwidth and spectral efficiency are two prime capacity governing attributes, of a system [33]. The current system, faces challenges due to the high frequency bandwidth. Therefore, the investigation of the unused high frequency bands can prove to be beneficial. The mmWave band stretches from 3GHz to 300GHz. The studies show that the capacity and the data rates could be increased multiple times even with a small section of mmWave band [34]. Such high data rates are possible to achieve with the aid of steering antennas and mmWave technology. Lately, it is found that mmWave technology of 2.6 GHz frequency spectrum can help in boosting the system performance of current 700 MHz band. Therefore, full exploitation of the mmWave band opens tremendous new possibilities in capacity hikes. The concept behind mmWave technology is that, high bandwidth provision opens up possibilities of high data rates and bandwidth expansion, which in turn increase the capacity [35]. Blending B5G system architecture with mmWave technology will bring fast and smooth system operation. Moreover, cost effective in hardware technology, high gain steerable antennas, can be supported by mmWave communication systems.

The mmWave technology needs to be analysed in all perspectives, in order to ripe its maximum advantage. One of the challenges in exploitation of mmWave band is the associated path loss. At higher frequencies, path loss is eminent. The antenna size depends on its carrier frequency, with an inverse proportion. Therefore, mmWave systems demand small sized antennas. However, this increases the aperture size of the antenna, which in hand increases the pathloss. The solution of this problem is if the antenna aperture is kept constant at one or both the ends, the pathloss remains unaffected or even decreases [36]. Another challenge in mmWave communications is the blocking. Micro-waves exhibit the property of diffraction therefore, they suffer from blockages. However, mm-Waves diffract less than micro-waves and propagates spectacularly, but this causes increased effects of blockage. The researches show that if the distance between the transmitter and the receiver is increases then, the path loss in line of sight (LOS) increases, but the blockage decrease [37]. High frequencies also suffer from high penetration and absorption losses. However, this could be overcome by large BS spacing. The Dopplers effect defines the mobility and carrier frequency of the system technology. The signal is said to have Doppler Spread, if the received signal carrier has dissimilar shifts. To reduce the effects of Dopplers spread, the angular spread should be minimized, in mmWave communications. The mmWave technology also face challenges in the link acquisition during link setup as well as handoffs. Therefore, the problem is multiple scanning is required, to acquire the angular positions of the users and the BS. Furthermore, mmWave technology demands new investigations for reduction in the hardware complexity and advancements in system architecture in order to reduce the power consumption.

1.2.5. Artificial Intelligence

Traditionally, the mathematical and statistical models used to design wireless networks need expert knowledge for processes like coding, modulation, and detection. In practical scenarios, hardware impairments, time variations due to high mobility, delay, and other factors can lead to signal distortions. Hence, perfect information of system characteristics cannot be found. Therefore, conventional designs may not always work well in practical scenarios. AI provides a new way of designing wireless networks with big data training to enhance its performance even with imperfect system characteristic information. Therefore, AI will be one of the prime technologies of 6G. AI is the intelligence applied by machines to perform a task that includes learning, perception, reasoning, planning, problem-solving, and manipulation.

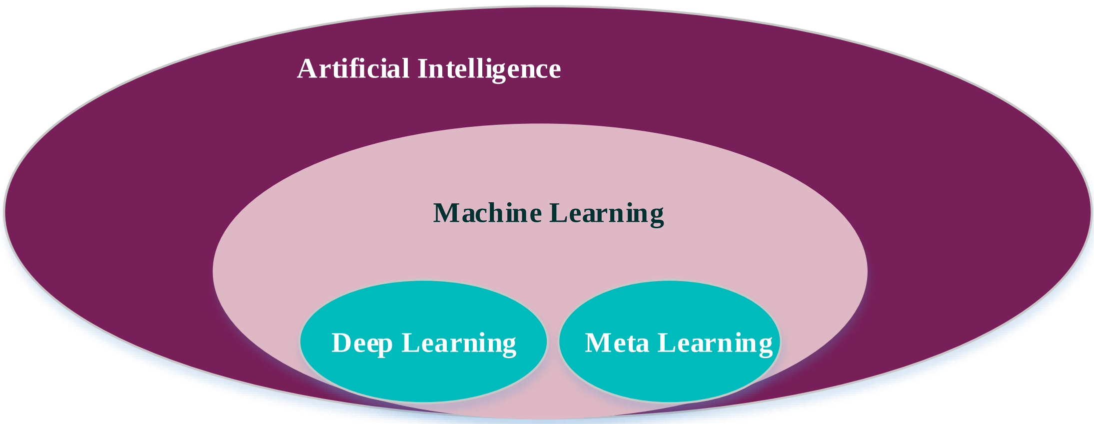

Fig. 1.3. Broad sub-branches of AI.

The 6G networks will mandate intelligent use of control, computing, and storage from the network core to edge. The AI can be integrated with different layers of OSI to replace or transform features that require expert knowledge, for example; AI-enabled autoencoders in the physical layer, AI-enabled security enhancements, and resource allocation in the data-link layer, and AI-enabled mobility management and load balancing in the network layer. The three prime applications of 6G which can be supported by AI are big data analysis, automated and closed-loop optimization, and intelligent wireless communication. The AI-assisted big data analysis can aid performance, fault, behavior, and decision analysis of network operations. The AI-assisted automated and closed-loop optimization can support optimization in extremely dynamic application scenarios. The AI-assisted intelligent wireless communication can help in end-to-end network optimization and mitigating the effects of hardware impairments. AI can also be used to predict the development, infection rate, and spread of the epidemic such as COVID-19. Fig. 1.3 shows the broad sub-branches of AI; which are ML, DL, and meta-learning.

- **Machine Learning**

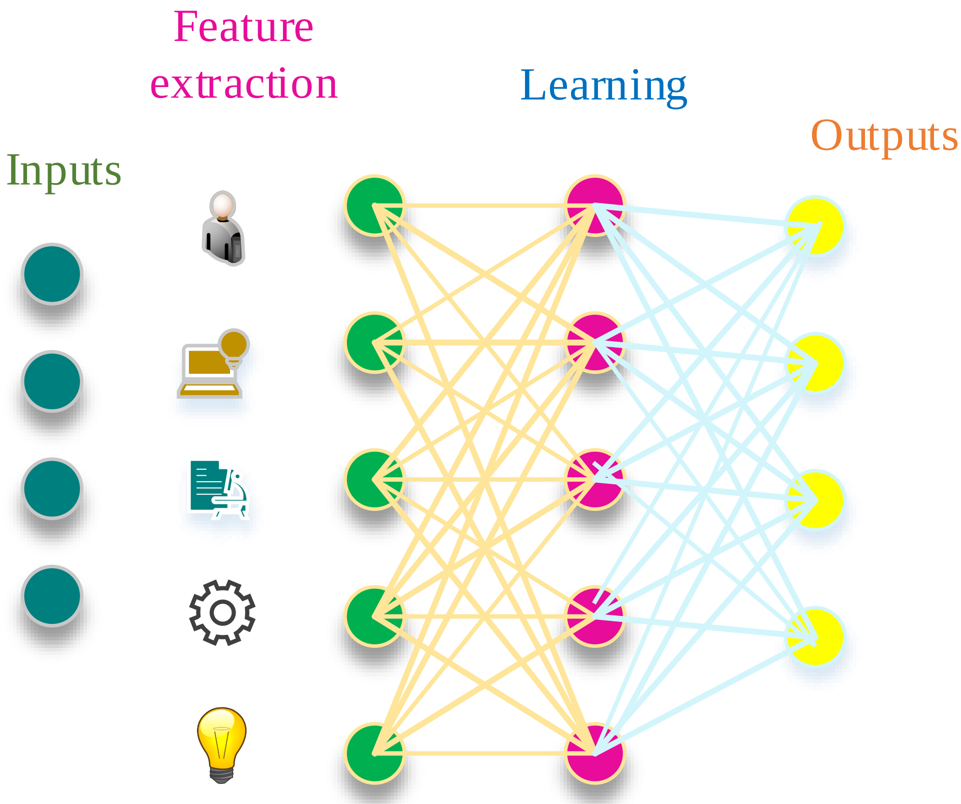

Fig. 1.4. Machine learning.

Due to the limitations of modeling and algorithmic deficiencies of the conventional model-driven algorithm, data-driven ML is gaining research interest lately [37]. Fig. 1.4. demonstrates machine learning. The conventional model-driven approach is ideal when the underlying models are accurate. However, when the system operates in a complex and unfamiliar propagation environment, the conventional model-driven approach lacks effective modeling. Therefore, in such scenarios incorporating ML can be beneficial. In ML, a machine can learn, operate, and enhance its operations, based on the attained operational knowledge and experience. With the growing demands of connectivity, a lot of innovation is required for 6G networks, and tools of ML can play a key role in resolving problems in wireless systems. Table 1.1. shows potential 6G technologies and potential 6G advancements/algorithms.

Table 1.1: Potential 6G technologies and potential 6G advancements/algorithms

Technology	Function	Potential Advancements/Algorithm enablers for 6G	Advancements Description
massive MIMO	Increasing the capacity	OAM for supporting 3D DFT approximation,	Support 3D DFT approximation

	Link reliability Spectral efficiency Security	Holographic radio to increase beam accuracy AI algorithms	Increase beam accuracy
mmWave Communication	Extreme wide bandwidths Enhanced capacity Spectral efficiency Data-rates	New hardware developments New interference mitigation scheme AI and ML algorithms	Improve signal quality Flexible, easily adapted, improved performance
THz communication	High data rates Extreme wide bandwidths Security Low-sensitivity to attenuation and interference	High gain steered directional antennas New method of spatially-oversampled antennas New physical layer design New designs of phase-tracking reference signal New architectures for phased array device and condensed computational approaches AI algorithms	Alleviate atmospheric attenuation Enhanced energy efficiency Much wider bandwidth Improve robustness against phase noise distortion Enhance power amplifier output power efficiency
AI and ML techniques for communication	Intelligent learning, perception, reasoning, planning, problem solving and manipulation Enhance system's performance even with imperfect system characteristic information	Layered AI, layer-free AI, cross-layer AI Supervised learning, unsupervised learning, and reinforcement learning. Deep Neural Network (DNN) Deep Boltzmann Machines Meta-learning	Intelligent control, computing, and storage Intelligent system fault management Proactive and self-sustaining intelligent network
NOMA	Massive connectivity and capacity Reduce latency Aid improvement in spectrum efficiency and fairness	New interference mitigation techniques New clustering and resource allocation techniques AI algorithms Unsupervised machine learning	Enhanced system performance Achieve flexible, autonomous, and adaptive environments

1.3 Motivation

Due to various challenges in 5G, B5G/6G drives researcher's interest. Moreover, with the goal of global connectivity in B5G/6G the number of devices, BS density, number of antennas, and use of larger bandwidths in the wireless communication network is expected to surge prodigiously. The main motivations behind choosing this topic are:

- To fulfill the application demands of users, the B5G/6G networks are anticipated to employ various frequency bands (e.g., RF, mmWave, THz, etc.). Different frequency bands have different advantages and limitations, e.g., RF frequencies can travel long distances however, they are ineffective if fulfilling Gbps rates. Whereas higher frequencies can achieve tremendous data services but suffer from high atmospheric losses. So a way must be found to efficiently employ electromagnetic spectrum to satisfy the various B5G/6G application demands.

- Due to the wide spectrum, and high spatial reuse mmWave and THz wave has been recognized for significantly improving the data rates in HetNets. However, mmWave and THz signals undergo high propagation losses. Moreover, due to high penetration loss, they are also highly sensitive to blockage which is required to be considered and condensed while designing the system.
- Rapid growth in electricity consumption, prodigious amount of greenhouse gas emissions, energy crises, and phenomenal carbon emissions from this sector is a great concern for the environmental. Therefore, it is necessary to design a green 6G network.
- To realize larger coverage and performance robustness, D2D communications and relaying techniques can be employed for THz wireless communications. Moreover, clustering is a key feature to attain an improved performance in NOMA systems. Clustering in NOMA is defined as grouping several users to be served classically in a beam. Design of an efficient clustering technique is vital, as diverse methods of selecting diverse channel gains may lead to dissimilar strategies of signal power distribution, and this ultimately influences SIC application and rates of the system.
- The mobile base stations (BS)s can provide a much broader coverage range than terrestrial static BSs. Additionally, the Flying BSs are very cost-efficient and manually operable and can serve to offload the communication data traffic. Efficient deployment of mobile small cells must be designed to enhance energy efficiency.

1.4 Research Gaps

This chapter, with help of literature survey, finds the gaps and problems in current hybrid system models. We address this concern in the current chapter by laying specific focus on the objectives outlined in the next section.

- **Under-explored efficient B5G hybrid system model**

  Combining the advantages of mmWave communication, RF communications, mMIMO, D2D and NOMA in a two-tier network can provide huge benefit in B5G wireless communication systems. However, hybrid system model using mmWave, massive MIMO, NOMA, RF and D2D remains terra-incognita. Moreover, advantages of exploiting D2D networking remains unexploited in a hybrid millimeter-wave, massive-MIMO and NOMA small-cell communication system.
- **High energy consumption in B5G hybrid system model**

  Efficient utilization of system energy in a hybrid millimeter-wave, massive-MIMO and NOMA communication system is prime requirement. Employment of NOMA technology helps in enhancing the energy efficiency of a network. Efficient implementation of NOMA operation can further improve the systems energy efficiency. Complete exploration of NOMA and D2D networks for enhancing energy efficiency of in a hybrid millimeter-wave, massive-MIMO and NOMA D2D enabled communication system remain unexplored.

- **Uncharted efficient NOMA clustering methods for B5G hybrid system model**
  Efficient NOMA clustering can help in efficient system implementation. Antenna parameters consideration is important for reducing system interference and efficient clustering in a hybrid millimeter-wave, massive-MIMO and NOMA D2D enabled communication system. However, it remains unanalyzed.
- **Under-explored B5G mobile small-cell systems**
  High density of users on small areas such as movies and stadiums large data transmission load on the macro-cell base stations. It is challenging to provide fair broadband wireless services by the MBS at such high-density areas. Also, the wall penetration loss in indoor scenarios such as offices, movie theatres etc., results in high signal attenuation. The mobile small cell base stations can be set up on as a flying BSs to deliver on demand services to the remotely located users. Investigation of mobile small-cell systems for serving high mobility users and efficiently utilizing system's energy is critical. Energy optimization of NOMA enabled mobile small-cell systems remains unexplored.
- **Unplumbed efficient clustering in B5G mobile small-cell systems**
  Blind zones of the wireless communication coverage in ocean communication are common due to lack of infrastructure. This issue can be effectively addressed by deployment of the mobile small cell base stations. The mobile small cell base stations can offer attention for such blind zones with onshore. Efficient NOMA clustering can help in efficient system implementation and reduce system interference. However, efficiently clustering the users in NOMA enabled mobile small-cell D2D system remains unexplored.

1.5 Objectives

In this chapter, the objectives for the PhD thesis are formed according to the direction given by literature survey and aforementioned research gaps for further exploration of B5G system.

- **First objective** is implementation of a hybrid beyond 5G system model using millimeter-wave, massive-MIMO and NOMA with D2D enabled small-cell communication network. As hybrid system model using mmWave, massive MIMO, NOMA, THz, RF and D2D remains terra-incognita. Further, exploitation of advantages of D2D networking in hybrid millimeter-wave, massive-MIMO and NOMA small-cell communication system.
- **Second objective** is energy efficiency optimization of a hybrid millimeter-wave massive-MIMO NOMA with D2D enabled beyond 5G network using a novel battery efficient NOMA technique. With rise in communication devices and new applications, there will explosion in the system's energy consumption. Further, rapid growth in electricity consumption, prodigious amount of greenhouse gas emissions, energy crises, and phenomenal carbon emissions from this sector is a great concern for the

environmental. Energy saving and efficient utilization is prime important for hybrid millimeter-wave massive-MIMO NOMA with D2D enabled beyond 5G network. Therefore, our objective is energy efficiency optimization of a hybrid millimeter-wave massive-MIMO NOMA with D2D enabled beyond 5G network using a novel battery efficient NOMA technique.

- **Third objective** is implementation of an efficient user clustering approach in hybrid mmWave massive-MIMO NOMA with D2D enabled beyond 5G small-cell network using antenna angle bound clustering technique. The clustering of users in a group, for resource allocation in the NOMA system, is restricted by the locations of the users. Antenna Angle bound (AAB) clustering scheme is proposed, which uses the parameters of the antenna, like antenna beamwidth and direction, to decrease the interference of the hybrid millimeter-wave massive-MIMO NOMA with D2D enabled beyond 5G small-cell network and enhance the network rates. Therefore, we implement of an efficient user clustering approach in hybrid millimeter-wave massive-MIMO NOMA with D2D enabled beyond 5G small-cell network using antenna angle bound clustering technique.
- **Fourth objective** is implementation of an energy efficient mobile small-cell for beyond 5G networks using NOMA technology. Unmanned aerial vehicles when deployed as mobile small cell base stations, can provide much broader coverage range than terrestrial base stations. Additionally, such the mobile small cell base stations are very cost-efficient and manually operable. This makes them appropriate for numerous mission-critical applications. The employment of mobile small cell BSs can offer better coverage and high-quality of service to users with poor channel conditions. Therefore, our objective is implementation of an energy efficient mobile small-cell for beyond 5G networks using NOMA technology.
- **Fifth objective** is energy efficient clustering in a mobile small-cell using NOMA D2D technique in beyond 5G networks. The total energy of the mobile small cell base station is limited. Thus, to advance the performance of the beyond 5G system and reduce communication energy, collaboration of NOMA, D2D technology and mobile small cells can prove to be proficient. Efficient clustering can reduce system interference and have positive impact on sum rate and energy efficiency. Therefore, our objective is energy efficiency clustering in a mobile small-cell using NOMA D2D technique in beyond 5G networks.

1.6 Research Methodology

As the order to make progress in the direction of future B5G wireless communication networks, the more data rate and power for transmission, processing and reception has become a prime criterion for B5G wireless communication networks. In this regard, technologies such as THz, millimeter-wave, massive-MIMO, NOMA, D2D and small cells play an important role in designing the B5G systems.

- The main objective this research is to design a hybrid beyond 5G communication system model depending on the user mobility.

- Designing a hybrid beyond 5G system model using millimeter-wave, massive-MIMO and NOMA with D2D enabled small-cell communication network, for a static user system.
- Developing a NOMA based technology for energy optimization of the designed hybrid mmWave, massive-MIMO and NOMA D2D enabled small-cell network.
- Developing an efficient user clustering scheme for the designed hybrid beyond 5G communication mmWave, massive-MIMO NOMA D2D enabled small-cell network.
- Designing of energy efficient NOMA enabled mobile small-cell, for mobile users.

FLOWCHART OF RESEARCH METHODOLOGY

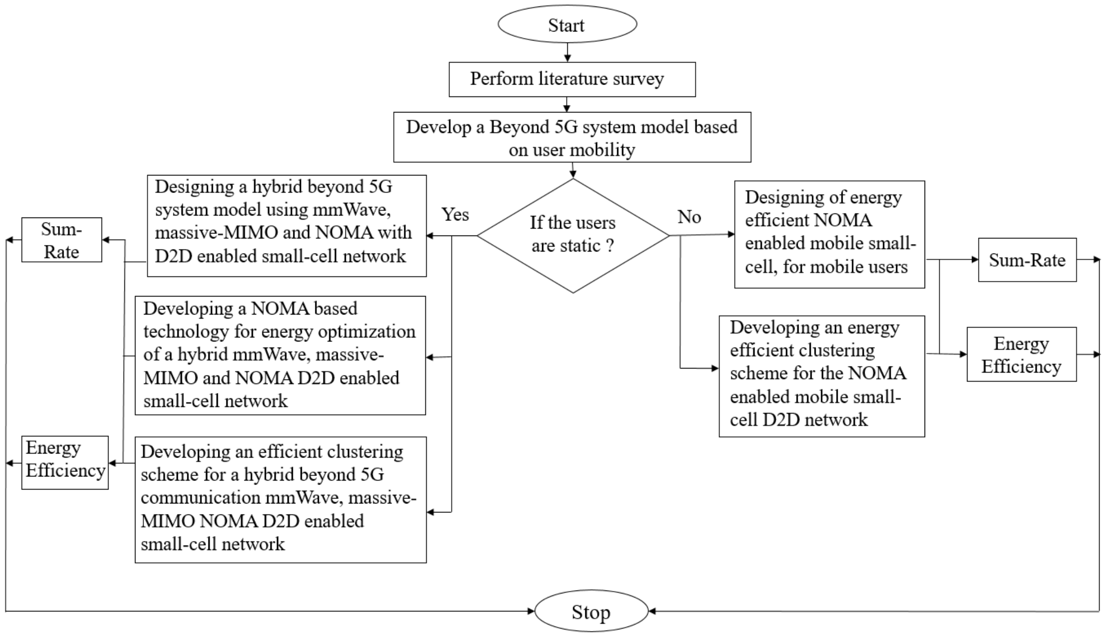

1.7 Organization of Thesis

The rest of the thesis is organized as follows:

In chapter 2, a literature survey has been done. Literature survey is prime job to understand the basics of any system. It will also ascertain about current research circumstances and the possibilities of future research in that field. In this chapter, a survey has been done in five phases related to the work of the thesis. The first phase of the survey has been done on various technologies for implementing a hybrid beyond 5G system model using millimeter-wave, massive-MIMO and NOMA with D2D enabled small-cell communication network. The second phase of the survey has been done on finding using a novel battery efficient NOMA technique to enhance the efficiency of a hybrid beyond 5G system model using millimeter-wave, massive-MIMO and NOMA with D2D enabled small-cell communication network. The third phase of the survey has been done on finding efficient user clustering approach for hybrid millimeter-wave massive-MIMO NOMA with D2D enabled beyond 5G small-cell network. The fourth phase of the survey has been done on finding techniques for designing energy efficient mobile small-cell for beyond 5G networks. The fifth phase of the survey has been done for finding an energy efficiency clustering technique in a B5G mobile small-cell network using NOMA D2D technique.

In chapter 3, a general intelligent autonomous, ultra-dense and super flexible B5G/6G cellular network architecture has been proposed. It describes the 3D network integration of space, aerial, terrestrial and underwater networks to provide full wireless coverage and make a large-dimension-space-air-ground-underwater network. It shows dexterous integration of various techniques simultaneously fulfilling diverse service requirements. It also demonstrates interconnectivity among the different emerging technologies like THz communication, mmWave communication, inter satellite communication, ultra-massive MIMO network, Internet of Everything (IoE), AI, ML, NOMA, intelligent reflecting surface technology, vehicle-to-vehicle communication, mobile and static small-cell networks, holographic verticals, cell-free networks, under water communication, and much more. It also incorporated cloud-centric Internet and fully decoupled RAN architecture for enhancing flexibility and efficiency. The proposed architecture has features such as on-demand network scaling, anywhere and anytime network, and self-evolving, self-adaptive, self-aware, and self-interpretive network functions. In general, the proposed B5G/6G architecture may offer a decent platform for standardization of 6G network.

In chapter 4, a hybrid beyond 5G system model using millimeter-wave, massive-MIMO and NOMA with D2D enabled small-cell communication network is implemented. The main contribution of this chapter is combining the advantages of THz communications, mmWave communication, RF communications, mMIMO, and NOMA in a two-tier 6G HetNet, and a novel application specific channel selection (ASCS) scheme. ASCS scheme, conferring to the application demand of the small cell users the small cell base station (SBS) switches downlink frequency channel dynamically. This aids in the efficient utilization of the spectrum. Additionally, to decrease the transmission load and energy cost at the BS due to the huge bandwidth of mmWave/THz-wave each BS is enabled with caches. The contributions of this chapter are analyzed and compared it with the conventional methods which use mmWave/RF channels. The potential merits of this proposed approach are analyzed through simulation with respect to sum rate, energy efficiency, and throughput.

In chapter 5, using a novel battery efficient NOMA technique energy efficiency of a hybrid millimeter-wave massive-MIMO NOMA with D2D enabled beyond 5G network is optimized. The higher frequency bands such as THz and mmWave aids delivering data rates in Gbps and Tbps range. However, these higher frequencies cannot penetrate buildings, this can become a major problem in designing B5G/6G of mobile communication networks. Moreover, with rise in communication devices and new applications, there will explosion in the system's energy consumption. With the intention to unravel these issues, the main contribution of this chapter is hybrid green 6G HetNet with THz blockage alleviation (TBA) and modified cooperative NOMA (MCN) methods. The TBA method employs D2D communication where the devices redirect the propagating signal to evade the obstructions in the communication path and clinch the communication. The MCN integrates the benefits of the NOMA technology and cooperative communication. The procedures designed in MCN to forward signal to the end-user via cooperative NOMA communication are based on the power levels of the users, aiming efficient use of user power levels and interference mitigation. The total energy efficiency is defined as proportion of the archived data rate of the signal and the energy utilized in transmitting the signal. The reduction in interferences in MCN have positive impact on the signal-to-interference noise ratio (SINR) and data rate of the system and the cooperative communication aids in saving the transmission power at the BS. Therefore, the MCN enhances the energy efficiency. The potential merits of this proposed approach are analysed through simulation in terms of the sum rate, power consumption and energy efficiency than the conventional systems.

In chapter 6, an efficient user clustering approach in hybrid mmWave massive-MIMO NOMA with D2D enabled beyond 5G small-cell network using antenna angle bound clustering technique is implemented. THz communication has attracted the interest of researchers to realize the swelling future needs for higher data rates and greater connectivity. Also, mMIMO, and NOMA based techniques with multiple antennas too allow the system to enlarge the capacity and deliver high multiplexing gains. Therefore, the THz communication, mMIMO, and NOMA based technologies are considered vital parts of the 6G wireless communication systems. In this chapter, we design a 6G hybrid system model employing THz communication, mMIMO, cooperative NOMA, and D2D communication with macrocells and small cells. Further, we propose Antenna Angle Bound (AAB) clustering technique to enhance the sum rate of the proposed 6G hybrid system model. The proposed ABB clustering technique employs antenna parameters such as beam angle and beamwidth to form clusters and mitigate interference. The simulation results are given to validate the better performance of the proposed 6G hybrid system model in assessment with the traditional models. Moreover, the employment of the proposed ABB clustering technique in the proposed 6G system model is observed to attain an improved sum rate, significant power saving, and enhanced energy efficiency.

In chapter 7, an energy efficient mobile small-cell for beyond 5G networks using NOMA technology is implemented. The wireless communication traffic is expected to explode in the coming years. The flying BS is a promising solution to offload such traffic and deliver high rate, cost-effective, energy-efficient, flexible, and reliable services B5G/6G systems. Moreover, the deployment of flying BSs can effectively cover remote areas that terrestrial BSs are unable to cover. These attractive benefits have recently urged increasing enthusiasm in both the academic world and industry escalating an explosion of new mobile BS applications, such as unmanned aerial vehicles (UAVs)-enabled data harvesting, UAV-enabled wireless power, UAV-enabled relaying and dissemination, etc. Reducing the global communication energy consumption is a prime objective in 6G wireless communication system design. To design an energy-efficient 6G system, path optimization of flying BS is vital. This chapter integrates the advantages of THz, mMIMO, NOMA, and flying BSs to form a green 2-tier 6G HetNet. Later, this chapter propose a track selection scheme (TSS) for flying BS. The proposed TSS dynamically selects the finest flying BS path to decrease the flight time, and improve the energy efficiency of the two-tier 6G HetNet. The simulations inspect the performance of the proposed scheme and compare it with traditional approaches with respect to sum rate, flying latency, power consumption, and energy efficiency.

In chapter 8, an energy efficiency clustering technique in a mobile small-cell using NOMA D2D technique in beyond 5G networks is designed. As the number of users is expected to rise in 6G wireless networks, installation of additional BSs will be required for signal transmission. Mobile small cell BS (MSBS) can effectively solve this issue. Moreover, with an upsurge in the number of users, the power allocation and clustering will get enormously complex. As the system topology becomes dynamic with mobile small cell BS, this issue will escalate. The employment of machine learning (ML) tools enables systems to learn and adapt without direct human control and pull-out inferences from data patterns even in dynamic environments. Therefore, ML-based systems can support addressing this problem via the learning-based mechanism for making near-optimal decisions. This chapter combines mobile BS, THz communication, mMIMO, NOMA, and D2D technologies in a 6G HetNet environment. The main contribution of this chapter is a power allocation and clustering scheme to maximize the sum rate of the proposed 6G mobile small cell system. A novel fuzzy logic system that exploits channel gains to design optimum power allocation in NOMA is proposed. Further, this chapter propose a clustering scheme that effectively integrates user device antenna parameters, NOMA, and D2D communication to reduce interference and enhance the energy efficiency of MSBS. Through simulations it can be seen that the proposed schemes for mobile small cell-based 6G HetNet can realize enhanced system performance, compared with the traditional methods with respect to sum rate, power consumption, and energy efficiency.

CHAPTER 2

LITERATURE SURVEY

This chapter briefs the resent research works on analysis of HetNet, NOMA, mmWave, D2D, mMIMO and THz technologies. This literature survey helps in showing new research directions in the field of fundamental and promising B5G technologies.

M. Youssef et al. [38] in this paper considered a system with mixed data traffic. In this paper, to achieve QoS requirements like latency for real time users, a problem of subband allocation is studied. The subband resource allocation problem is studied in distributed and centralized antenna systems for both OMA and NOMA. By considering characteristics of each traffic type, a subband allocation method low complexity suboptimal solution based on matching theory balance between throughput and fairness. In this low-complexity matching theory solution the subband resource assignment problem is displayed as a two-sided one-to-many matching game. In this, the set of subbands and the set of users form two disjoint sets where, a subband can be allocated to at most one user, granting a user to be matched with more than one subband. In terms of real time users QoS requirements satisfaction, the simulation displays that the proposed allocation method based on matching theory significantly outstrips previous greedy approaches by up to 63%. Further, to control the number of subbands per antenna an iterative method for distributed antenna systems is proposed in the paper. Moreover, it is found that when distributed antenna systems is combined with matching theory the real-time user QoS satisfaction surges by more than 30%, compared to its centralized antenna systems.

Z. Ding et al. [39] in this paper considers a system of NOMA assisted orthogonal time frequency space modulation networks, where the spectrum is shared between the high and low mobility users. Taking channel conditions as basis the spectrum is shared between different users. The NOMA aided orthogonal time frequency space modulation networks, uses the spectrum resources accessible in both the delay-Doppler plane and time-frequency plane therefore, the users moving with high speed can be assisted in the delay-Doppler plane, and the low-mobility users can be assisted with the time-frequency plane. Hence, this improves the overall spectral efficiency. In a system of users with different mobility profiles, such a spectrum sharing method can help scenarios of 5G and beyond wireless communication. This paper proposed a beamforming design optimization problem to maximize the data rates of the users with low-mobility NOMA while ensuring targeted data rates for the high-mobility users.

X. Li *et al*. [40] in satellite communication few constrains like latency, some time-critical sensing applications are very strenuous. Therefore, authors in this paper proposes a NOMA network of unmanned aerial vehicle assisted hybrid satellite (HSUAV) unified framework. The satellite connects with the terrestrial users with the assistance of a UAV relay, in a NOMA network. In this paper, under imperfect CSI the outage probability of near and far users are analysed in the considered unified framework network. Furthermore, the throughput of the system is estimated and discussed. In high SNR regions the asymptotic behaviour is explored and the diversity order are obtained and discussed. Moreover, the location of UAV is optimized to improve the performance of the system. Where, the distance between UAV and users is minimized, to improve the sum rate. The simulation results show that there are error floors for the outage probability due to the non-ideal CSI. Further, simulations show that specifically for the far users the proposed scheme outclasses the arbitrary UAV-location method.

F. Kara [41] in this paper considered a diamond relaying network employing cooperative NOMA and studied error performance of the system and derived bit error probability. Further, the authors provide closed form of error floor and bit error probability in high SNR regions. The authors also found that in NOMA diamond relaying network are non-equiprobable symbols in the second phase of communication and their error probabilities are derived. Additionally, it is proved that, for all symbols non-equiprobable communication must be considered. Future direction of the work can be the symbol error rate analysis of NOMA systems for M-QAM. It is shown that the error performance in terms of achieved data rates the NOMA diamond relaying network outperforms NOMA cooperative relay systems. Moreover, it is concluded that the NOMA diamond relaying network could be beneficial in distributed coded schemes, (such as LPDC, Turbo coding or Polar coding) to enhance the error performance.

V. Aswathi et al. [42] in this paper considers a downlink cognitive radio system, employing cooperative NOMA in the secondary network, to send messages for secondary users. In this paper, the near users act as relays, in either full duplex or half duplex modes for the far users. For the considered full/half duplex cooperative NOMA systems the outage probability for the secondary users is derived and analysed. The constrains like maximum endurable interference power and maximum transmit power are also found for the primary users and at secondary users respectively. For guaranteeing equal outage performance for secondary users and reducing the system outage probability, the power allocation coefficient is are also analysed in this paper. Numerical and simulation results show that on comparison with the default power allocation method, the proposed that optimal power allocation factor can significantly decrease the system outage probability.

E. M. Almohimmah et al. [43] in this paper considered a visible light communication network employing NOMA. NOMA helps in improvement of spectral efficiency but at the cost of amplified data detection error. Authors in this paper considers system with higher order modulation techniques with imperfect SIC. For quadrature amplitude modulation (QAM) of any order, closed form expression of the symbol error rates is derived. Further, for higher order modulation in NOMA VLC systems, the paper derives the power allocation constraint to guarantee that in the superimposed constellation decision regions of the symbols do not cross or overlap. The results of the simulations conclude that with appropriate power allocation in NOMA VLC systems, the user symbol error rates can be reduced.

S. Dhanasekaran et al. [44] in this paper, a system with cooperative NOMA where secondary users acts as decode and forward relay for the primary users to share the spectrum. Due to fixed decode and forward relay, the channel can be accessed by the secondary user in all the alternate timeslots, while maintaining the QoS requirements of the primary user. The proposed half duplex spectrum sharing scheme employing NOMA lets the secondary and the licensed user operate together while maintain the average bit error rate and data rate performance of the primary users. To examine primary user performance the bit error rate closed-form expression is derived and validated through simulation results. Further, the simulation results illustrate that the cell-edge user can be served while maintain the fairness and QoS. The proposed system can achieve improved results in low SNR regime, having constraint on the transmit power is concluded.

L. P. Qian et al. [45] in this paper tries to address the issue of poor QoS issue due to less computational resources in large resource demanding applications, in IoT devices. To cope with this issue, mobile edge computing solution is provided which reduces the computation workloads the cell edge users. Authors in this paper significantly offloads the work of edge servers, to reduce the latency, through NOMA scheme. Joint resource allocation optimization layered-algorithm is studied, at the edge server and IoT smart terminal. Through the proposed optimal offloading solution, a scenario of multiple smart terminals is studied to find the optimal grouping amongst various edge server for serving the IoT users. The analytical results show the efficiency of the proposed NOMA based computation offloading in IoT devices.

K. N. Doan et al. [46] in this paper, works on technologies like NOMA using Rayleigh fading channels and cache-enabled users is analysed. The authors study the combination of caching-NOMA to improve the cache usefulness and the effectiveness of NOMA. The user collaboration is not required in such a scheme, which reduces many issues like security and privacy of the users. The probability of signal decoding by all the users is maximized to optimize the QoS requirements and user fairness. Further, two power allocation optimization solutions were studied which are divide-and-conquer-based technique and the other one is deep reinforcement learning technique. The first method is a simple and flexible method of user pairing and helps to obtain closed-form expression and the second machine learning based power allocation helps in fast user request responses as well as supports sharing of the entire bandwidth by all the users. Lastly, the simulation results show the proposed methods performance in contrast with the performance of the conventional power allocation methods.

J. Ding et al. [47] in this paper considers a clustering model of MIMO-NOMA system. To reduce the system's power consumption the authors, investigate new strategy for cluster beamforming. The approach helps in eliminating the peer effect during beamforming. The main focus of the authors is to solve the two problems. First, resource management in user clustering as collision game in large scale MIMO where users cluster size is flexible. Second, to build a joint optimization problem of NOMA power allocation and MIMO beamforming. It was found that various factors like channel coefficient and radius of users are affects the MIMO NOMA cluster power consumption. Through simulations the comparison analysis of the proposed scheme and traditional schemes is shown, and the results verify that the proposed scheme is efficiently reduces total power consumption and total number of coalitions. Further, for clustering, on comparison of different MIMO-NOMA it is found that the scheme of allocation of a set of power allocation for each user is outperforms, the scheme of power allocation as a single allocation coefficient for each user, in terms of power reduction.

L. Liu et al. [48] in this paper, the authors identify the problem of the SIC iterative receiver that it has mismatch between error detection and multi user decoding, for the MIMO channel. To solve this issue for MIMO NOMA, the authors provided a matching condition between the detector and decoders. For iterative detection, this matching condition helps in derivation achievable rate. For a MOMO NOMA system, the authors consider iterative linear minimum mean square error detector, where numerous single-antenna equipment concurrently connect with a multiple-antenna BS. Two cases were considered in the paper; systematic and non-systematic MIMO NOMA. Through simulations the authors found that for any number of users the systematic and non-systematic MIMO NOMA can achieve optimum capacity and optimum sum capacity respectively. Moreover, to match linear minimum mean square error detector, an irregular repeat-accumulate error correcting code is designed. The mathematical findings show that the performance of the proposed iterative error detector is improved in comparison with the conventional detection methods in terms of bit error rate within 0.8 dB from the related capacity bounds.

D. Tong et al. [49] in this paper addresses the intra-cluster interference in MIMO NOMA systems, through widely linear processing structure. In the proposed framework, complex power allocation coefficients are used to organise the in-phase signals. Authors found that the inter-cluster interference can be eliminated through the proposed widely linear MIMO-NOMA and as well as can also remove semi intra-cluster interference, in a general case. Whereas, both inter cluster and intra cluster interferences can be entirely removed another case named as, user pairing case. Over the performance evaluation of the proposed framework it is found, that through orthogonally phased of complex power allocation coefficients, the outage probability drops to minimum. Further it is found, that the proposed system MIMO NOMA framework outstrips the existing system. Thereafter, the proposed framework is comprehensively extended to the case of both complex and real signals. The outcomes of simulation confirm that the performance of the proposed framework is better than the traditional MIMO NOMA system.

K. He et al. [50] in this paper investigates the ultra-reliable low-latency requirements of MOMO NOMA network. Compressed sensing technique for mission-critical machine-type communication, is introduced to solve this issue. A tensor compressed sensing frame is proposed to minimize the transmit time intervals, for decreasing the latency in MIMO NOMA systems. In the tensor compressed sensing frame, the compressed sensing signatures are allocated to numerous users as well as to different symbols of a time slot and to various time slots. For multiuser detection, the authors proposed a condition for compressed sensing signatures. The upper bound of the proposed system were found by considering imperfect channel state information. The simulation results show that high time slot overload and user overload can be achieved through the proposed system. Furthermore, it is found that the block error rate is lower in the proposed tensor compressed sensing frame when compared to the conventional frame.

S. Park et al. [51] in this paper investigates beamforming techniques in MIMO-NOMA in a downlink scenario. The identified difficulty in optimal power allocation was the transmission power budget per cluster relating to the transmission power of MIMO NOMA antenna must have some limit. The authors propose a user pairing method in NOMA cluster, by considering different channel qualities for power allocation. Moreover, through transmit power budget, the sum spectral efficiency is optimized. With different beamforming techniques like zero-forcing, regularized zero-forcing and maximum ration transmission, the systems spectral efficiency was investigated. The analysis shows that highest sum spectral efficiency is achieved in a MIMO NOMA system with zero forcing beamforming and the spectral efficiency for weak users benefits from regularized zero-forcing beamforming technique.

A. Nasser et al. [52] in this paper authors studied power allocation and interference cancelation techniques for MIMO NOMA HetNets. The authors propose a scheme title as power allocation as based on coordinated beamforming and interference alignment. To cope with the issues like optimal power allocation and interference mitigation a non-convex power allocation problem is generated, and the proposed scheme solves this issue by modelling the problem as a non-cooperative game. It comprises of two stages, in the first stage interference alignment and coordinated beamforming is done first and then the inter cluster interference cancellation, is managed for small and macro cells respectively. In the second stage, through power allocation, the cross-tier interference is coped at macro and small cell BSs. Via simulations it is verified that the proposed technique is performs better than orthodox techniques in terms of system's outage probability and sum rate.

Z. Ding et al. [53] in this paper, authors find that it is difficult to realize a perfect channel state information system. A downlink massive MIMO NOMA scenario with BS communicating with several users is considered. A low-feedback NOMA massive MIMO transmission technique is proposed by the authors. The proposed technique divides a massive MIMO NOMA system into several separated SISO NOMA channels. The analytical and simulation results are evaluating the proposed scheme for two scenarios namely one-bit feedback scenario and with perfect user ordering. In one-bit feedback scenario, the BS has information about each user channel gain is above or below the threshold, as each user checks its channel gain with the predefined threshold and informs the BS. In perfect information of the ordering of the system user, in this scenario the need not know the global channel state information.

Y. Li et al. [54] in this paper investigates spectrum sharing in the massive MIMO NOMA downlink scenario. Considering successive interference cancellation, the authors investigates the intra-cluster and inter-cluster pilot contamination. The authors try to assure that the secondary co-channel interference at primary users must be under the primary interference temperature. Therefore, the transmission constraints on the secondary massive MIMO NOMA BS are derived. Further, secondary massive MIMO NOMA sum rates is investigated. Thus, the joint impact of imperfect channel state information, intra-cluster pilot contamination, and imperfect successive interference cancellation is examined. The simulation results verify that the proposed massive MIMO NOMA spectrum-sharing system outdoes the orthodox OMA system in terms of achievable data rates.

X. Liu at al. [55] in this paper, found that the complexity of the hardware in cooperative massive MIMO NOMA increases with the system efficiency. The further analysis is done on the efficient three-dimensional massive MIMO NOMA resource utilization. As the channel variations constrains the hardware complexity of the massive MIMO NOMA systems, an efficient scheduling algorithm for antenna selection is proposed. The main goal of the proposed massive MIMO NOMA system is to upsurge the system sum rate. Further, for serving multiple users, the authors propose a cooperative relaying NOMA by using three dimensional resources. To minimize the hardware complexity of the receiver, a simplified collaborative NOMA assisted relaying is introduced. The results of numerical analysis show that the proposed user selection and antenna selection schemes reduces the complexity of the system without affecting its performance. The proposed collaborative NOMA assisted relaying performs better than the other techniques, for a special case of high target rates, with condensed complexity.

M. Zeng et al. [56] in this paper investigates the security issues in massive MIMO NOMA systems by exploiting artificial noise. With BS minimum mean square error, uplink communication is considered. After the estimation of the channel state information, the BS precedes the information to be secured and the adds artificial noise into it. Further, the secrecy rate is calculated for the proposed system in the downlink scenario. For large antenna array the and high BS transmission power an analysis of asymptotic secrecy performance is carried out, to find the key parameters of confidentiality performance of the massive MIMO NOMA system under consideration. For uplink and downlink scenarios a joint power allocation is introduced for maximizing the system's sum secrecy rates. Moreover, to increase the energy efficiency, an optimization algorithm is proposed. The simulations show the secrecy performance optimization algorithm of the proposed system is proved to be higher than the other conventional algorithms. Lastly, through simulations it is validated that the secrecy performance of proposed massive MIMO NOMA system outperforms the massive MIMO OMA systems.

D. Zhang et al. [57] in this paper studied a non-regenerative cooperative massive MIMO NOMA system with maximum mean square error successive interference cancellation receiver design. The SINR is derived from tools like matrix analysis and a deterministic equivalent. Further, sum rate and capacity were analysed with the help of previously derived SINR. The study found that the ratio of number of transmitter antennas and number of the relay devices helps in determining the system performance. The simulations demonstrate that the sum rate and capacity have positive correlation with the average power, number of transmitter antennas and users, and number of relays have negative correlation with the massive MIMO NOMA system performance. Further, it is found that the proposed system has capacity improvements when compared to conventional cooperative MIMO NOMA and cooperative massive MIMO OMA.

K. Senel et al. [58] in this paper, studies the possible advantageous role of power domain NOMA when collaborated with massive MIMO system. The authors found that, as the NOMA systems outperforms the OMA systems, this does not conclude that the NOMA systems have maximum efficiency when employed with massive MIMO networks with condition of a greater number of antennas at the BS than at the users. Earlier spatial multiplexing was studied with linear multi-user beamforming. The introduced system is studied for the LoS and NLoS beamforming scenarios in massive MIMO NOMA systems. It is found that the sum rate was improved with line-of-sight beamforming scheme. The authors also demonstrate that, over different user positions, massive MIMO is superior to NOMA concerning the sum rate, still in some cases the performance of NOMA is improved for a specific user clustering.

D. Kudathanthirige et al. [59] in this paper investigates pilot assignment and user clustering for multi cell mMIMO NOMA systems. The proposed massive MIMO NOMA system design is generalized for system's over-loading as well as under-loading to control the spatial covariance matrices of users. In the proposed system the users having matrices are linearly dependent are placed in the same cluster and for mitigating the cluster pilot contamination, the pilots are assigned orthogonally. To decrease the training overhead, users in different clusters share the same pilots. The authors found that the pilot contamination, in the different cluster pilot-sharing users with asymptotically independent covariance matrices, can be mitigated. The downlink rates were analysed. Though, in case of overloading systems, in order to be served by single frequency resource, the users in the same cluster, sharing the same spatial direction, have to share pilots. For mitigating the adverse effect of the near far effect, improving the sum rates and fairness, transmission power control policies are designed by the authors. The results of the analysis verify that the pilot contamination in intra-cluster and inter-cluster arises reuse of pilot in the underload system. Further, it is found that as the number of BS antennas increases the data rates surge with zero forcing precoding.

X. Chen et al. [60] in this paper presents study of the spectral efficiency improvement techniques massive MIMO NOMA systems. The authors propose algorithm for user scheduling and user pairing for simultaneously pairing and selecting users for communication. The proposed user pairing technique chooses the two users in such a way that they both contribute for maximizing the system's sum rate. Interference cancellation combining technique is further introduced to reduce the interference between the user pairs, through constrain on the number of BS antennas and user antennas. The simulation results verify that the proposed user pairing algorithm outperforms the conventional algorithms with respect to sum rate and outage probability.

E. P. Simon et al. [61] in this paper, analysis of massive MIMO NOMA in indoor as well as outdoor environments is presented. The proposed system exploits the user clustering and multi user beamforming in massive MIMO NOMA systems. The authors used the maximum ratio transmission and zero forcing precoding techniques to investigate the sum rate capacity of the mMIMO NOMA systems. Through inter beam power allocation is studied for intra cluster user power allocation. It can be seen from the simulations that the massive MIMO NOMA system with zero forcing precoding design performs in low SNR regions. Whereas, through clustering greatly correlated users the studies found that maximum ratio transmission precoding achieves performance gain in all SNR regions. Further the authors found that, in indoor as well as outdoor environment, zero forcing outperforms maximum ratio transmission precoding for all SNR values.

W. A. Al-Hussaibi et al. [62] in this paper investigates improvements in fairness, sum capacity, number of connected devices and reduction in the system's complexity in mMIMO NOMA systems through proposed receiver antenna selection scheme. Based on the number of accessible radio frequency chains at the BS a scheme is proposed for user clustering for mMIMO NOMA systems. The authors derive the capacity and sum rate region equations over Rayleigh fading channels for the proposed system scheme. The authors further investigate, optimal power allocation and user clustering through proposed receiver antenna selection scheme for maximizing the sum rate. Through simulation results and numerical analysis, the efficiency of designed algorithms is evaluated for mMIMO NOMA systems. The results show that the improvements in connectivity and sum rate capacity with available number of radio frequency chains, while satisfying the constraint of the minimum rates. Moreover, the authors found trade-offs between system performances, user-fairness and hardware complexities in terms of serving more users.

L. Zhu et al. [63] in this paper, evaluate the system capacity for mmWave NOMA systems. Authors studies that in large phase array mmWave NOMA systems are generally classified by the beamforming in transmitter or receiver side when compared to the conventional NOMS systems. The authors investigate the challenges due to beamforming while designing mmWave NOMA systems. The authors found that the systems sum rate gets affected by beamforming affects. The relative angle between NOMA users may get offset by the conventional beamforming techniques. Authors found that the proposed multi beamforming technique enhances the system performance. Further, authors examine the joint design of the user pairing and power allocation for the considered mmWave NOMA systems. Moreover, a hybrid of NOMA and spatial division multiple access is examined, to address the problems of multi-user interference cancellation and multi-user precoding.

Z. Wei et al. [64] in this paper, authors study resource allocation in hybrid mmWave NOMA systems through multiple beams. Authors studied that previously, on each RF chain, beam splitting is introduced to serve multiple users through the same analog beam. Therefore, to make full use of multi-user diversity and to introduce flexibility in the system authors proposed a technique to server multiple users having arbitrary distribution of angle-of-departure. For sum rate improvement, the authors proposed a new technique for resource allocation in two stages. The first stage groups the users and allocates antenna resources with a presumption that only analog beamforming is available. This stage uses coalition game theory for enhancing the sum rate of the system. The second stage, tries to solve the sum rate non convex optimization problem of power allocation, considering constraints on the QoS. The results of the simulation show that an optimal solution for resource allocation, in a closed form can be achieved in each stage. Moreover, the authors show that the proposed scheme enhances spectral efficiency compared to other mmWave NOMA or mmWave OMA schemes.

N. Rupasinghe et al. [65] studied the unmanned aerial vehicle broadband data communication in mmWave NOMA system scenario. The unmanned aerial vehicle is considered as the BS for stadium communications, though mmWave NOMA transmission. Authors found the importance of information collection about the quality of channel becomes a drawback for practical scenarios. To eliminate this problem and of tracing and feeding back the channel state information the authors proposed a limited feedback mmWave NOMA technique. The authors studied that in the limited feedback NOMA system, user angle can be exploited in beamforming technique. It was found that the users can be distinguished and the user area becomes broader with respect to their angles, at the transmitter side. For example, when the footmark of the transmission beam is sufficiently wide in horizontal angle on the ground, the performance of the schemes based on the sum rate and outage angle outperforms the scheme where the user ordering is based on their distances. This makes the proposed user angle feedback scheme a better substitute for the conventional distance feedback schemes. The derivations and simulations show that the probability of outage and the sum rate of the proposed system is less than the other distance or ordering based feedback schemes.

L. Zhu et al. [66] in this paper, investigates a downlink hybrid beamforming scenario in mmWave NOMA systems. Depending on the user channel conditions the authors designed an algorithm for user clustering. Depending to the high or low correlation amongst the users, the users were grouped in same or different groups respectively. This method of grouping helps in mitigating the interference between users in different groups. Thereafter, the authors investigate the problem of power allocation and joint hybrid beamforming, with constrains on the minimum rates per user, for sum rate maximization. The proposed power allocation method was divided into two problems namely; inter and intra cluster power allocation. The results of the simulation verify that the sum rate of the proposed scheme outperforms the traditional mmWave OMA schemes. Furthermore, it was found that the energy efficiency performance in the proposed hybrid beamforming scheme better than other schemes and the proposed technique can significantly reduce the inter cluster interference.

Y. Song et al. [67] in this paper studies are a mmWave and NOMA as two prime technologies for future mobile communications. The security issues are the main focus of this paper. The study is based on power allocation in cognitive style, maintaining the primary user’s QoS. To cope with the eavesdroppers, a guard zone sector is created through directional beamforming. Moreover, to decrease the complexity of the channel arrangement, users from an internal and external sector rings are chosen for employing NOMA. The performance of secrecy through random geometry of users and eavesdroppers is evaluated by the authors, in terms of outage probability of secrecy, throughput of secrecy and outage probability of the connection. The simulation analysis confirms that the performance of the secondary users in the proposed system is better than the other conventional OMA systems, and the performance of the primary users remain the same for NOMA and OMA schemes. Furthermore, it is found that, with proper setting of the parameters the secrecy throughput of the secondary user in proposed system is higher than the mmWave OMA system.

D. Fan et al, [68] in this paper, examine transmission and channel estimation techniques for hybrid mmWave NOMA systems. The authors propose a channel estimation technique based on iterative index detection to find channel gain and direction of arrival of each transmission. Further, to decrease the inter beam interference, a hybrid precoding technique is designed which is based on the transmission angle domain. To maximize the sum rate, the authors further studied a power allocation and user scheduling non-convex problem. This problem is decomposed into distinct sub problems of power allocation and user scheduling. The problem of user scheduling solved by two-sided many-to-one matching model and the power allocation problem is cracked through iterative optimization procedure. The performance superiority of the proposed user scheduling and channel estimation scheme is verified through the simulations.

K. Belbase et al. [69] in this paper studied the a cooperative mmWave NOMA systems and the probability of coverage of the system. In the proposed system the relay receives its own signal as well as the signal for the destination, transmitted by the source. To examine the coverage probability, the authors proposed two schemes for relay selection, to select the users which can meet the threshold rates. In the relay selection schemes, the relays are selected on the basis of their location; either near to the source or destination. Decoding sets based on the location are considered to find the probability of the coverage. Through simulations the authors found that both the proposed relay selection schemes perform better than the mmWave OMA schemes. As the proposed work is based on cooperative scheme because of no direct link between source and destination. The authors suggest that if a direct communication link is available between the source and the destination then the system can decide to either exercise direct or cooperative communication as a direction for the future works.

J. Li et al. [70] in this paper examines the agile-beam mmWave NOMA systems to investigate the sum rate and the coverage probability of the proposed scheme. Firstly, scenario was considered by the authors where the users for communication were selected by the proposed user pairing method considering distance as well as angle characteristics. The BS is equipped with a uniform linear array system. Then, depending on the angle of the users, the BS changes between the single and multiple-beam transmission strategy transmission. From a group of far users, the BS randomly chooses a user and then evaluates the minimum difference in the angles with the near users, for user pairing. The proposed pairing strategy was investigated through simulations. The efficiency of the proposed user pairing scheme uses channel sparsity to form a flexible mmWave NOMA agile beam transmission scheme. geometry. The simulations show the efficiency of proposed scheme its superiority over the conventional mmWave OMA schemes in terms of sum rate and coverage probability.

Z. Wei et al. [71] in this paper analyses, beamwidth control strategy is investigated in a mmWave NOMA system to improve the energy efficiency through a proposed scheme of optimal resource allocation. By sharing frequency resources amongst users, the authors try to enhance the system's energy efficiency. Moreover, the authors studied that, through the proposed scheme of controlling the beamwidth and widening the beamwidth, the number of simultaneously served users can rise. The authors proposed, two methods for beamwidth control, based on the conventional and Dolph-Chebyshev beamforming. Due to the proposed beam control methods the, power loss in the main lobe was considered to introduce an analog beamformer method. This method aims to reduce the power losses. Thereafter, an efficient resource allocation problem is studied to improve the energy efficiency of the system, considering minimum required data rates as a constraint. Moreover, a coalition game-based NOMA clustering algorithm is designed to find an optimal solution of the problem. The results of the simulation show that the proposed algorithm is effective and has fast convergence. Furthermore, superiority of the proposed scheme in terms of energy efficiency over the conventional OMA schemes were also verified.

M. Zeng et al. [72] in this paper investigates a massive MIMO NOMA system employing mmWave uplink communication for energy efficiency intensification. Authors propose a NOMA two user clustering technique based on difference between their channel gains and the correlation between their channels. Authors found that, the number of radio frequency chains and the beamforming technique can help in reducing the complexity of the transceiver as well as the energy consumption of the system. Therefore, to decrease the number of radio frequency chains at the BS the authors designed an analog-digital hybrid beamforming technique. Based on the proposed hybrid beamforming technique, the authors introduced iterative power allocation method in order to increase the system's energy efficiency, while considering all the QoS requirements. Further, the authors proposed an enhancement in the NOMA technique. In uplink communication, the proposed enhanced NOMA technique takes advantage of the global knowledge available at the BS, where the interference of the weak user is mitigated for the other cluster users. The simulation results show the superiority of the proposed scheme over OMA scheme in terms of energy efficiency.

X. Hu et al. [73] in this paper, studies error in angular estimation in a massive MIMO NOMA system employing mmWave communication for evaluating the algorithms for power control and user clustering. The sum rate performance of the system is derived in a closed form function. From this function the authors found an asymptotic approximation rate analysis. The analytical studies found that when the BS has a huge amount antenna, then the rates is inversely proportional to the number of antennas to the number of beams ratio and directly proportional to the spatial direction distance. To reduce the interference between the clusters a cluster grouping algorithm based on the spatial direction distance is introduced by the authors. This algorithm shows considerable improvement in the systems performance in contrast to the conventional schemes via simulations.

N. Wang et al. [74] in this paper analyses pilot contamination attack on mmWave NOMA massive MIMO networks. Authors found that the recognition of the pilot contamination attack is difficult due to the superimposition coding used in NOMA communications. Authors found that the virtual channel model of the system will show a characteristic of channel sparsity and this characteristic can be used to differentiate pilot contamination attack case from the normal case. Therefore, for recognition of the pilot contamination attack, the authors proposed two schemes for dynamic and static system models. For attaining improved detection performance, machine learning and peak estimation algorithm-based model is also introduced. The results of the simulation results validate the efficiency of the proposed schemes. The results show that the detection rate in static and dynamic system models can reach 100% and 95% respectively.

P. Liu et al. [75] in this paper examines a massive MIMO NOMA system employing mmWave communication. Authors found that the energy consumption in communication networks is a big issue in massive MIMO systems with large number of radio frequency chains. Therefore, the authors investigate a power allocation scheme to intensity the energy efficiency of the considered system. Zero forcing precoding is used in this paper through beam selection. Then, an optimization problem for enhancing the energy efficiency is formed. Thereafter, this optimization problem was converted into a convex optimization problem, by the authors. Then the authors used iterative algorithm for to derive the power allocation coefficients. The convergence method is then analysed by the authors, and found that the suboptimal solution for each iteration.

The results of the simulation verify the superiority of the proposed power allocation algorithm in terms of energy efficiency, over the conventional schemes.

V. Mandawaria et al. [76] in this paper investigates massive MIMO NOMA system employing mmWave system to enhance its weighted sum energy efficiency. Through successive convex approximation method, the weighted sum energy efficiency is analysed, then through first-order Taylor approximation is used for further analysis. This approximation is taken as a generalized convex program, which is then converted into conic program to decrease the computation time. Further, using dual decomposition authors proposed an algorithm for weighted sum energy efficiency, to decrease the time required in calculations. When compared with successive convex approximation methods the calculation time is reduced by two orders in the proposed scheme. Through simulations it is found that NOMA has higher weighted sum energy efficiency than OMA scheme.

Table 2.1. Literature Survey

Ref. No.	Description of Algorithm	Perfor-mance Indicators Optimized	Up-link/ Down -link	System Model	Year
Objective 1: Implementation of a hybrid beyond 5G system model using millimeter-wave, massive-MIMO and NOMA with D2D enabled small-cell communication network.					
[77]	Authors found that the number of simultaneous users at the same resource cannot exceed the number of RF chains in the MIMO beamspace model. To overcome this issue, the authors proposed a beamspace mmWave MIMO-NOMA model. A zero-forcing based precoding scheme is formed to condense the inter-beam interferences in the system. Further, the sum rate and a joint inter and intra-beam power is optimized through a proposed dynamic power allocation scheme via an iterative algorithm. The results of the	Data rate, Spectral Efficiency and Energy Efficiency	Down link	mmWave MIMO NOMA	2017

	simulation show that the proposed beamspace model can outperform the existing models in terms of spectrum and energy efficiency.				
[78]	Analysis of an uplink mmWave massive MIMO NOMA system is presented in this paper. The clusters of two users are designed depending on the correlation and difference in their channel gain. The authors found that hybrid analog-digital beamforming method can aid reducing the number of RF chains at the BS. Thereafter, a non-convex power allocation optimization problem is formed based on a hybrid analog-digital beamforming method. This non-convex problem is then solved through an iterative power allocation algorithm with QoS constraints. The simulation results show that the energy efficiency of the proposed system outperforms the conventional systems.	Energy Efficiency	Up-link	mmWave massive MIMO NOMA	2019
[79]	Authors found that the issue of high energy consumption in 5G massive MIMO systems is a major problem. A study of mmWave massive MIMO NOMA systems is carried	Spectral Efficiency and Energy Efficiency	Down link	mmWave massive MIMO NOMA	2019

	out with the purpose of improvement in energy efficiency via optimization of power allocation in the cluster based beamspace model. In the considered scenario of the paper, the precoding matrix is found according to the selected beams from the BS. Thereafter, the energy efficiency optimization problem is formulated as fractional programming. This problem is transformed into convex optimization problem solved via iterative optimization algorithm to get power allocation coefficients. The simulation results show that the system's energy efficiency through the proposed method is superior than the conventional methods.				
[80]	Authors in this letter studied the system model of mmWave massive MIMO NOMA network. The considered system model assumes a limited number of RF chains at the BS, and proposes a hybrid analog-digital precoding technique. Based on this proposes a hybrid analog-digital precoding technique a problem of power allocation is formulated to maximize the energy efficiency. Further, with the help of an iterative algorithm the solution of the optimization problem is found. The results of the simulations show that for lesser number of RF chains,	Energy Efficiency	Down link	mmWave massive MIMO NOMA	2017

	the energy efficiency under the proposed hybrid precoding is superior than under digital precoding.				
[81]	Based on a hybrid precoding scheme, a power allocation and power splitting scheme are proposed to improve the energy efficiency in SWIPT system	Spectral Efficiency and Energy Efficiency	Down link	mmWave massive MIMO NOMA	2019
[82]	In this paper, analysed the mmWave massive MIMO-NOMA systems with simultaneous wireless information and power transfer (SWIPT), where each user, via a power splitting receiver, is able to get both information and energy. For each beam one user is chosen according to a proposed cluster-head selection algorithm. Thereafter, for all the beams, analog and digital precoding are designed, depending on the cluster head and channel gain, respectively. Through power allocation and SWIPT power splitting factor optimization the sum rate is enhanced, and to solve the optimization problem an iterative optimization algorithm is developed. The results of the simulation analysis show that the spectrum and energy efficiency of the proposed system is higher than the other OMA based SWIPT systems.	Energy Efficiency, weighted sum energy efficiency, run time	Down link	mmWave massive MIMO NOMA	2019

Research Gap: There are very few articles related to millimeter-wave, massive-MIMO and NOMA system model but these articles have not exploited the advantages of exploiting D2D networking in a hybrid millimeter-wave, massive-MIMO and NOMA small-cell communication system					
Objective 2: Energy efficiency optimization of a hybrid millimeter-wave massive-MIMO NOMA with D2D enabled beyond 5G network using a novel battery efficient NOMA technique					
[83]	In this paper, capacity of the mmWave massive MIMO NOMA systems is analysed. Initially, by extending the random single-path model, a simplified mmWave model is introduced with angle of arrival. Thereafter, this model is categorized into low and high SINR regimes, for capacity analysis. In low and high SNR regimes the capacity is determined through StieltjesShannon transform and statistic and eigenvalue distribution, respectively. The observations show that SNR and the number of users have positive correlations with the capacity of the system in the low SNR regime, where as in the high-SNR regime have the number of LOS paths has positive on the capacity. The results of the simulations show that the achieved capacity through the proposed model shows significant improvements.	Capacity	Down link	mmWave massive MIMO NOMA	2017

[84]	Authors found that, to minimize the cost of the hardware in mmWave massive MIMO NOMA systems, finite resolution analog beamforming can be used. However, this may lead to imperfection in beam alignment with the channels moreover, multiple users might be allotted in identical beams. In this letter, a new NOMA scheme employing finite resolution analog beamforming technique is proposed, to mitigate the reduced degrees of freedom induced by finite resolution analog beamforming technique in the system. The results of the simulations show that the proposed system shows excellent performance in terms of outage probability.	Outage Probabilit y	Down link	mmWav e massive MIMO NOMA	2017
[85]	In this paper, authors found that in a dense user deployment scenario, various users can have similar beam signatures. This can lead to a strong mutual interference. Therefore, the authors considered a multi-cell mmWave massive MIMO NOMA system and investigated the effects of proposed angle-domain NOMA scheme on it. This scheme is proposed to simultaneously schedule a user at cell edge and a user at cell centre, on each spatial downlink beam, and reduce the	Average Data Rate and Average Sum Rate	Down link	mmWav e massive MIMO NOMA	2020

	interference. Thereafter, to optimize the transmission and sum rate, precoder is designed and categorized into outer and inner precoder, based on beam signatures and, joint optimization precoder decoder and cooperative NOMA, respectively				
[86]	In this paper, authors studied a cooperative relay network using NOMA. The main aim of the study is to maximize the Global Energy Efficiency. Through decomposing non-convex energy optimization problem into bilateral optimization problem, the global energy efficiency is optimized. The results of the simulations show that the proposed system shows excellent performance in terms of global energy efficiency optimization.	Global Energy Efficiency	Down link	NOMA	2018
[87]	Authors in this paper, propose dynamic resource allocation for suboptimal sub-channel assignment algorithm, using NOMA. Through methods like, two- side matching method, Lyapunov, linear and Lagrangian optimization the problem of energy efficiency is solved. The results of the simulations show that the proposed scheme outperforms the conventional OMA schemes.	Energy Efficiency and Average Energy Efficiency	Down link	NOMA	2018

Research Gap: There is no work where exploration of NOMA and D2D networks for enhancing energy efficiency of in a hybrid millimeter-wave, massive-MIMO and NOMA D2D enabled communication system is analyzed.					
Objective 3: Implementation of an efficient user clustering approach in hybrid millimeter-wave massive-MIMO NOMA with D2D enabled beyond 5G small-cell network using antenna angle bound clustering technique.					
[88]	In this paper, considered a massive MIMO-NOMA uplink system with receive antenna selection. Authors proposes a scheme to group two users in a cluster based on available number of RF chains at BS and are categorised as low-power and high-power cluster. The authors propose power allocation, user clustering, and RAS algorithms, to condense the computational energies, fairness and to maximize sum rate under constraints of minimum rate requirement and received power consumption. The simulation results show that through the proposed scheme up to two-fold increase in connectivity for a limited number of RF chains can be achieved.	Average Sum Rate	Down link	mmWave massive MIMO NOMA	2019
[89]	In this paper, to decrease power consumption the authors proposed a cluster beamforming strategy for MIMO-NOMA systems. Through power allocation and beamforming vector optimization the schemes try to cancel peer effects of multi user clustering. Moreover, a coalition game approach is used to optimize	Sum Rate	Up-link	Massive MIMO-NOMA	2019

	the proposed clustering technique, with flexible cluster size. The results of the simulation show that the proposed approach outperforms the MIMO NOMA clustering counterparts.				
[90]	In this paper, to reduce power consumption the authors proposed a cluster beamforming strategy for MIMO-NOMA systems. Through power allocation and beamforming vector optimization the schemes try to cancel peer effects of multi user clustering. Moreover, a coalition game approach is used to optimize the proposed clustering technique, with flexible cluster size. The results of the simulation show that the proposed approach outperforms the MIMO NOMA clustering counterparts.	Power Reduction	Down link	MIMO-NOMA	2019
[91]	In this letter, authors aim to maximize the sum rate through optimum power allocation and clustering technique, for MIMO NOMA systems. Based on user channel gains first, the active users are categorized two clusters types high power and low power. Thereafter, NOMA is used to control the inter cluster and intra cluster power, for efficient cluster formation. The simulations demonstrate that the proposed	Average Sum Rate	Up-link	MIMO-NOMA	2019

	system has improved sum rate than multi user MIMO system.				
[92]	In this paper, a user clustering strategy and power allocation strategy is examined a hybrid NOMA system. A problem of weighted sum maximization is formed based on clustering and power allocation problem. The clustering problem is considered as partition formations and coalitional games and solved through global optimal and low complexity techniques. Thereafter, based on successive convex approximation iterative algorithm the power allocation problem is solved. The results of the simulations show that the proposed schemes outperform the random structured schemes in terms of weighted sum rate.	Weighted Sum Rate, Fairness	Down link	NOMA	2019
Research Gap: Efficient NOMA clustering can help in efficient system implementation. Antenna parameters consideration is important for reducing system interference and efficient clustering in a hybrid millimeter-wave, massive-MIMO and NOMA D2D enabled communication system. However, it remains unanalyzed.					
Objective 4: Implementation of an energy efficient mobile small-cell for beyond 5G networks using NOMA technology.					
[93]	In this paper, analysis of deployment of the mobile small cell to improve total in-service time is carried out. First the authors formulated the problem as NP-hard and ratio inapproximable. Thereafter, authors propose a	Total in-service Time, Total Travel distance of small cell	Down link	Mobile Small Cell	2017

	mobile small cell deployment algorithm. The proposed algorithm is one of the best approximation algorithms to overcome problem of service un-availability during cell movement. The results of the simulations show improvement in the in-service time as compared to the static cell deployment technique.				
[94]	In this paper, authors found that it is vital to consider vehicle mobility and provide dynamicity in allocating small-cell BS and power, in high mobility vehicle-to-small-cell (V2S) network. To solve this issue, authors proposed power control and cell association optimization improve long lasting system-wide performance and utility and lower the rate of handoffs. The optimization problem is solved by standard gradient-scheduling method and transforming it into a problem of weighted sum rate maximization. Thereafter, based on Karush-Kuhn-Tucker optimality conditions the authors propose hierarchical power control algorithm for weighted sum rate maximization. show that the proposed algorithm performs better performance in terms of spectrum-energy efficiency and handover rate for the joint optimization of cell association and power control.	Weighted Sum-Rate, Fairness	Down link	Vehicle-to-Small-Cell Network	2017

[95]	Authors in this paper found that the conventional macro-cell systems suffer from high traffic in HetNets. Therefore, authors studies deployment of dynamic small-cells to offload the traffic and hence, reducing the total power consumption. The dynamic small-cell deployment is analysed for two scenarios; to communicate with uniform and nonuniform distributed user locations. In the first scenario, the number of users in small cell and macro cell are assumed to be same. Thereafter, based on the distance between macro and small cell BS, for the small cell BSs operation mode selection, an optimal location-based algorithm is designed, to condense the total power utilization. Further, a scenario of different user distribution in small and macro cell is considered, and the problem is considered as NP-hard. To solve this problem authors proposed density and location-based algorithm.	Total Power Consumpti on	Down link	Static Macro Cell-Small Cell HetNet	2016
[96]	In this paper, authors found that, in an uplink system, the distance of a user is different from each small cell BSs in a NOMA system. Therefore, right selection of small cell BS for a user, is important. However, this problem is associated with co-channel interference management and power control. Therefore,	Total Power Consumpti on, Fairness	Up-link	Static Small Cell NOMA network	2017

	authors formulated a power allocation and BS association optimization problem, to minimize total transmit power and utility maximization. To solve this problem, authors propose a coalition formation game theory-based algorithm. The results of the simulations show that the proposed algorithm gives superior performance in terms of power consumption and system utility.				
[97]	Authors in this paper found that it is difficult find the energy and spectral efficiency in a high mobility vehicular small cell system. Therefore, authors in this paper give attention to handovers and interference management of the system. To solve this problem, NOMA is employed while designing the vehicular small cell system architecture in this paper. Moreover, for power control and cell association optimization a hierarchical power control solution is proposed to maximize the energy and spectral efficiency. The simulation results show that the proposed architecture shows significant improvement in spectral and energy efficiency	Weighted Sum-Rate, Fairness, Power Consumption	Down-link	Vehicular Small Cell NOMA Network	2017
Research Gap: Investigation of mobile small-cell systems for serving high mobility users and efficiently utilizing system's energy is critical. Energy optimization of NOMA enabled mobile small-cell systems remains unexplored.					

Objective 5: Energy efficiency clustering in a mobile small-cell using NOMA D2D technique in beyond 5G networks.					
[98]	In this paper, authors found that NOMA technology can be beneficial in bandwidth improvement in the communication systems. For sum rate maximization, the authors define power allocation and clustering technique for the considered system. Putting quality of service constraints on dynamic service rate and minimum service rate, the authors investigated the sum rate maximization problem. First, sum rate is investigated through power allocation optimization with arbitrary cluster size. Thereafter, a user clustering solution is proposed for random number of users with a random cluster size. An exhaustive search algorithm is used for optimization. The simulation results show that the sum rate is enhanced through proposed technique with reduction in computational complexity.	Sum-Rate	Down -link	Static Cell NOMA system	2018
[99]	The authors in this letter studies user clustering and power control for NOMA systems to reduce the power consumption. The authors considered conventional decoding power at the receiver side and transmission power utilized in	Total Power Consum-ption	Down link	Static Cell NOMA system	2018

	transmission. The power consumption minimization problem is transformed from nonconvex form, into equivalent problem with linear rate constraints. Thereafter, compressive sensing and penalty method are used to solve the problems. The results of the simulations show that the effectiveness of the proposed algorithm is superior than the popular matching-based algorithm.				
[100]	The authors in this paper found that the users are unaware of the transmission information of other users in NOMA uplink communication, and each user transmits independently. Therefore, the problem of simultaneous transmission arises as multiple users cannot be grouped to transmit a single composite uplink power signal. To solve this problem, the authors use two-step power allocation method for NOMA uplink system. First, multiple users are grouped into small cell like clusters, according to their locations and a cluster transmission node is defined for each cluster. Users lying inside the cluster carries out individual uplink transmission independent from the cluster transmission node. Thereafter, multiple users are multiplexed by	Sum-rate, Outage Proba-bility	Up-link	Static Cell NOMA system	2019

	the cluster transmission node, in a single composite uplink power signal. The results of the analysis validate that the proposed technique is superior from the access OMA technique.				
[101]	In this paper, throughput analysis of NOMA uplink and downlink systems is carried out. By optimising power allocation and user clustering sum throughput maximization problem is formulated. By exploiting the gain difference in channels of the users, they ate grouped into single or multiple groups. Thereafter, optimal power allocation coefficients are derived for any cluster size using KKT optimality conditions. The results of the simulations show the significance of proposed network over OMA networks.	Sum-Throughput	Uplink and Downlink	Static Cell NOMA system	2016
Research Gap: Efficiently clustering the users in NOMA enabled mobile small-cell D2D system remains unexplored.					

CHAPTER 3

B5G/6G WIRELESS NETWORK ARCHITECTURE

This chapter puts light on the what is lacking in previous architectures and why there is a requirement of new architecture for B5G/6G. This chapter further proposes a general 6G wireless network architecture which may provide a good platform for future 6G standardization network.

3.1 Introduction

The B5G/6G is envisioned as a platform for connecting everything; people, things, and even intelligence. The first source of induction for the need for the development of B5G/6G is to keep addressing the world's insatiable demands and insistence on better service experiences. Moreover, a unified platform needs to be designed to enable new industries and new services that 5G will be unable to achieve. The prime engine of continuous research is envisioning to raise the bars to attain, ultra-fast wireless speed, high mobility, full coverage, increased bandwidth, connectivity, and greater security while reducing the energy consumption and achieving ultra-low round-trip latency, to such a level that is unachievable with 5G. Prime objectives of B5G/6G systems are identified as:

- *1~10 Tbps Data rates in real-world:* 360° VR/AR services need data rates up to 500Mbps. Applications and services like holographic communications, IoE, 3D video communication, 4K 8K, AR, etc. will demand much high data rates than promised by 5G.
- *Tremendous number of connected devices*: With the rise of mobile users, the development of smart cities, and cell densification the network capacity requirements also increase. Static Base Station (BS) cannot fulfil these demands. Therefore, the facility of relocation offered by mobile BSs can offload the data traffic of the static BSs.
- *Every time everywhere services*: B5G/6G envisions to cover the entire surface of the earth with communication links. This 3-Dimensional (3-D) nature of coverage will surpass the coverage capabilities of 5G.
- *Perceived availability almost 100%:* Network services must essentially be always available is one of the key B5G/6G visions and motivation.
- *10~100µs round trip Latency*: To support real-time, emergency, and IoE based applications, B5G/6G will require to reduce backhaul congestion and Radio Access Network (RAN) congestions. Short-packet transmissions, dynamic transmission, and signalling overhead because of these congestions. B5G/6G aims to address these issues to achieve low latency access networks.
- *High bandwidth in the unit area*: It is a requirement to extensity the connections in a specific area, with higher bandwidth, for a longer duration.

- *Safety and Security of the Information*: Presently, massive user data is stored in networks in form of activity logs, text messages, geo-tagged voices, etc. Securing confidential online data from eavesdroppers, increasing cyber-security and encryption tools are a few of the vital goals of B5G/6G.
- *Shrinking the Energy usage*: Reduction in power consumption and development of green technologies while achieving high target data rates and providing enormous connectivity, is a fundamentally important design aspect of B5G/6G.

3.2 Comparison of 5G and B5G/6G architectural requirements

In 6G, the employment of edge cloud computing interfaces and elements will grow in an immediate information service, which cannot be fetched through centralized search engines. The edge intelligence service platform can be used for framing highly dynamic and local resources, information, and service market. Such a marketplace can maximize economic value through increasing infrastructure utilization, and efficiently matching supply and demand, within the industry. Features such as on-demand network scaling, anywhere and anytime network, and self-evolving network functions, will be considered in the design of 6G networks. All the network nodes should be homogeneous, this will allow most of the traffic and devices to employ resources at the edge of the network. Fig. 3.1 shows the comparison of 5G and B5G/6G architecture key points.

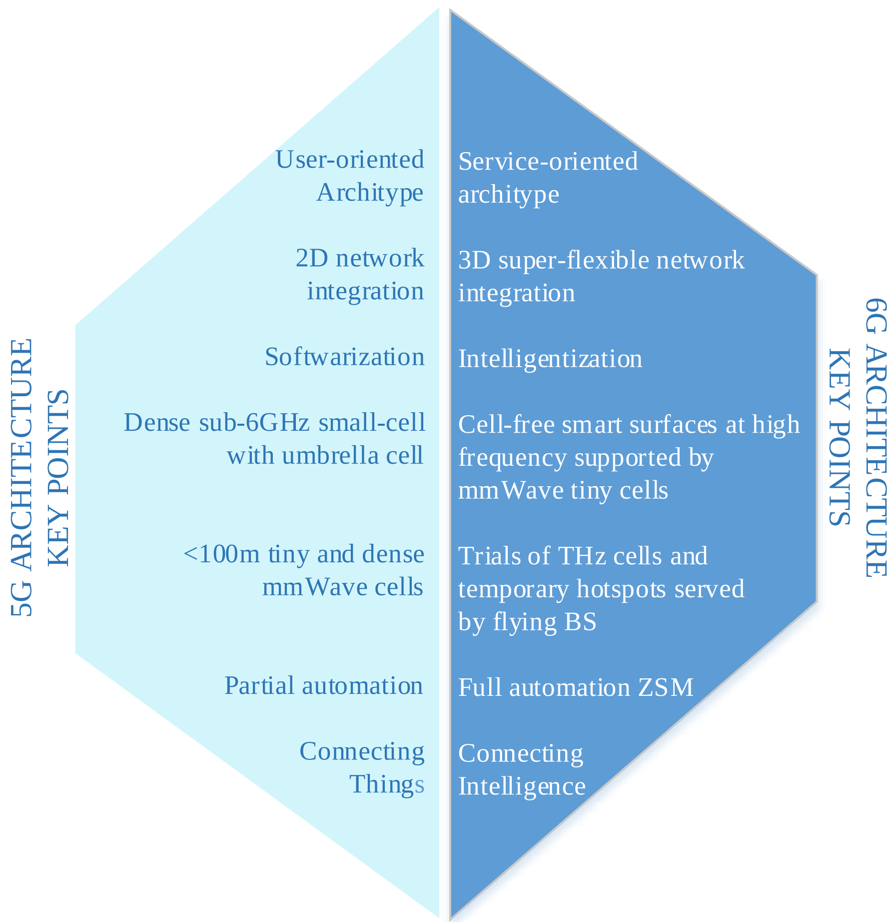

Fig. 3.1. Comparison of 5G and 6G architecture key points, ZSM: zero-touch network and service management.

All the terminals should be allowed to enter and exit freely and easily, to make the 6G network ultra-scalable. To fulfill dynamic contextual and event-defined requirements, AI and ML are envisaged to play a prime role. It will also aid in connecting business-level solutions and network services, through self-orchestration, self-configuration, and self-optimization of resources, with fewer human interventions. The roles of operators and stakeholders will change, to bring demand and supply together. Distributed ledgers technology may give rise to innovations in establishing markets for data and resources or maintaining trust with inter-stakeholder. To ensure sustainability, inclusion, and transparency, new techniques of resource sharing and matching will emerge. Ultimately, regulations will assist the emergence of a new wireless system. Table 3.1 shows requirements of 5G vs. B5G/6G.

Table 3.1: Requirements of 5G vs. B5G/6G

KPI	5G	B5G/6G
Peak Data-rate	20 Gbps	1Tbps
User-experience Data-rate	0.1 Gbps	1Gbps
Area Traffic Capacity	10 Mb/s/m^2	1Gb/s/m^2
Connection Density	10^6 devices/km^2	10^7 devices/km^2
User-Plane Latency	0.5 ms	<0.1 ms
Control-Plane Latency	10 ms	<1ms
Mobility	350-500 km/h	1000 km/h
Relative Spectral Efficiency	~3-5x relative to 4G	>3x relative to 5G
Downlink Spectral Efficiency	30bps/Hz	100 bps/Hz
Energy Efficiency	not specified	1 Tb/J
Relative Energy Efficiency	>1000x relative to 4G	>10x relative to 5G
Reliability	1-10^{-5}	1-10^{-9}
Position Precision	centimeter level	meter level
Receiver Sensitivity	about -120 dBm	<-130 dBm
Delay Jitter	not specified	1µs
Coverage Percentage	about 70%	>99%
Security	not specified	support
Frequency Bands	Sub 6 GHz mmWave for fixed access	Sub 6 GHz mmWave for mobile access

		Exploration of higher frequency and THz bands (above 300GHz) Non-RF (e.g., optical, VLC, etc.)
Device Types	Smartphone, Sensors, Drones	Sensors and Digital Linear Tape devices, Connected Robotics and Autonomous Systems (CRAS), Extended Reality (XR) and Brain Computer interface equipment, Smart implants
Architecture	Dense sub-6 GHz small BS with umbrella macro-BS mmWave small cell for about 100m softwarization 2D coverage	Cell-free smart surfaces at high frequency supported by mmWave, tiny cells for mobile and fixed access, and trial son THz tiny cells Temporary hotspots served by flying BSs Intelligentization Full 3D coverage
Typical Scenarios	Enhanced Mobile Broadband (eMBB) Ultra-reliable Low Latency Communication (URLLC) Massive Machine Type Communication (mMTC)	Further Enhanced Mobile Broadband (FeMBB) Extremely-reliable Low Latency Communication (ERLLC) Extremely Low Power Communication (ELPC) Long Distance Mobility Communication (LDHMC) Ultra-massive Machine Type Communication (umMTC) Human-centric services Multipurpose services
Applications	VR/AR/360° Videos	Holographic Verticals

	UHD Videos V2X IoT Smart City/Factory/Home Telemedicine Wearable Devices	Tactile/Haptic Internet Fully Automated Driving Industrial Internet Space Travel Deep-Sea Sightseeing Internet of Bio-Nano-Things

3.3 B5G/6G Network Architecture

The B5G/6G network architecture is envisioned as intelligent autonomous architecture that will be able to intelligently manage network configuration based on predefined multiple choices in a deterministic manner. Intelligent interpretation, prophecy, and decision based on real-time data, and numerous latency applications need the ability to identify and adapt to unexpected environments. Therefore, future communication network needs to be self-adaptive, self-aware, and self-interpretive. Closed-loop automation in B5G/6G will aid, descend the complexity of orchestration and service management with ZSM, and 100 percent operation automation, bringing self-optimization, self-healing, and self-protection capabilities in the network. With the expansion of smart homes, cities, and societies, and with the growth of robotic and autonomous systems, the demands for integration of machine-to-machine and human-to-machine in terms of communications, will increase. Therefore, for realizing IoE, the B5G/6G networks will be ultra-dense and super flexible. The B5G/6G architecture will dexterously integrate various techniques to simultaneously fulfill diverse service requirements. Moreover, B5G/6G architecture will integrate space, aerial networks, terrestrial and underwater networks for achieving 3D global connectivity. The proposed B5G/6G architecture aims to provide full wireless coverage and make a large-dimension-space-air-ground-underwater network.

The aerial network segment of proposed B5G/6G architecture can be largely classified into two classes, high altitude platforms (HAP) and low altitude platforms (LAP), which generally operate in the stratosphere and several kilometers respectively. HAP can support wider coverage and LAP can support rapidly deploying and reconfigurable short-range communication. Unmanned aerial vehicle (UAV) LAP can be deployed as flying BSs or relay nodes for supporting long-distance or emergency communications. Proposed architecture integrates LEO satellite, GEO satellite, HAPs, and UAV-based LAPs in a network. Aerial networks generally work in low-frequency mmWave or microwave bands. Through the dense deployment of flying or floating BSs like LAP and HAP respectively, a reliable and flexible communication connection is aimed by proposed architecture in remote areas or emergencies. The flying BSs can support the integration of terrestrial and non-terrestrial networks, and floating BSs can support the integration of space networks and flying BSs.

For most human activities terrestrial networks will continue to be the prime wireless coverage, solution provider. To provide services of the Tbps rate, the THz band will be exploited. Thus, technologies like mmWave communication, VLC can provide cellular traffic offloading. In future B5G/6G wireless communication, the spectrum of terrestrial networks will exploit in a way that has not been exploited in previous generations. Thus, apart from the RF band, the terrestrial network will exploit the electromagnetic spectrum, starting from low-frequency, microwave, mmWave, visible and THz band. More number of small cell BSs will be deployed since bands like mmWave and THz suffer from high path loss. Therefore, the terrestrial networks will be ultra-dense heterogeneous networks.

Underwater networks in the proposed architecture will provide wireless coverage and Internet services even in the deep sea and broad sea activities, through smart underwater objects such as Autonomous Underwater Vehicles (AUV) and Remotely Operated Vehicle (ROV). Internet of Underwater Things (IoUT) is expected to interconnect smart underwater devices. The B5G/6G underwater networks will focus to provide uninterrupted services in military or commercial-based applications. Undersea communication mainly deploys RF, optical, and acoustic communication. Supplementary underwater hubs can be deployed to achieve high-speed bidirectional data transmissions in undersea networks. IoUT will ensure disaster prevention, oil and gas pipeline monitoring, pollution detection, water quality monitoring, and control, etc. However, underwater technology can be more complicated than space technology, even the clearest water has 1000 times the attenuation of clear air, due to many reasons including sea pressure. Underwater networks have an unpredictable and complex underwater environment. Since water exhibits diverse propagation characteristics, intricate network deployment can be deployed for ensuring reliable wireless communications, severe physical damage to equipment, cope with signal attenuation, leaving numerous problems to be solved. Potential network architecture of B5G/6G is shown in Fig. 3.2. The proposed B5G/6G architecture comprises of “intelligent physical, datalink and network layers”, where B5G/6G is capable of self-adaptive, self-aware and self-interpretive, self-learning and self-optimization, self-protection, and self-healing capabilities, by integrating advanced AI technologies, data collection, sensing, and domain-specific signal processing methods. Further it has following capabilities:

- Providing training to the transmitter, channel, and receiver, for joint optimization.
- Innovating end-to-end physical layer design and plummeting the receiver complexity.
- Refining physical layer performance, especially in high mobility scenarios.
- Realizing optimal user scheduling through intelligent traffic prediction and channel estimation based on trained DL models.
- Optimizing data offloading and service paradigm and optimizing multiple connections through traffic prediction.
- Optimizing handover process through mobility prediction.
- Realizing optimal data transmission paths through mining beneficial information directly from raw network data and learning routing strategies.
- Realizing optimal BS and user clustering, and monitoring the cluster size in a dynamic network environment.

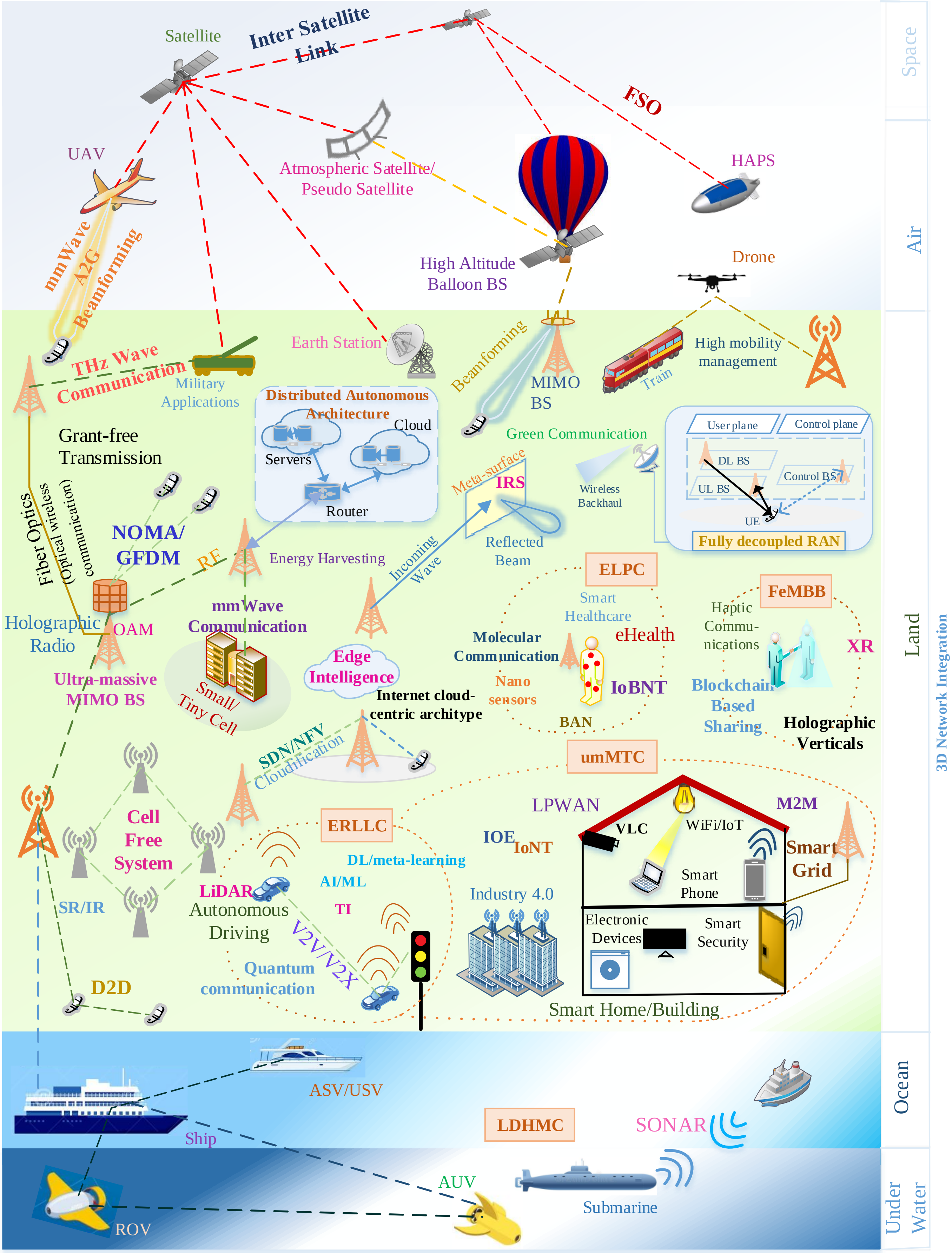

Fig. 3.2. Proposed network architecture of B5G/6G

CHAPTER 4

IMPLEMENTATION OF A HYBRID BEYOND 5G SYSTEM MODEL USING MILLIMETER-WAVE, MASSIVE-MIMO AND NOMA WITH D2D ENABLED SMALL-CELL COMMUNICATION NETWORK

In this chapter, a hybrid system model for B5G/6G is proposed using millimeter-wave, massive-MIMO and NOMA with D2D enabled small-cell communication network. Combining the advantages of THz communications, mmWave communication, RF communications, mMIMO, and NOMA in a two-tier 6G HetNet, this chapter further propose a novel application specific channel selection (ASCS) scheme. In the proposed ASCS scheme, conferring to the application demand of the small cell users the SBS switches downlink frequency channel dynamically. This aids in the efficient utilization of the spectrum. Additionally, to decrease the transmission load and energy cost at the BS due to the huge bandwidth of mmWave/THz-wave each BS is enabled with caches. This chapter also comprises of a pseudo code that will be helpful for developing the ASCS scheme.

4.1 Introduction

Over the past few years, wireless communication networks have experienced ground-breaking progress. The fifth-generation (5G) of mobile communication networks supports many growing verticals including enhanced mobile broadband, machine-to-machine (M2M) communications, and applications such as e-commerce, contactless payment, virtual and augmented reality (VAR), etc. However, with the evolution of the needs of society, there has been a noticeable escalation in a surfeit of emerging use cases that 5G cannot assist satisfactorily. For example, even the millimeter wave (mmWave) frequency bands within 5G cannot support microsecond (μs)-level latency and Tera-bits per second (Tbps)-level rates required in the next generation of VAR [102]. Additionally, with the development of industrial automation, Industry 4.0 will be preceded by Industry X.0. The 5G is designed for $10^6 km^2$ connectivity density metric and the connectivity density of upcoming Industry X.0 will surpass these set parameters. Moreover, a rise in the connection density will also upshoot the demands for enhanced energy efficiency, to a level that 5G cannot fulfill [102]. Subsequently, this together with societal needs has driven the need for a generational leap beyond current wireless systems i.e., 6G systems.

Spectrum unification and the simultaneous employment of spectrum from completely diverse frequency bands such as the conventional mobile bands, the mmWave bands, and Terahertz (THz) bands, is recognized as prime element for 6G networks. Fig. 4.1 shows the electromagnetic spectrum from microwaves to visible light. The advancement of the used radio frequency (RF) spectrum (i.e., 1 Hz to 3000 GHz) has extended the available spectrum for 5G in the section below 6 GHz as well as opened up an utterly new spectrum in the mmWave region, which will also be continued in beyond 5G networks. The 5G New Radio (NR) standards

[103], have encompassed frequencies just below 30 GHz and at 40 GHz. Whereas, the employment of a complete mmWave spectrum up to 100 GHz and beyond is foreseen for the sixth generation (6G) of mobile communication networks. Furthermore, 6G is expected to explore the road towards the THz spectrum, along with full deployment of the mmWave band [104]. Communication in the THz band is being analyzed by the researchers as it provides an edge over legacy networks by offering enormous bandwidths in huge unregulated frequency regions. The short wavelengths of the mmWave and THz wave allow enormous spatial multiplexing gain and provide astonishingly precise output in imaging, sensing, spectroscopy, and many other 6G use cases. While, many losses are associated with mmWave and THz wave bands such as spreading loss, atmospheric loss, diffraction loss, shadowing loss, and scattering loss. The transmitter's energy must be directed on a confined space to avoid the high path loss associated with high frequencies. mMIMO technology provides the chance to electronically direct the signals by regulating the phase of the propagating signals over numerous antennas. To adeptly function, the employment of mMIMO technology can be advantageous at mmWave and THz frequencies. Further, NOMA can serve multiple users simultaneously using a single resource block. Thus, NOMA technology is also beneficial in improving the spectral efficiency of the system. HetNet can offer high spatial reuse and high-frequency reuse. If RF, mmWave, THz, mMIMO, and NOMA technologies are deployed in a HetNet scenario, they can improve the spectral efficiency of the system to a great extent.

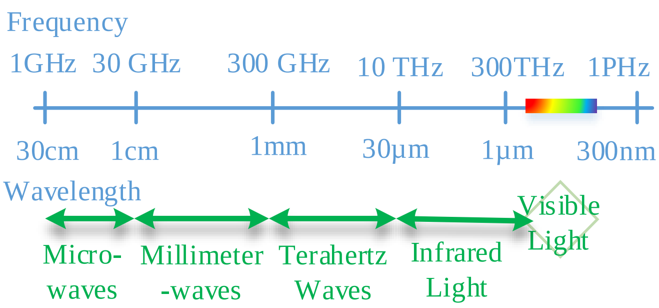

Fig. 4.1. Electromagnetic spectrum from microwave to visible light.

4.2 System Model

We study a 6G downlink two-tier HetNet scenario where a N number of small cells are deployed inside a macro cell. Each cell consists of a BS at the center of the cell. Each BS employs mMIMO and is equipped with N_S antennas. The set of all BSs are denoted as $\hat{\mathrm{S}} = \{1, 2, 3, \dots, \mathrm{S}, \mathrm{S}+1\}$, where $\mathrm{S}+1$ is macro-BS (MBS) and remaining $\{1, 2, 3, \dots, S\}$ are SBSs. All the users are distributed in a stochastic fashion, inside the coverage of macrocell. The set of users is defined as $U = \{U_1, U_2, \dots, U_s, \dots, U_{S+1}\}$. As our system employs NOMA in the downlink, all the users are served in clusters. Each user is grouped into C clusters; $U_s = \{u_{s,1}^1, u_{s,1}^2, \dots, u_{s,c}^i, \dots, u_{s,C}^1, u_{s,C}^2, u_{s,C}^{\cdots}\}$, where $u_{s,c}^i$ is i^{th} user in c^{th}cluster of s^{th} BS. Each BS is equipped with N_{rf} RF chains, which are made equal to the number of clusters to achieve multiplexing gain. Cache storage is enabled at each BS. An error-free fronthaul link connects each BS to a central controller, with C_s^{FH} capacity. As Macrocell has a wide coverage range, MBS employs RF frequency. As THz and mmWave performed better at short distances in the proposed system, the SBS employs RF, mmWave, or THz according to the proposed application-specific channel selection (ASCS) scheme. Fig. 4.2 shows the considered cache-enabled downlink 6G system model. The notations used in the chapter are shown in Table 4.1.

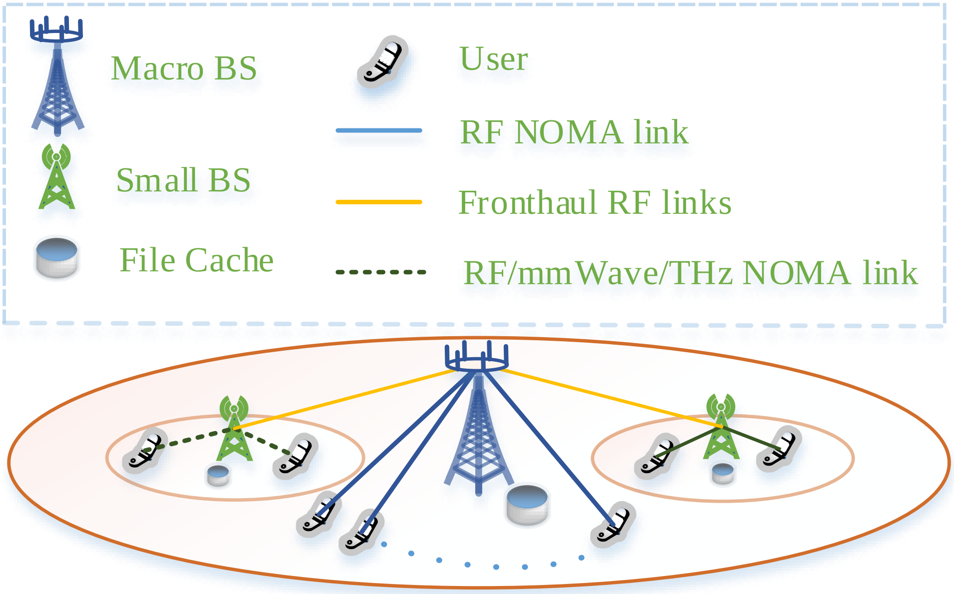

Fig. 4.2. Cache-Enabled Downlink 6G System Model.

TABLE 4.1: NOTATIONS

N_S	Number of antennas at each BS
$\hat{S}$	Set of BSs
U	Set of Users
$u_{s,c}^{i}$	i^{th} user in c^{th}cluster of s^{th} BS
Ǣ	Set of applications
A_s	Set of applications requested by users of s^{th} BS
$a_{p_{s,c}}^{\ i}$	$a_p \| a_p \in$ Ǣ application requested by i^{th} user in c^{th}cluster of s^{th} BS.
$G_{s,c}$	Number of users in c^{th}cluster of s^{th} BS
$p_{s,c}$	The power control factor of cluster c in s^{th} BS
Ᵽ$_{s,c}$	The transmit power of cluster b of BS s is denoted by
$z_{s,c}$	The set of user signals in cluster b of BS s is denoted as
Ḫ	Set of channels
$h_{s,c}^{i}$	Downlink channel of i^{th} user in c^{th}cluster of s^{th} BS.
$y_{s,c}^{i}$	Received signal at i^{th} user in c^{th}cluster of s^{th} BS.
$v_{s,c}^{i}$	Additive white gaussian noise at i^{th} user in c^{th}cluster of s^{th} BS.
$SINR_{s,c}^{i}$	Signal to interference and noise ratio (SINR) of user i in cluster c of BS s
$R_{s,c}^{i}$	Achievable rate at i^{th} user of c^{th} cluster of BS s

The BSs transmit signals to the users in the downlink. Let, $G_{s,c}$ be the total number of users in c^{th}cluster of s^{th} BS, then transmitted superimposed signal from s^{th} BS to $G_{s,c}$ is given as

$$x_{s,c} = \sum_{i=1}^{G_{s,c}} \sqrt{p_{s,c}^{i} \mathrm{P}_{s,c}}\, z_{s,c}^{i} \tag{4.1}$$

where the power control factor of cluster c in s^{th} BS is represented as $p_{s,c} = \{p_{s,c}^{1}, p_{s,c}^{2}, \dots, p_{s,c}^{G_{s,c}}\}$, the transmit power of cluster c of BS s is denoted by $\mathrm{P}_{s,c}$ and is limited by $\sum_{i=1}^{C} \mathrm{P}_{s,c} \leq \mathrm{P}_{s}$, $\forall s \in \hat{\mathrm{S}}$ for apiece cluster, where P_{s} is the transmitter power of BS s, and the set of signals of users in cluster c of BS s is denoted as $z_{s,c} = \{z_{s,c}^{1}, z_{s,c}^{2}, \dots, z_{s,c}^{G_{s,c}}\}$.

Subsequently, the transmitted signal is received by the users over the $S \times C \times U_S$ channel matrix $\breve{\mathrm{H}}$. $\breve{\mathrm{H}} = \{\breve{\mathrm{H}}_1, \breve{\mathrm{H}}_2, \dots, \breve{\mathrm{H}}_s, \dots, \breve{\mathrm{H}}_S | \breve{\mathrm{H}}_s = \{h_{s,c}^{1}, \dots, h_{s,c}^{G_{s,c}}\}\}$. Then, the received signal at i^{th} user in cluster c of s^{th} BS can be given by

$$y_{s,c}^{i} = h_{s,c}^{i} w_{s,c} \sqrt{p_{s,c}^{i} \mathrm{P}_{s,c}} z_{s,c}^{i} + I_{s,c,i}^{1} + I_{s,c,i}^{2} + I_{s,c,i}^{3} + v_{s,c}^{i} \tag{4.2}$$

$$I_{s,c,i}^{1} = h_{s,c}^{i} \sum_{j=1, j\neq s}^{S+1} \sum_{j=1}^{C} w_{j,c} x_{j,c} \tag{4.3}$$

$$I_{s,c,i}^{2} = h_{s,c}^{i} \sum_{j=1, j\neq c}^{C} w_{s,j} x_{s,j} \tag{4.4}$$

$$I_{s,c,i}^{3} = h_{s,c}^{i} w_{s,c} \sum_{j=1}^{G_{s,c}} \sqrt{p_{s,c}^{j} \mathrm{P}_{s,c}}\, z_{s,c}^{j} \tag{4.5}$$

where, $v_{s,c}^{i} \sim CN(0, \sigma_c^2)$ is the additive white gaussian noise (AWGN) with zero mean and variance σ_c^2, $w_{s,c}$ is the precoding vector, and $I_{s,c,i}^{1}$, $I_{s,c,i}^{2}$, and $I_{s,c,i}^{3}$ denotes inter-cell interference, inter-cluster interference, and intra-cluster interference experienced by i^{th} user in c^{th}cluster of BS s.

Consequently, the signal to interference and noise ratio (SINR) of user i in cluster c of BS s is given by

$$SINR_{s,c}^{i} = \frac{p_{s,c}^{i} \mathrm{P}_{s,c} || h_{s,c}^{i} w_{s,c} ||^2}{\sigma_c^2 + \sum_{j=1, j\neq s}^{S+1} \sum_{j=1}^{C} \mathrm{P}_{j,c} || h_{s,c}^{i} w_{j,c} ||^2 + \sum_{j=1, j\neq c}^{C} \mathrm{P}_{s,j} || h_{s,c}^{i} w_{s,j} ||^2 + \sum_{j=1}^{G_{s,c}} p_{s,c}^{j} \mathrm{P}_{s,c} \left|\left| h_{s,c}^{i} w_{s,c} \right|\right|^2} \tag{4.6}$$

Through the capacity model in [25], the rate at i^{th} user of c^{th} cluster of BS s is given by

$$R_{s,c}^{i} = \frac{B}{C} log_2(1 + SINR_{s,c}^{i}) \tag{4.7}$$

The BS cache model is presented as follows. It is assumed that the cache state information $\mathrm{Q}_{f,s}$ is preordained, and is given by

$$Q_{f,s} = \begin{cases} 1 & if\ file\ is\ f\ is\ cashed\ by\ BS\ s \\ 0 & Otherwise \end{cases} \quad (4.8)$$

If the file is not cached by SBS, then it is required to be retrieved from the MBS over the fronthaul link. On the other hand, the file can be directly retrieved from the cache, if the SBS has cached the file requested by the small cell user. The archived rate of the fronthaul link from MBS to SBS s is given by

$$R_s^{Fh} = \sum_{c=1}^{C} \sum_{i=1}^{G_{s,c}} R_{s,c}^{i}(1 - F_{s,c}^{i}) \quad (4.9)$$

where, $F_{s,c}^{i}$ denoted cache efficiency coefficient which can be given by

$$F_{s,c}^{i} = \sum_{f=1}^{M_{s,c}^{i}} Q_{f,s} \quad (4.10)$$

where, $M_{s,c}^{i}$ is the number of files requested by i^{th} user in c^{th} cluster of BS s. Many works study the modeling of cache efficiency, which is is an uncertain area. Though, it is outside the scope of our paper. Meanwhile, attention is paid to a cache model with an identified cache efficiency. The total power consumption of BS s [105] can be expressed as

$$P_s = P_s^{cir} + \xi(\sum_{c=1}^{C} P_{s,c}) \quad (4.11)$$

where, P_s^{cir} is the power of BS s circuit, ξ is the drain efficiency of the power amplifier. P_s^{cir} can be expressed as

$$P_s^{cir} = P_S + N_R P_R + N_s P_P + N_s P_A \quad (4.12)$$

where, N_R is the number of RF chains, P_S is the power consumption of baseband, P_R, P_P, and P_A is power consumption at each RF chain, phase shifter, and amplifier respectively. The energy efficiency [105] can be expressed as

$$\mathrm{EE}_{system} = \sum_{s=1}^{S} \frac{\sum_{c=1}^{C} \sum_{i=1}^{G_{s,c}} R_{s,c}^{i}(1-F_{s,c}^{i})}{P_s^{cir} + \xi(\sum_{c=1}^{C} P_{s,c})} \quad (4.13)$$

The channel model of THz, mmWave, and RF band is discussed. The THz band channel gain [105] of i^{th} user in c^{th} cluster of BS s is given as

$$h_{s,c}^{i}(f,d) = \sqrt{N_S}(\sqrt{\frac{1}{L(f,d)}} \Omega \alpha\left(\varphi_{s,c}^{i}\right)) \quad (4.14)$$

here, Ω denotes the antenna gain, $L(f,d)$ denotes path loss at d distance away from the BS at frequency f, φ is the angle of departure, $\alpha(\varphi)$ represents array steering vector which is given by

$$\alpha(\varphi) = \frac{1}{\sqrt{N_S}}\left[1, \dots, e^{j\pi[n sin\varphi]}, \dots, e^{j\pi[(N_S-1)\sin\varphi]}\right]' \quad (4.15)$$

where, $[A]'$ represents the transpose of matrix A, and j is the imaginary unit, i.e., $j^2 = -1$. The non-line of sight (NLoS) paths are formed by scattered, reflected, and diffracted signals. Due to weak scattering and diffracting ability in the THz band, these paths are generally neglected. The effect of NLoS link can be ignored when LoS link is present, as NLoS link pathloss is greater than the line of sight (LoS) link path loss [26]. In the THz band, the pathloss explicitly consists of molecular absorption loss and spreading loss which cannot be ignored. The pathloss of THz signal at frequency f and traveled distance d is given as follows:

$$L(f,d)^{THz}[dB] = 20\ log_{10}\left(\frac{4\pi}{\lambda_c}\right) + 10k(f)d\ log_{10}e \tag{4.16}$$

here, λ_c is the wavelength of the carrier frequency and $k(f)$ is frequency-dependent medium absorption coefficient. The atmospheric attenuation of THz channels is significantly higher in water vapor molecules than in air molecules. For ease, only the impact of water molecules in atmospheric attenuation is considered in this paper. The frequency absorption coefficient parameters $k(f)$ are given in [105].

For the mmWave channel model [106], the channel gain in (14) becomes:

$$h_{s,c}^i = \sqrt{\frac{N_s}{L(d)\rho_{s,c}^i}} \sum_{k=1}^{\rho_{s,c}^i} \gamma_{s,c,k}\ a_{UE}(\phi_{s,c,k}^i) a_{BS}^*(\theta_{s,c,k}^i) \tag{4.17}$$

here, a_{UE} and a_{BS} are uniform linear arrays array response vectors. The a_{UE} and a_{BS} are of the form $a(\theta) = \left[1\ e^{-j\theta}\ \dots\ e^{-j(N_s-1)\theta}\right]^* / \sqrt{N_s}$. The virtual angle of arrival (AOA) and virtual angle of departure (AOD) for k^{th} path from BS s to user i in cluster c, is denoted by $\phi_{s,c,k}^i$ and $\theta_{s,c,k}^i$ respectively. Here, $\rho_{s,c}^i$ are the number of paths between the BS s and user i, in cluster c, the small-scale fading gain on k^{th} path is signified by $\gamma_{s,c,k}$, and a^* represents the complex conjugate of a. The virtual AOA and AOD are related to the corresponding physical angles as $\theta = 2\pi \text{Ƃ} \sin(\varsigma) / \lambda_c$ where Ƃ signify the spacing between the antennas, ς and θ are respectively the physical and virtual angles. The path loss $L(d)$ of mmWave channel model [107] at traveled distance d is given by;

$$L(d)^{mm}[dB] = 20\ log_{10}\left(\frac{4\pi}{\lambda_c}\right) + 10\gamma log_{10}(||d||) + \text{ʂ}_{s,c}^i \tag{4.18}$$

where γ represents the pathloss exponent, $\text{ʂ}_{s,c}^i \sim CN(0, \xi^2)$ denotes Gaussian distribution with zero mean and ξ^2 variance.

For the RF channel model, the Rayleigh fading channel is considered with Gaussian distribution of $h \sim CN(0, \beta)$ [108] with zero mean and β variance, The large-scale fading characterized by β encompass penetration losses, pathloss, shadowing losses, and antenna gains in NLoS path. Channel gain for RF is given by

$$h_{s,c}^i = 10^{-(L(d)^{RF}/10)} \tag{4.19}$$

The pathloss for RF channel [109], at traveled distance d (km), is given as follows:

$$L(d)^{RF}[dB] = 148.1 + 37.6log_{10}(d) \quad (4.20)$$

4.3 Proposed Approach

The users in the small cell use different services and applications such as online gaming, high definition (HD) video, ultra-HD video, real-time communication, virtual reality (VR), augmented reality (AR), military application, Tbps wireless local area network (WLAN) system, holographic communication, etc. The set of applications is denoted by $\bar{Æ} = \{\tilde{A}_1, \tilde{A}_2, \tilde{A}_3\}$. These applications require data rates in Mbps, Gbps, or Tbps. The relation between different applications and their required data rate is shown in Table 4.2.

Application $\tilde{A}_1$ requires 100 Mbps − 200 Mbps data rate, $\tilde{A}_2$ requires 200 Mbps − 20 Gbps data rate, and $\tilde{A}_3$ requires 20 Gbps − 1 Tbps data rate. The downlink channel for signal transmission from SBS to the small cell users is determined adaptively, according to the application requested by the small cell users. Each user in SBS requests an application; $A_s(t) = \{a_{p_{s,1}^1}(t), a_{p_{s,1}^2}(t), \ldots, a_{p_{s,c}^i}, \ldots, a_{p_{s,C}^1}(t), a_{p_{s,C}^2}(t), a_{p_{s,C}^{\cdots}}(t)\}$, where $a_{p_{s,c}^i}(t)$ denotes $a_p | a_p \in \bar{Æ}$ application requested by i^{th} user in c^{th}cluster of s^{th} BS at t^{th} time instance. Let the total number of users in c^{th}cluster of s^{th} BS be denoted as $\hat{c}_{s,c}$.

Table 4.2: Relation Between Various Applications and Required Data rates

Application	Required Data rate
$\tilde{A}_1$	100 Mbps − 200 Mbps
$\tilde{A}_2$	200 Mbps − 20 Gbps
$\tilde{A}_3$	20 Gbps − 1 Tbps

Following ASCS, at time instance t, if one or more users request application $\tilde{A}_3$, then the SBS employs the THz channel model in the downlink. At time instance t, if no user in the small cell requests $\tilde{A}_3$ in addition, one or more users are request application $\tilde{A}_2$, then the SBS employs the mmWave channel model in the downlink. If all the users in the small cell at time instance t are request applications $\tilde{A}_1$, then the SBS employs the RF channel model for downlink communication. Algorithm 4.1 explains the ASCS. The computational complexity of Algorithm 1 is O(TSC$\hat{c}_{s,c}$).

Algorithm 1 for ASCS

for $t = 1 \; to \; T$

for $s = 1 \; to \; S$

for $c = 1 \; to \; C$

for $i = 1 \; to \; \hat{c}_{s,c}$

a) **if**

$A_s(t) \nexists$ {$\tilde{A}_2, \tilde{A}_3$:$\tilde{A}_2, \tilde{A}_3$ ∈ $\bar{Æ}$ } **then**

$h^i_{s,C}(t) \leftarrow h^{RF}_{s,user}$

b) **elseif**

$A_s(t) \nexists$ {$\tilde{A}_3$:$\tilde{A}_3$ ∈ $\bar{Æ}$ } **and** $A_s(t) \exists$ {$\tilde{A}_2$:$\tilde{A}_2$ ∈ $\bar{Æ}$ } **then**

$h^i_{s,C}(t) \leftarrow h^{mmWave}_{s,user}$

c) **else**

$A_s(t) \exists$ {$\tilde{A}_3$:$\tilde{A}_3$ ∈ $\bar{Æ}$ } **then**

$h^i_{s,C}(t) \leftarrow h^{THz}_{s,user}$

end if

end for

end for

end for

end for

4.4 Simulation results

In this section, we present the simulation results to examine the efficacy of the proposed ASCS Algorithm 1 and compare it with other conventional schemes. Particularly, the effects of the proposed ASCS scheme on spectrum efficiency, energy efficiency, and throughput are compared. Moreover, the comparison of energy efficiency with different cache efficiency coefficients is also shown. To reduce the computational complexity, we set the number of SBS, $S = 2$. The considered simulation parameters are given in Table III. In the considered downlink system, MBS is in the cell center, and SBS is in the coverage of MBS. The user distribution is random throughout the cell, within the scope of their allied BS. All the considered system model uses the RF channel at MBS. We labeled the HetNet system with the proposed ASCS scheme as 'ASCS'. HetNets using mmWave and RF channel at SBS, are labeled as 'mmWave' and 'RF' respectively. Fig. 3 shows the comparison of spectrum efficiency of HetNet with the proposed ASCS scheme with HetNets using mmWave and RF channel at SBS.

TABLE 4.3: NUMERICAL PARAMETERS FOR THE SCENARIO

Parameters	Value
THz carrier frequency	0.34 THz
mmWave carrier frequency	73 GHz
RF carrier frequency	2 GHz
Bandwidth at BS employing THz channel	10 GHz
Bandwidth at BS employing mmWave channel	1 GHz
Bandwidth at BS employing RF channel	10 MHz
Radius of MBS	500 m
Radius of SBS	40 m
Minimum distance between users	0.1 m
Noise Power σ^2	-174 dBm/Hz
Number of SBS, S	2
Cache efficiency, $F_{s,c}^{i}$	0.1, 0.3, 0.5
SBS transmitter power	5 W
Baseband power consumption $\mathbb{P}_S$	200 mW
RF chain power consumption, $\mathbb{P}_R$	160 mW
Phase shifter power consumption, $\mathbb{P}_P$	40 mW
Amplifier power consumption, $\mathbb{P}_A$	20 mW
Drain efficiency of relay amplifier, ξ	0.75%

Fig. 4.3 shows the comparison of sum rate of HetNet with the proposed ASCS scheme with HetNets using mmWave and RF channel at SBS. The number of users is increased from 10 to 50. It can be seen from Fig. 4.3 that the sum rate of 'ASCS' performs better than that of 'mmWave' and 'RF'. The users in demanding applications with the data rate of the range of 200 Mbps - 20 Gbps in HetNets using RF channel and users in demanding applications with the data rate of the range of 20 Gbps - 1 Tbps in HetNets using mmWave at SBS suffer from low data rates. The ASCS scheme employs high and low-frequency bands (i.e., THz, mmWave, and RF bands) dynamically according to the user demands. Therefore, all the users with different application requirements are served proficiently guaranteeing no user suffers from a low data rate. Moreover, the carrier frequency of high-frequency bands offers huge spectrum bandwidth. In a few instances, the available spectrum bandwidth is becoming significantly larger than mmWave and RF band. This causes an increase in the sum rate of ASCS.

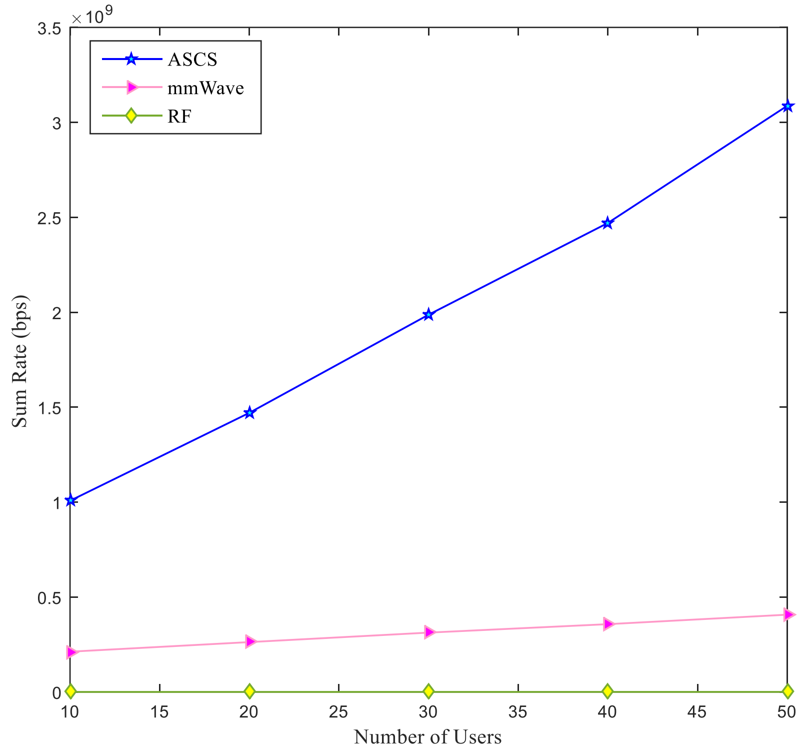

Fig. 4.3. Sum Rate v/s Number of users.

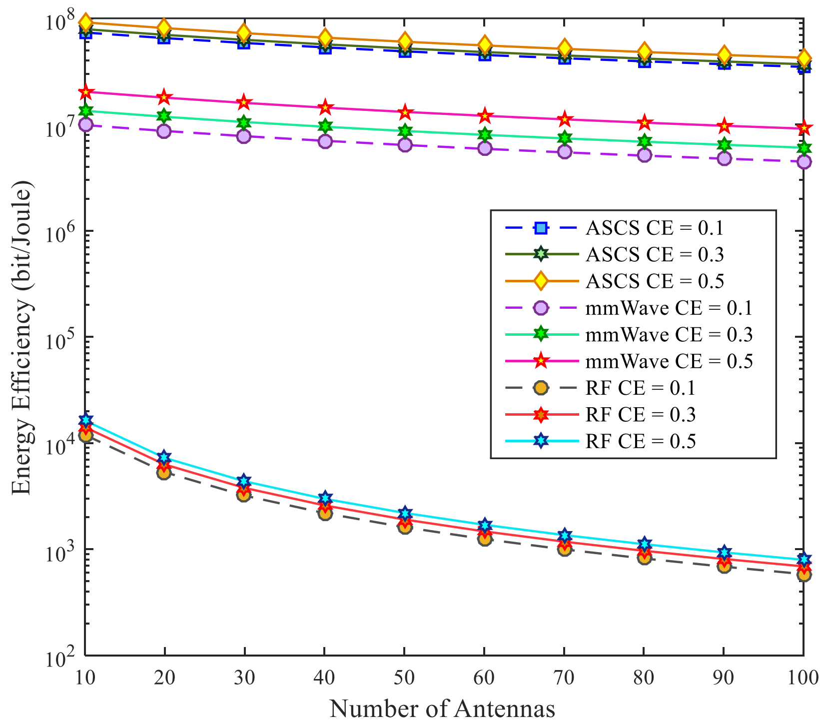

Fig. 4.4. Energy Efficiency v/s Number of antennas.

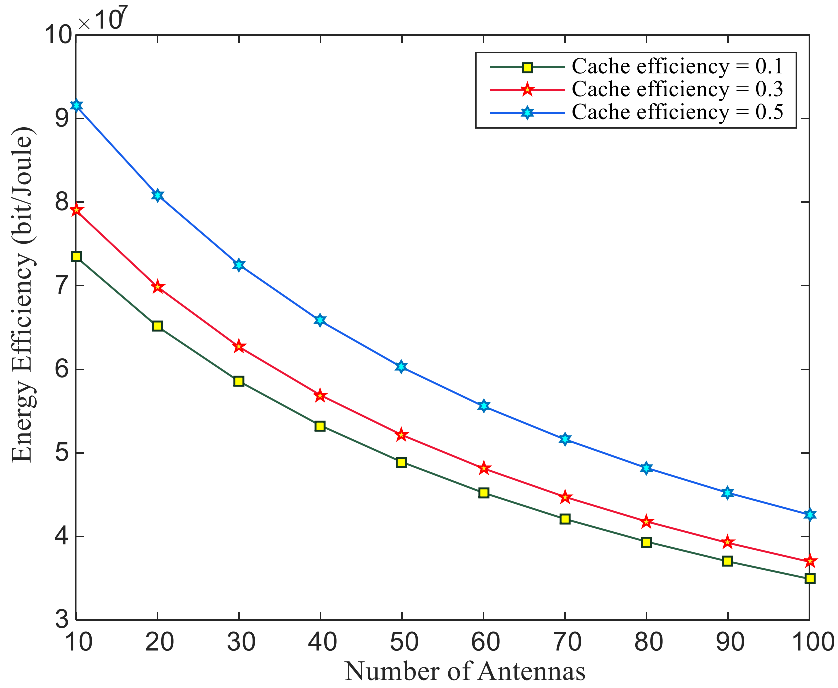

Fig. 4.5. Energy efficiency of ASCS scheme v/s Number of antennas.

For different cache efficiency coefficients, Fig. 4.4 compares the energy efficiency of considered HetNet employing the proposed ASCS scheme, with HetNets using mmWave and RF channel at SBS, which are labeled as 'mmWave CE and 'RF CE' respectively in logarithmic scale. The energy efficiency of HetNet with the proposed scheme is labeled as 'ASCS CE' in Fig. 4.4. Further, Fig. 4.5 explicitly shows the energy efficiency of the ASCS scheme concerning the number of antennas for different cache efficiency coefficients. The number of antennas is increased from 10 to 100. It can be seen from Fig. 4.4 and Fig. 4.5, that with an increase in the number of antennas at the transmitter the energy efficiency decreases, as the power consumption at the antennas rises. A progressive increase in the value of energy efficiency can be seen with the coefficient of cache efficiency. This is due to the significant increase in the sum rate by incorporation of local cache files at BS, as the required files can be directly acquired via the local cache files. Moreover, with the ASCS scheme, the cross-tier interference can be ignored when the SBS employs mmWave or THz band at downlink due to the different bands across the tiers. The cross-tier interference is taken into account only when SBS employs an RF band, and otherwise, it is ignored. Consequently, it has a positive impact on the sum rate and energy efficiency.

CHAPTER 5

ENERGY EFFICIENCY OPTIMIZATION OF A HYBRID MILLIMETER-WAVE MASSIVE-MIMO NOMA WITH D2D ENABLED BEYOND 5G NETWORK USING A NOVEL BATTERY EFFICIENT NOMA TECHNIQUE

In this chapter, the energy efficiency of a hybrid millimeter-wave massive-MIMO NOMA with D2D enabled beyond 5G network is optimized using a novel battery efficient NOMA technique. Further this chapter propose modified cooperative NOMA (MCN) and THz blockage alleviation (TBA) methods. The TBA method aids in ensuring the end-to-end signal communication in presence of obstructions in the path. The TBA method uses device-to-device (D2D) communication to redirect the signal to evade hindrances in the propagation path. TBA method also aids in reducing the interference and hence, improving the SINR and achievable rates. The MCN helps in reducing the power consumption and efficiently utilizing the system's energy. The MCN integrates cooperative relaying technique with NOMA. This supports in reducing the transmission power at the BS and outstretch the signals to the users at the edge of the cell, which have poor channel qualities or cannot build direct links with the BS. Aiming efficient use of user power and interference mitigation, this chapter design two procedures in MCN to forward signal to the end-user based on the power levels of the users. Further, the proposed methods are analyzed in terms of key performance parameters.

5.1 Introduction

The M2M communications, IoT, and vehicular communication are developing expeditiously. With time, the global penetration of wireless portable devices will increase with mushrooming rate. The number of wireless network nodes likely to be measured in trillions to deliver enormous global connectivity [110]. Technologies such as Tactile internet, is expected to be used in numerous applications including transport, entertainment, industrial, and healthcare, and has low latency requirements. Very small end-to-end delays affects the whole network as it needs to reduce the processing-time, over-the-air propagation time, and transportation-time. Moreover, reliability is crucial for various upcoming wireless communications scenarios including industrial internet, autonomous systems, haptic communication and healthcare. The requirements of high privacy, security, and reliability are expected to escalate with time. The 5G is incapable to meet such demands. Consequently, a combination of societal desires and technological innovations that aid to empower such requirements are the key drivers for a generational leap towards B5G/6G of mobile communication networks.

The 6G networks anticipates enhancement in the network capacity, and link capacity compared with previous generations. Many 6G application including holographic communication, extended reality (XR) and ultra-high-definition video demands very high bandwidth and data rates. Consequently, this has inspired researchers to go on the way to explore wireless communication in higher frequency bands, which have significantly larger bandwidths, and are less congested [111]. However, working at higher frequencies not only opens the door to numerous resources but also extensive open problems. Radio design at higher frequencies turns out to be more intricate. Moreover, the propagation losses at higher frequencies due to various factors such as rain attenuation, scattering, dispersion, free-space path loss, gaseous attenuation, and variation of atmospheric refractive index are considerably higher. Further, to improve spectrum efficiently NOMA and mMIMO are another two promising techniques. NOMA simultaneously serves multiple users, by superimposing the signals at the transmitter and sending them to multiple users over a single channel. This decreases the latency and complexity of resource allocation at the BS. Through SIC the receiver separates the signals [112]. Also, the massive number of antennas in mMIMO technology produces more spatial data streams, enhanced throughput, greater multiplexing gain, and consequently, improves the spectral efficiency of the system [113]. Moreover, mMIMO helps in improving link reliability as it is less prone to fading [114].

5.2 System Model

The considered downlink 6G HetNet is shown in Fig. 1, where a macro cell deploys S small-cells inside it. Macro-BS (MBS) and small-BSs (SBS)s employ mMIMO-NOMA and each are enabled with N_B antennas and N_{RF} RF chains. $\text{Ɓ} = \{1, 2, 3, \dots, \text{ƀ}, \dots, \text{Ƀ}, \text{Ƀ} + 1\}$. denotes set of all BSs, where, $\{1, 2, 3, \dots, \text{Ƀ}\}$ are SBSs and $\text{Ƀ} + 1$ is MBS. All the users are spread arbitrarily within the MBS coverage. $\hat{\text{U}} = \{\text{Ų}_1, \text{Ų}_2, \dots, \text{Ų}_{\text{ƀ}}, \dots, \text{Ų}_{\text{Ƀ}+1}\}$ denotes set of all the single antenna users. NOMA employed at the BS groups all the users into Ñ clusters signified by $\text{Ų}_{\text{ƀ}} = \{\text{ų}^1_{\text{ƀ},1}, u^2_{\text{ƀ},1}, \dots, u^i_{\text{ƀ},\tilde{\text{n}}}, \dots, u^1_{\text{ƀ},\tilde{\text{N}}}, u^2_{\text{ƀ},\tilde{\text{N}}}, u^{\cdots}_{\text{ƀ},\tilde{\text{N}}}\}$, where $u^i_{\text{ƀ},\tilde{\text{n}}}$ is i^{th} user in $\tilde{\text{n}}^{th}$cluster of ƀ^{th} BS. The clusters served by each BS are allotted orthogonal time-frequency resources. Radio frequency (RF) band is employed for downlink communication at the MBS as regulated frequency bands have large coverage area. THz band is employed downlink communication at all the SBSs, as it performs better at short distances. Table 5.1 shows the notations used in this chapter.

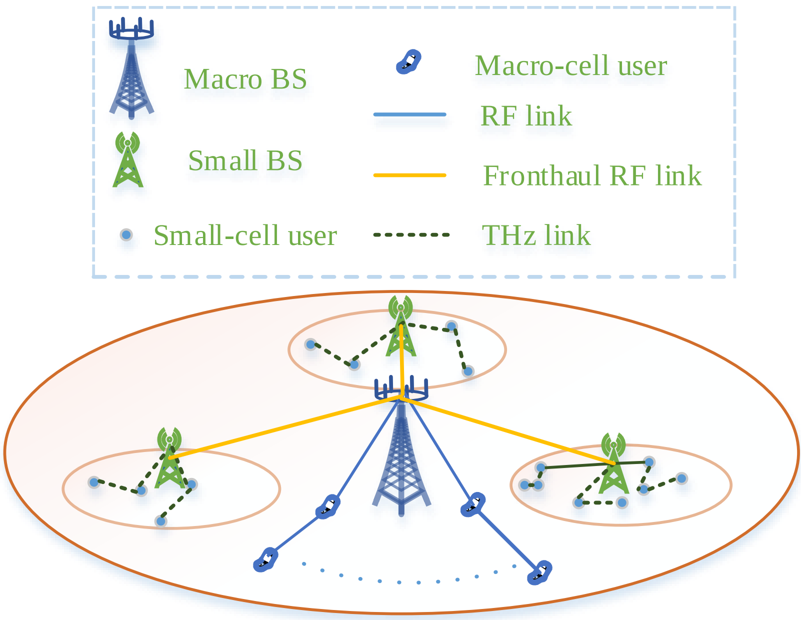

Fig. 5.1. Considered Downlink 6G HetNet.

TABLE 5.1: NOTATIONS

S	Number of SBS
N_B	Number of antennas at each BS
Ɓ	Set of BSs
Û	Set of Users
Ñ	Number of clusters all the users are divided into
$u^{i}_{ƀ,ñ}$	i^{th} user in $ñ^{th}$cluster of $ƀ^{th}$ BS
$K_{ƀ,ñ}$	Number of users in $ñ^{th}$cluster of $ƀ^{th}$ BS
$ɋ_{ƀ,ñ}$	The power control factor from $ƀ^{th}$ BS to $ñ^{th}$cluster
$ꝑ_{ƀ,ñ}$	The transmit power from $ƀ^{th}$ BS to $ñ^{th}$cluster
$x_{ƀ,ñ}$	The set of signals for $ñ^{th}$cluster in $ƀ^{th}$ BS
Ɦ	Set of channels
$h_{ƀ,i}$	Downlink channel of $u^{i}_{ƀ,ñ}$
$ŵ_{ƀ,i}$	The precoding vector of $u^{i}_{ƀ,ñ}$
$ŷ_{ƀ,i}$	Received signal at $u^{i}_{ƀ,ñ}$
$ň_{ƀ,i}$	Additive white gaussian noise at $u^{i}_{ƀ,ñ}$
ȸ	Drain efficiency of power amplifier
$ꞵ_t$	The transmit power of user $ų^{t}_{Ƀ+1}$
B	The bandwidth of channel employed at BS
$Ṕ_A$,	The power consumption per power amplifier
$Ṕ_{RF}$	The power consumption per RF chain
$Ᵽ_B$	The power consumption of baseband
$Ṕ_P$	The power consumption per phase shifter
$λ_c$	The wavelength of the carrier frequency
Ʊ	The antenna gain
φ	The angle of departure
$ɑ(\varphi)$	The array steering vector
$ţ(f)$	The frequency dependent medium absorption coefficient

The BSs transmits signals to the users in downlink. Let, $ƀ^{th}$ BS has total $K_{ƀ,ñ}$ users in $ñ^{th}$cluster, then the transmitted downlink signal from $ƀ^{th}$ BS to $ñ^{th}$cluster is given as

$$s_{ƀ,ñ} = \sum_{i=1}^{K_{ƀ,ñ}} \sqrt{ɋ^{i}_{ƀ,ñ} ꝑ_{ƀ,ñ}}\, x^{i}_{ƀ,ñ} \qquad (5.1)$$

where $ɋ_{ƀ,ñ} = \{ɋ^{1}_{ƀ,ñ}, ɋ^{1}_{ƀ,ñ}, \dots, ɋ^{K_{ƀ,ñ}}_{ƀ,ñ}\}$ and $ꝑ_{ƀ,ñ}$ denotes the power control factor and transmit power of cluster ñ in BS ƀ, respectively. $x_{ƀ,ñ} = \{x^{1}_{ƀ,ñ}, x^{2}_{ƀ,ñ}, \dots, x^{K_{ƀ,ñ}}_{ƀ,ñ}\}$ represents the set of signals for cluster ñ in BS ƀ.

Remark 1: For each cluster the transmit power is limited by $\sum_{ñ=1}^{Ñ} ꝑ_{ƀ,ñ} \le ꝑ_{ƀ},\ \forall ƀ \in Ƀ,$ *where* $ꝑ_{ƀ}$ *is the transmitter power of BS* ƀ, *and the power control factor* $ɋ_{ƀ,ñ}$ *is limited by* $\sum_{i=1}^{K_{ƀ,ñ}} ɋ^{i}_{ƀ,ñ} = 1, \forall ƀ \in Ƀ, ñ \in Ñ$. Then, the signals are received over the $Ƀ \times Ñ \times Ų_{ƀ}$ channel matrix Ɦ. $Ɦ = \{Ɦ_1, Ɦ_2, \dots, Ɦ_{ƀ}, \dots, Ɦ_{Ƀ} \mid Ɦ_{ƀ} = \{h_{ƀ,1}, h_{ƀ,2}, \dots, h_{ƀ,K_{ƀ,ñ}}\}\}$. The signal received at $u^{i}_{ƀ,ñ}$ is given as

$$\hat{y}_{ƀ,i} = h_{ƀ,i}\hat{w}_{ƀ,i}\sqrt{ƣ_{ƀ,ñ}^{i}p_{ƀ,ñ}}x_{ƀ,ñ}^{i} + \check{I}_{ƀ,ñ,i}^{1} + \check{I}_{ƀ,ñ,i}^{2} + \check{n}_{ƀ,i} \tag{5.2}$$

$$\check{I}_{ƀ,ñ,i}^{1} = h_{ƀ,i}\sum_{j=1,j\neq ñ}^{Ñ}\hat{w}_{ƀ,j}s_{ƀ,j} \tag{5.3}$$

$$\check{I}_{ƀ,ñ,i}^{2} = h_{ƀ,i}\hat{w}_{ƀ,i}\sum_{j=1}^{K_{ƀ,ñ}}\sqrt{ƣ_{ƀ,ñ}^{j}p_{ƀ,ñ}}\,x_{ƀ,ñ}^{j} \tag{5.4}$$

where $\hat{w}_{ƀ,i}$ is the precoding vector, $\check{n}_{ƀ,i} \sim CN(0,\sigma_{ƀ,i}^{2})$ is the additive white gaussian noise (AWGN) with zero mean and variance $\sigma_{ƀ,i}^{2}$ and $\check{I}_{ƀ,ñ,i}^{1}$ and $\check{I}_{ƀ,ñ,i}^{2}$ represents multi-cluster interference and intra-cluster interference of $u_{ƀ,ñ}^{i}$.

The SINR of signal received at $u_{ƀ,ñ}^{i}$ is given as

$$SINR_{ƀ,i} = \frac{ƣ_{ƀ,ñ}^{i}p_{ƀ,ñ}||h_{ƀ,i}\hat{w}_{ƀ,i}||^{2}}{\sum_{j=1,j\neq ñ}^{Ñ}p_{ƀ,j}||h_{ƀ,i}\hat{w}_{ƀ,j}||^{2}+\sum_{j=1}^{K_{ƀ,ñ}}ƣ_{ƀ,ñ}^{j}p_{ƀ,ñ}\left|\left|h_{ƀ,i}\hat{w}_{ƀ,i}\right|\right|^{2}+\sigma_{ƀ,ñ}^{2}} \tag{5.5}$$

Let B be bandwidth of channel employed at BS. The achievable rate at $u_{ƀ,ñ}^{i}$ according to the capacity model as given in [105], is given by

$$R_{ƀ,i} = \frac{B}{Ñ}log_{2}(1 + SINR_{ƀ,i}) \tag{5.6}$$

The total power consumption of $ƀ^{th}$ BS [112] is expressed as summation of transmit power and circuit power can be given as

$$Ṕ_{ƀ} = Ṕ_{ƀ}^{cir} + ȸ(\textstyle\sum_{ñ=1}^{Ñ}p_{ƀ,ñ}) \tag{5.7}$$

where ȸ is the drain efficiency of power amplifier, $P_{ƀ}^{cir}$ is the circuit power of BS ƀ which can be expressed as;

$$Ṕ_{ƀ}^{cir} = N_{B}Ṕ_{A} + N_{RF}Ṕ_{RF} + N_{B}Ṕ_{P} + Ṕ_{B} \tag{5.8}$$

where, $Ṕ_{A}$, $Ṕ_{RF}$, and $Ṕ_{P}$ is power consumption per power amplifier, per RF chain and per phase shifter respectively. $Ᵽ_{B}$ is power consumption of baseband. N_{RF} is number of RF chains. The energy efficiency is elucidated as ratio of achieved capacity to the total power consumption and can be given as

$$EE = \sum_{ƀ=1}^{ƀ+1}\frac{\sum_{ñ=1}^{Ñ}\sum_{i=1}^{K_{ƀ,ñ}}R_{ƀ,ñ}^{i}}{Ṕ_{ƀ}} \tag{5.9}$$

In this subsection, THz channel model and RF channel model is provided. In THz, the pathloss of non-line of sight (NLoS) link is considerably larger than line of sight (LoS) link hence, effect of NLoS link can be ignored [105]. The THz band channel gain [16] of $u_{ƀ,ñ}^{i}$ is given as

$$h_{ƀ,i}(f,đ) = \sqrt{N_B}(\sqrt{\frac{1}{L(f,đ)^{THz}}}Ʊα\left(\varphi_{ƀ,ñ}^{i}\right)) \quad (5.10)$$

here $L(f,đ)^{THz}$ signifies path loss at frequency f and at đ distance away from the BS, Ʊ represents the antenna gain, φ is angle of departure, α(φ) represents array steering vector which is given by

$$α(\varphi) = \frac{1}{\sqrt{N_B}}\left[1, \dots, e^{j\pi[nsin\varphi]}, \dots, e^{j\pi[(N_B-1)\sin\varphi]}\right]^T \quad (5.11)$$

In THz communication, the losses due to molecular absorption and spreading cannot be neglected. THz signal pathloss of at frequency f and at distance đ is given as

$$L(f,đ)^{THz}[dB] = 20\, log_{10}\left(\frac{4\pi}{\lambda_c}\right) + 10ʈ(f)đ\, log_{10}e \quad (5.12)$$

here $ʈ(f)$ is frequency dependent medium absorption coefficient, λ_c is wavelength of the carrier frequency. In THz band the atmospheric attenuation of water vapor molecules is considerably larger than that of other air molecules. Therefore, simplicity, in atmospheric attenuation only the effect of water molecules is considered in this paper, which is used in our simulation. The frequency absorption coefficient $ʈ(f)$ parameters are shown in [105].

Rayleigh fading channel model for RF, with Gaussian distribution of $h \sim CN(0, \varepsilon)$ [112] with zero mean and variance ε is considered in this paper. The channel gain for RF is given as

$$h_{ƀ,i} = 10^{-(L(đ)^{RF}/10)} \quad (5.13)$$

The pathloss for RF channel [112], at travelled distance đ is given as

$$L(đ)^{RF}[dB] = 148.1 + 37.6log_{10}(đ) \quad (5.14)$$

5.3 Proposed THz Blockage Alleviation (TBA) Method

Fig. 4.2 shows proposed TBA method. As THz signals cannot penetrate walls, buildings, trees, etc., they suffer from huge losses. TBA is utilized to overcome this issue in THz signals. TBA method encompasses SBS, users and device-to-device communication. In this method, the SBS transmits the superimposed signal in $ñ^{th}$ cluster. When direct signal from the SBS cannot reach the users due to blockages on the path the users in the cluster employ decode and forward method to redirect received signal to the next users. This helps to evade blockages in the path.

All the BSs employs NOMA. As NOMA, users with higher channel gain can decode the signal of users with lower channel gain through SIC, without any power allocation constraints. However, users with worse channel gain cannot decode signals of users with higher channel gain employing SIC. Thus, interference faced from signals of users with higher channel gain acts as intra-cluster interference. TBA method also aids in mitigating these interferences.

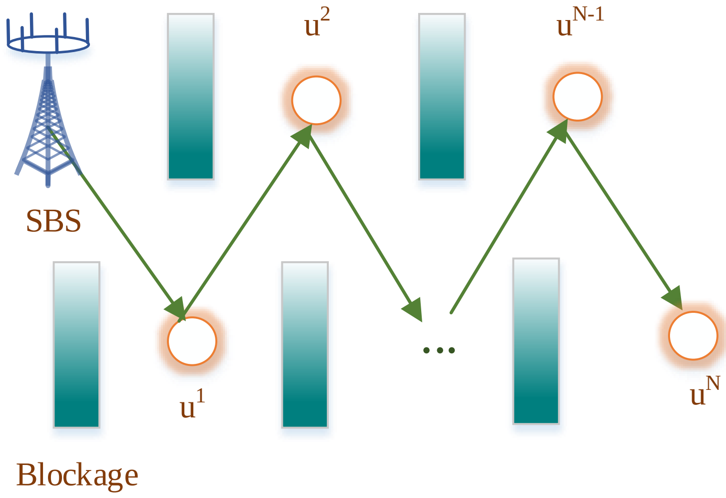

Fig. 5.2. THz Blockage alleviation method

The superimposed signal transmitted by $ƀ^{th}$ SBS to $ñ^{th}$cluster is given as in (1). The users in $ñ^{th}$cluster have channel gains ordered as $|h_{ƀ,1}|^2 \geq |h_{ƀ,2}|^2 \geq \cdots \geq |h_{ƀ,K_{ƀ,ñ}}|^2$. In TBA method, the $ɥ^1_{ƀ,ñ}$ receives the superimposed signal given as

$$\hat{y}_{ƀ,1} = h_{ƀ,1}\hat{w}_{ƀ,1}s_{ƀ,ñ}+\breve{I}_{ƀ,ñ,1} + \check{n}_{ƀ,1} \quad (5.15)$$

$$\breve{I}_{ƀ,ñ,1} = h_{ƀ,1}\sum_{j=1,j\neq ñ}^{Ñ}\hat{w}_{ƀ,j}s_{ƀ,j} \quad (5.16)$$

$\breve{I}_{ƀ,ñ,1}$ shows the inter cluster interference. Then $ɥ^1_{ƀ,ñ}$ employs SIC to obtain signals of users with weaker channel gains; $h_{ƀ,1}\hat{w}_{ƀ,1}\sum_{i=2}^{K_{ƀ,ñ}}\sqrt{ɋ^i_{ƀ,ñ}ƥ_{ƀ,ñ}}\,x^i_{ƀ,ñ}$ and subtracts it from the received signal $h_{ƀ,1}\hat{w}_{ƀ,1}(s_{ƀ,ñ} - \sum_{i=2}^{K_{ƀ,ñ}}\sqrt{ɋ^i_{ƀ,ñ}ƥ_{ƀ,ñ}}\,x^i_{ƀ,ñ}) + \breve{I}_{ƀ,ñ,1} + \check{n}_{ƀ,1}$ to obtain its signal; $h_{ƀ,1}\hat{w}_{ƀ,1}\sqrt{ɋ^1_{ƀ,ñ}ƥ_{ƀ,ñ}}x^1_{ƀ,ñ} + \breve{I}_{ƀ,ñ,1} + \check{n}_{ƀ,1}$. Thereafter, $ɥ^1_{ƀ,ñ}$ forwards the signal $\sum_{i=2}^{K_{ƀ,ñ}}\sqrt{ƥ_1}\,x^i_{ƀ,ñ}$ to $ɥ^2_{ƀ,ñ}$. Here, $ƥ_1$ is the transmission power of $ɥ^1_{ƀ,ñ}$. The signal received at $ɥ^2_{ƀ,ñ}$ is given as;

$$\hat{y}^2_{ƀ,ñ} = h^{1,2}_{ƀ,ñ}\hat{w}^{1,2}_{ƀ,ñ}\sum_{i=2}^{K_{ƀ,ñ}}\sqrt{ɋ^{1,i}_{1,ñ}ƥ_{1,ñ}}\,x^i_{ƀ,ñ}+\breve{I}_{ƀ,ñ,2} + \check{n}^{1,2}_{ƀ,ñ} \quad (5.17)$$

then $ɥ^2_{ƀ,ñ}$ employs SIC to obtain its signal and forwards $\sum_{i=3}^{K_{ƀ,ñ}}\sqrt{ɋ^i_{2,ñ}ƥ_{2,ñ}}\,x^i_{ƀ,ñ}$ to $ɥ^3_{ƀ,ñ}$. In this way, each user employs decode and forward method and the signals of users with highest channel gain are removed from the received signal. The $K_{ƀ,ñ}{}^{th}$ user need not apply SIC as the signal received at $K_{ƀ,ñ}{}^{th}$ user is given as

$$\hat{y}^{K_{ƀ,ñ}}_{ƀ,ñ} = h^{K_{ƀ,ñ}-1,K_{ƀ,ñ}}_{ƀ,ñ}\sqrt{ɋ^{K_{ƀ,ñ}}_{K_{ƀ,ñ}-1,ñ}ƥ_{K_{ƀ,ñ}-1,ñ}}x^{K_{ƀ,ñ}}_{ƀ,ñ}) + \breve{I}_{ƀ,ñ,K_{ƀ,ñ}} + \check{n}^{K_{ƀ,ñ}-1,K_{ƀ,ñ}}_{ƀ,ñ} \quad (5.18)$$

This eliminates the interference from signals of users with higher channel gain which perform as intra-cluster interference. Then, the signal received by each user in $ñ^{th}$cluster of $ƀ^{th}$ SBS after SIC in matrix form is given by

$$\begin{bmatrix} \hat{y}_{ƀ,ñ}^{1} \\ \hat{y}_{ƀ,ñ}^{2} \\ \vdots \\ \hat{y}_{ƀ,ñ}^{K_{ƀ,ñ}} \end{bmatrix} = \begin{bmatrix} \hat{w}_{ƀ,ñ}^{ƀ,1} \\ \hat{w}_{ƀ,ñ}^{1,2} \\ \vdots \\ \hat{w}_{ƀ,ñ}^{K_{ƀ,ñ}-1,K_{ƀ,ñ}} \end{bmatrix} \begin{bmatrix} h_{ƀ,ñ}^{ƀ,1} \\ h_{ƀ,ñ}^{1,2} \\ \vdots \\ h_{ƀ,ñ}^{K_{ƀ,ñ}-1,K_{ƀ,ñ}} \end{bmatrix} \begin{bmatrix} x_{ƀ,ñ}^{1} & x_{ƀ,ñ}^{2} & \cdots & x_{ƀ,ñ}^{K_{ƀ,ñ}} \end{bmatrix} + \begin{bmatrix} \breve{I}_{ƀ,ñ,1} \\ \breve{I}_{ƀ,ñ,2} \\ \vdots \\ \breve{I}_{ƀ,ñ,K_{ƀ,ñ}} \end{bmatrix} + \begin{bmatrix} \check{n}_{ƀ,ñ}^{ƀ,1} \\ \check{n}_{ƀ,ñ}^{1,2} \\ \vdots \\ \check{n}_{ƀ,ñ}^{K_{ƀ,ñ}-1,K_{ƀ,ñ}} \end{bmatrix} \quad (5.19)$$

The SINR is described as ratio of received power and summation of noise power and interference power. Evidently, the TBA method reduces the interference power by eliminating intra-cluster interference. Therefore, this method avoid blockages, as well improves SINR and supports enhancement in the achievable rates.

5.4 Proposed Modified Cooperative NOMA (MCN)

Optimal use of energy resources is prime important in designing 6G communication systems. This section elaborates proposed MCN scheme to efficiently utilize the system's energy. Many a time, users at the cell border are incapable of receiving direct signals from the BS. In such cases, cooperative communication plays a major role in aiding communication, saving BS's energy, enhancing the cell coverage, and improving system reliability.

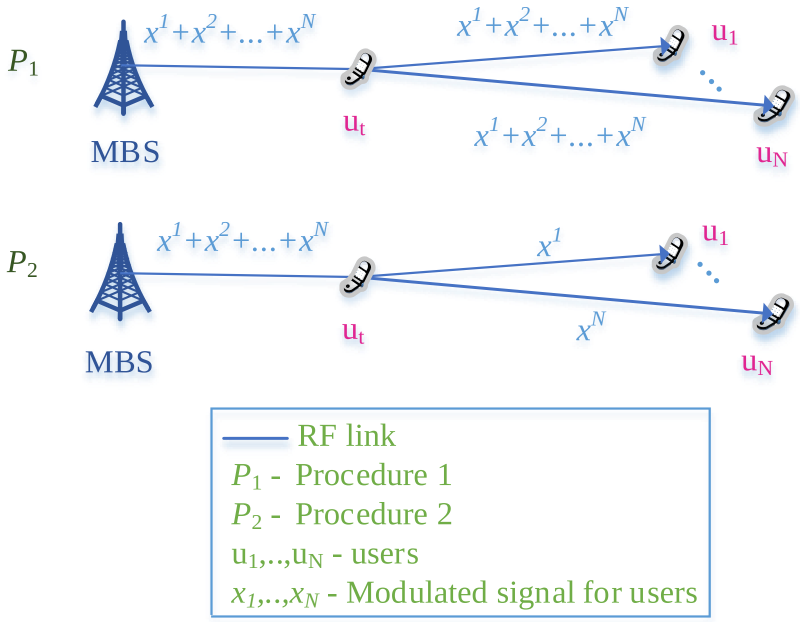

Fig. 5.3. Modified cooperative NOMA.

Fig. 5.3 shows modified cooperative NOMA. The $ñ^{th}$cluster in MBS is assumed to be at the cell edge and unable to form direct communication links with the MBS. Then, the MBS transmits the superimposed signal for ñ^{th}cluster to a nearby user $\text{ɥ}^t_{\text{Ƀ}+1}$. The rate at which the signal for $\text{ɥ}^i_{\text{Ƀ}+1,\text{ñ}}$ reaches $\text{ɥ}^t_{\text{Ƀ}+1}$ is given as

$$R^i_{\text{Ƀ}+1,\text{t}} = Blog_2\left(1 + \frac{\text{ɋ}^i_{\text{Ƀ}+1,\text{ñ}}\text{p}_{\text{Ƀ}+1,t}||h_{\text{Ƀ}+1,\text{t}}\hat{\text{w}}_{\text{Ƀ}+1,t}||^2}{\sum_{j=1}^{K_{\text{Ƀ}+1,\text{ñ}}} \text{ɋ}^j_{\text{Ƀ}+1,\text{ñ}}\text{p}_{\text{Ƀ}+1,t}\left||h_{\text{Ƀ}+1,\text{t}}\hat{\text{w}}_{\text{Ƀ}+1,t}\right||^2 + \sigma^2_{\text{Ƀ}+1,t}}\right) \tag{5.20}$$

Then, $\text{ɥ}^t_{\text{Ƀ}+1}$ forwards the signal for ñ^{th}cluster following either procedure P_1 or P_2. If the power level; ƥ_t of $\text{ɥ}^t_{\text{Ƀ}+1}$ is less than 50% of its maximum power then the procedure P_1 is employed, and if it is more than equal to 50% of its maximum power then the procedure P_2 is employed. In the procedure P_1 the user $\text{ɥ}^t_{\text{Ƀ}+1}$ amplifies and forwards the superimposed signal to the ñ^{th}cluster. The signal received at $\text{ɥ}^i_{\text{ƀ},\text{ñ}}$ via procedure P_1 is given as

$$\hat{\text{y}}_{t,i} = h_{t,i}\hat{\text{w}}_{t,i}\sqrt{\text{ƥ}_{t,i}}x^i_{\text{Ƀ}+1,\text{ñ}} + \check{\text{I}}^1_{\text{t},i} + \check{\text{I}}^2_{\text{t},i} + \check{\text{n}}^i_{\text{t},i} \tag{5.21}$$

$$\check{\text{I}}^1_{\text{t},\text{ñ},i} = h_{t,i}\sum_{j=1,j\neq\text{ñ}}^{\text{Ñ}} \hat{\text{w}}_{t,j}s_{\text{Ƀ}+1,\text{j}} \tag{5.22}$$

$$\check{\text{I}}^2_{t,\text{ñ},i} = h_{t,i}\hat{\text{w}}_{t,i}\sum_{j=1}^{K_{\text{Ƀ}+1,\text{ñ}}} \sqrt{\text{ƥ}_{t,j}}\, x^j_{\text{Ƀ}+1,\text{ñ}} \tag{5.23}$$

here $\text{ƥ}_{t,i}$ is the transmission power of $\text{ɥ}^t_{\text{Ƀ}+1}$ used in transmitting signal to $\text{ɥ}^i_{\text{ƀ},\text{ñ}}$. The SINR from $\text{ɥ}^t_{\text{Ƀ}+1}$ to $\text{ɥ}^i_{\text{ƀ},\text{ñ}}$ via P_1 is expressed as

$$SINR_{t,i} = \frac{\text{ƥ}_{t,i}||h_{t,i}\hat{\text{w}}_{t,i}||^2}{\sum_{j=1,j\neq\text{ñ}}^{\text{Ñ}} \hat{\text{w}}_{t,j}||h_{t,i}\hat{\text{w}}_{t,j}||^2 + \sum_{j=1}^{K_{\text{Ƀ}+1,\text{ñ}}} \text{ƥ}_{t,j}\left||h_{t,i}\hat{\text{w}}_{t,j}\right||^2 + \sigma^2_{t,i}} \tag{5.24}$$

As $\text{ɥ}^t_{\text{Ƀ}+1}$ has higher channel gain than the users in ñ^{th}cluster, $\text{ɥ}^t_{\text{Ƀ}+1}$ can decode messages of users in ñ^{th}cluster. In procedure P_2 the user $\text{ɥ}^t_{\text{Ƀ}+1}$ decodes the messages of the users in ñ^{th}cluster and forwards them the decoded messages. The signal received at $\text{ɥ}^i_{\text{ƀ},\text{ñ}}$ via procedure P_2 is expressed as

$$\hat{\text{y}}_{t,i} = h_{t,i}\hat{\text{w}}_{t,i}\sqrt{\text{ƥ}_{t,i}}x^i_{\text{Ƀ}+1,\text{ñ}} + \check{\text{I}}_{t,i} + \check{\text{n}}^i_{\text{t},i} \tag{5.25}$$

$$\check{\text{I}}_{t,i} = h_{t,i}\sum_{j=1,j\neq\text{ñ}}^{\text{Ñ}} \hat{\text{w}}_{t,j}s_{\text{Ƀ}+1,\text{j}} \tag{5.26}$$

The intra-NOMA interference in procedure P_2 has been cancelled. Therefore, the SINR from $\text{ɥ}^t_{\text{Ƀ}+1}$ to $\text{ɥ}^i_{\text{ƀ},\text{ñ}}$ is improved and is expressed as

$$SINR_{t,i} = \frac{\text{ƥ}_{t,i}||h_{t,i}\hat{\text{w}}_{t,i}||^2}{\sum_{j=1,j\neq\text{ñ}}^{\text{Ñ}} \hat{\text{w}}_{t,j}||h_{t,i}\hat{\text{w}}_{t,j}||^2 + \sigma^2_{t,i}} \tag{5.27}$$

The achievable rate from $\text{ɥ}^t_{\text{Ƀ}+1}$ to $\text{ɥ}^i_{\text{ƀ},\text{ñ}}$ is given by

$$R_{t,i} = \frac{B}{\text{Ñ}}log_2(1 + SINR_{t,i}) \tag{5.28}$$

The rate from MBS to $ų^{i}_{ƀ,ñ}$ according to decode and forward protocol [22] is given as

$$R_{Ƀ+1,i} = \frac{1}{2} min\{R^{i}_{Ƀ+1,t}, R_{t,i}\} \tag{5.29}$$

The total power consumption of $ų^{t}_{Ƀ+1}$ used in transmitting signal to $ų^{i}_{ƀ,ñ}$ expressed as summation of transmit power and circuit power can be given as

$$Ṕ_{ų} = Ṕ^{cir}_{ų} + ɘƥ_{t,i} \tag{5.30}$$

here of $ɘ$ is the drain efficiency of the user amplifier. The user circuit power $Ṕ^{cir}_{ų}$ is used in detecting, decoding and regenerating the signals. In P_1 the $ų^{t}_{Ƀ+1}$ detects and regenerates the signal, save it's the decoder energy. In P_2 the $ų^{i}_{Ƀ+1,ñ}$ detects the signal, save it's the decoder and regenerator energy. The total energy efficiency is defined as ratio of the archived data rate of the signal and the energy consumed in transmitting the signal. The MCN aids in mitigating interference and hence, enchaining the SINR and data rate. The cooperative NOMA system helps in reducing the transmission power at the BS. The circuit power at the user $ų^{t}_{Ƀ+1}$ is efficiently utilized in MCN through two proposed procedures P_1 and P_2 for signal transmission. In procedures P_2 the power level of $ų^{t}_{Ƀ+1}$ is more than 50% therefore, it efficiently aids in decoding the messages and the decoder circuit power is reduced at the users in $ñ^{th}$cluster. The MCN also aids enhancing energy efficiency of the system.

5.5 Simulation results

This section studies the efficiency of the proposed TBA and MCN in the considered downlink hybrid system model where TBA method and THz channel is employed at smallcells, and MCN and RF channel is employed at macrocell. The system results with proposed methods are labeled as 'TBA MCN THz RF'. The performance of the proposed scheme is compared with 'TBA MCN mmWave RF' where in the mmWave is employed at the smallcells in place of THz band, 'Basic THz RF' where in a THz band is employed at the smallcells and RF band is employed at the macrocell in a conventional downlink HetNet model and 'Basic mmWave RF' where mmWave band is employed at the smallcells and RF band is employed at the macrocell in a conventional downlink HetNet model. The comparative analysis is carried out between these four models in terms of sum rate, power consumption and energy efficiency.

The BSs are assumed at the center of the cell, and SBS within the coverage of MBS. It is assumed that the users are dispersed randomly throughout the cell inside the range of their associated BS. In this simulation, the number of SBSs S is taken as 3, the radius of MBS and SBS is set to 500 m and 5 m respectively. The number of antennas at each BS N_B is taken as 100. The carrier frequency of the THz, mmWave and RF band is taken as 0.34 THz, 73 GHz, and 2 GHz. The bandwidth B of THz, mmWave and RF channel is set as 10 GHz, 1 GHz, and 10 MHz. The minimum distance between the suers is set as 0.1 m. The maximum transmission power of MBS, THz SBS, mmWave SBS and user is taken as 42.7 dBm, 36.99 dBm, 30 dBm, and 10 dBm respectively. The power consumption per power amplifier $\acute{P}_A$, per RF chain $\acute{P}_{RF}$, baseband $Ꝑ_B$, and per phase shifter $\acute{P}_P$ is set as 160 mW, 20 mW, 200 mW, and 40 mW respectively. The amplifier drain efficiency ȸ is set as 0.75%. The noise power $\sigma^2_{ƀ,i}$ is set to -174 dBm/Hz.

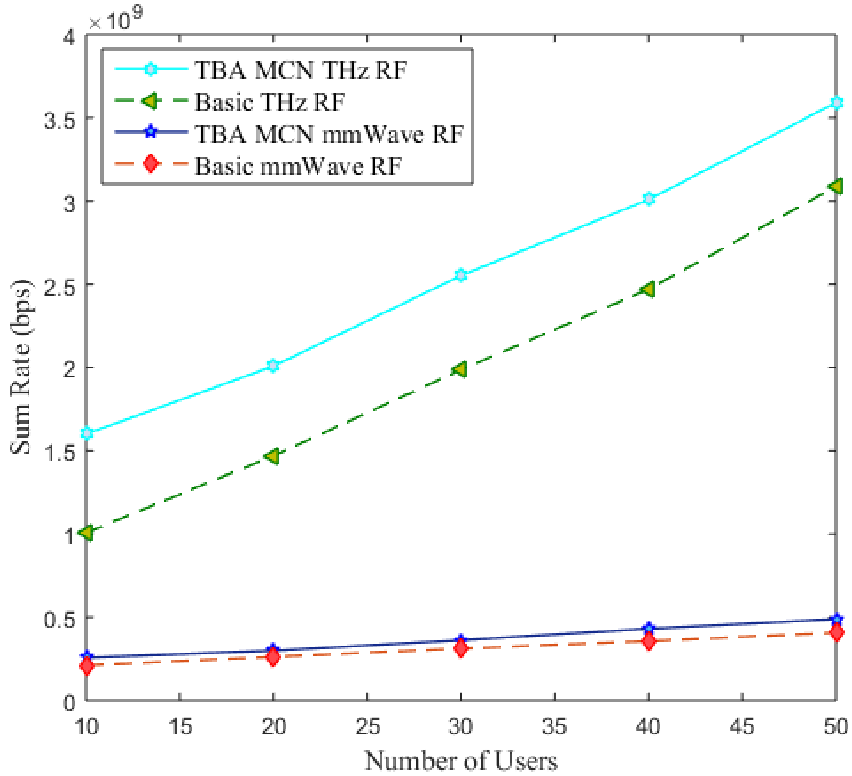

Fig. 5.4. Sum Rate v/s Number of users in a cell.

Fig. 5.4 shows the comparison of sum rate between the four aforementioned system models. From Fig. 5.4 it can be seen that the sum rate surges with the number of users and the sum rate of 'TBA MCN THz RF' is higher than 'Basic THz RF'. This is mainly due to TBA and MCN methods. The TBA method the used to avoid blockages also mitigates the intra-cluster interference, which aids in improving SINR and hence, the sum rates. On the other hand, one of the procedures in the MCN mitigates the intra-NOMA interference so, the SINR increases consequently the sum rate also improves. Further, the sum rates of 'TBA MCN THz RF' and 'Basic THz RF' are superior than 'TBA MCN mmWave RF' and 'Basic mmWave RF' this is due to larger bandwidth available in THz bands than mmWave bands.

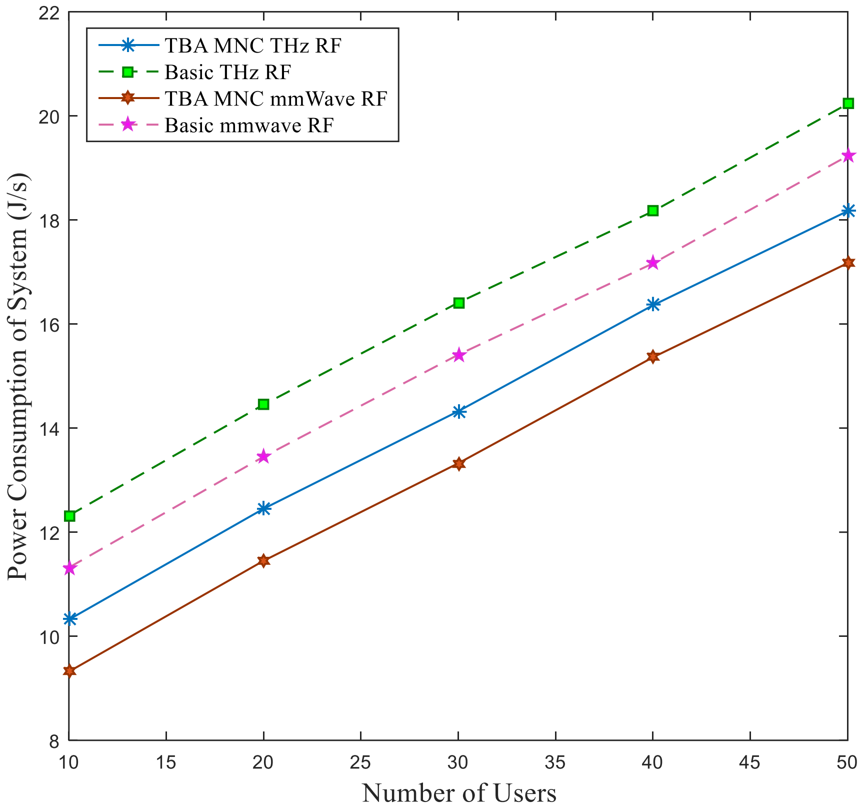

Fig. 5.5. Power consumption of system v/s Number of users.

Fig. 5.5 shows the comparison of system's power consumption of four HetNet models employing different methods for downlink signal communication and power consumption increases with increase in number of users. It can be seen from Fig. 5.5 that the power consumption of the 'Basic THz RF' and 'Basic mmWave RF' systems is more than the power consumption of the proposed 'TBA MCN THz RF' and 'TBA MCN mmWave RF' systems. As it can be seen from Fig. 5.5 the power consumption of 'TBA MCN THz RF' is less than 'Basic mmWave RF' and 'Basic THz RF'. This is due to the TBA and MCN aids in reducing the transmission load of the BS, as with the employment of cooperative methods, the BS requires smaller amount of power to transmit the superimposed signal to user which is comparatively nearer to BS. This aids in saving the BS power. Moreover, with MCN decoder circuit power consumption of users in $\tilde{n}^{th}$cluster is reduced in procedure P_2, this also aids in reducing the power consumption at the users' side. This shows that the power consumption of the system is affected by the proposed techniques and not by the carrier frequency used in the small cell.

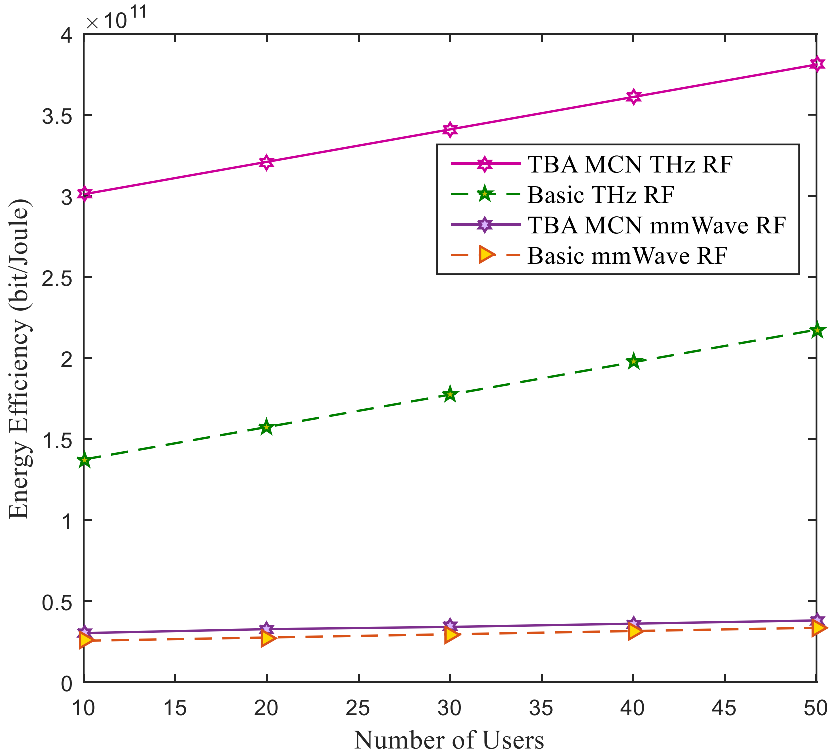

Fig. 5.6. Energy Efficiency v/s Number of users.

Fig. 5.6 shows the comparison of energy efficiency between the four system models. The total power consumption is defined as ratio of the archived data rate of the signal and the energy consumed in transmitting the signal. The proposed MCN aids in mitigating interference and hence, enchaining the SINR and data rate. When compared with the other models the Fig. 5.4 shows that the sum rate of the proposed 'TBA MCN THz RF' is higher and Fig. 5.5 depicts that its power consumption is least. Therefore, the energy efficiency of 'TBA MCN THz RF' is superior than the other systems. This is due power saving to efficient utilization of the system energy with MCN. The energy efficiency of 'TBA MCN mmWave RF' and 'Basic mmWave RF' are low as compared to 'Basic THz RF' and proposed 'TBA MCN THz RF'. This is due to larger bandwidth available in THz bands than mmWave bands can accommodate higher rates as can also be seen from Fig. 5.4.

CHAPTER 6

IMPLEMENTATION OF AN EFFICIENT USER CLUSTERING APPROACH IN HYBRID MILLIMETER-WAVE MASSIVE-MIMO NOMA WITH D2D ENABLED BEYOND 5G SMALL-CELL NETWORK USING ANTENNA ANGLE BOUND CLUSTERING TECHNIQUE

In this chapter, an efficient user clustering approach in hybrid millimeter-wave massive-MIMO NOMA with D2D enabled beyond 5G small-cell network using antenna angle bound clustering technique is implemented. This chapter first, design a 6G hybrid system model employing THz communication, mMIMO, cooperative NOMA, and device-to-device (D2D) communication with macrocells and small cells. Thereafter, this chapter propose Antenna Angle Bound (AAB) clustering technique to enhance the sum rate of the proposed 6G hybrid system model. The proposed ABB clustering technique employs antenna parameters such as beam angle and beamwidth to form clusters and mitigate interference. This chapter analyze simulation results to validate the superior performance of the proposed 6G hybrid system model in assessment with traditional models.

6.1 Introduction

So far, wireless communication networks are driven by the requirements of high data rates. This gave rise to the need for a thousand-time capacity escalation and spectrum scarcity [115]. The 6G wireless communication systems are anticipated to support simultaneously massive devices with different capabilities and needs. In comparison with conventional mobile broadband users, the scenarios of massive machine-type connectivity (mMTC), Internet of Everything (IoE), and ultra-reliable low latency communication (URLLC) are anticipated to fetch various types of connected devices into the network [116]. The 6G needs to support the high requirements of capacity enlargement which requires high spectrum resources. Exploring high frequencies like millimeter wave (mmWave) and Terahertz (THz) band opens an abundant spectrum for communication. The THz band ranges from 0.1 THz to 10 THz [117], which is three-four orders higher than the radio frequency (RF) band. this offers a huge spectrum. Apart from spectrum widening THz offers many other advantages therefore, it is a promising 6G technology. These benefits include robust confidentiality, supporting 100 Gbps or more data rates, high anti-interference capability, capable of supporting large capacity, communication security due to short pulse duration and narrow beam, has good directivity, and are appropriate for a few special scenarios as attenuates less thru penetrating few materials [118]. These features enable the use of THz in numerous ultra-high-speed short-range based 6G communications. The atmospheric and molecular attenuation of THz is higher than the conventional RF band however, by enhancing the transmitting and receiving antenna gains the THz communication can still achieve higher data rates for a short distance. To achieve high data rates with high energy efficiency in 6G communication networks, the non-orthogonal multiple access (NOMA) and massive multi-input multi-output (mMIMO) [119]-[121] are also required.

To support high data traffic, the NOMA concept was first suggested in [122] for wireless communication. Lately, NOMA has enticed significant interest of researchers and has been recommended for impending heterogeneous networks (HetNet) [123] and dense wireless communication networks [124]. The principal notion behind the working of NOMA is to employ the difference in the strength of the signal shaped by suitable power allocation and SIC to realize high performance. NOMA is a key multiplexing technique to enhance spectrum efficiency in 6G. In NOMA, the number of users is divided into groups. The channel gain of a group of users is arranged in decreasing order. In power division NOMA each user functions in the same time/frequency block where they are differentiated by their power levels. The power division NOMA allocates power to the signals of the user in the same order as their channel gains. Thereafter, NOMA superimposes signals for a group of users. Then, NOMA allocates a single resource block to a group of users and transmits the superimposed signal to the group of users. In this way, using the same resource block signals are transmitted to a group of users. The multiple access interference in the NOMA is eliminated for the user with lower allocated power through successive interference cancellation (SIC). The user with higher allocated power faces interference with the signals of the users with lower allocated power. The SIC successively cancels interference caused by the signal of higher allocated power [125]. First, the signal with the highest allocated power is detected, and then it is reconstructed. The reconstructed signal is then subtracted from the superimposed signal eliminating the interference caused by the signal with the highest power. In this way, the NOMA serves a group of users using the same time/frequency block. Therefore, NOMA can enhance spectral efficiency and consequently, it also can improve system throughput.

6.2 System Model

The proposed hybrid 6G system model is shown in Fig. 6.1. From the Fig. 6.1 it can be seen that there are three small cells inside a macro cell, having their respective base station (BS) at the center employing mMIMO NOMA. Each BS has N_T transmitting antennas. The small cells employ the proposed dynamic sectorization technique. $Ɓ = \{1, 2, .., b, .., B, B+1\}$ defines the set of BSs, where $\{1, 2, \dots, B\}$ are small cell base stations (SBS)s and is $b+1$ is the macro base station (MBS). $Ų = \{U_1, U_2, \dots, U_b, \dots, U_{b+1}\}$ defines the set of users. U_b comprises two types of users, D2D pairs and cellular users. Let the total number of cellular users in each cell be Ñ, and let there be total L clusters of cellular users in each BS. However, if the user density enormously varied throughout the cell, then areas with a higher density of users suffer from deprived services, and such approaches become incompetent.

Remark 6.1: *The transmit power of SBS earmarked for each user in D_n is $Ƿ_{D_n}$. The SBS uses NOMA therefore, the transmit power for each user will depend on its channel gain.*

To increase the efficiency of the proposed 6G system the small cells perform dynamic sectorization. The notations used in the paper are shown in Table II. In the traditional approaches, the cell is divided into Ɲ number of sectors. The set sectors in the small cell under SBS b are defined as $D_b =$

$\{D_{b,1}, D_{b,2}, \dots D_{b,n}, \dots, D_{b,\mathrm{N}}\}$. Each sector in the traditional approach of BS b is at an angle $Æ_{D_{b,n}}$ and distribute the power of the BS equally into the sectors, such as $Æ_{D_{b,n}} = \frac{360°}{\mathrm{N}}$. If the total transmit power of SBS b is denoted by $\mathfrak{p}_b$, in the traditional approaches the transmit power of SBS is divided into the sectors as $\mathfrak{p}_{D_{b,n}} = \frac{\mathfrak{p}_b}{\mathrm{N}}$ and the SBS transmits power earmarked for each user in D_n is $p_{D_{b,n}} = \frac{\mathfrak{p}_{D_{b,n}}}{Ú_{D_{b,n}}}$, where $Ú_{D_{b,n}}$ is the number of users in D_n. All BSs are anticipated to have impeccable channel state information (CSI) of the users. In the proposed 6G system with a dynamic sectorization technique, the SBS calculates the $Æ_{D_{b,n}}$ and $\mathfrak{p}_{D_{b,n}}$ according to the user density inside the small cell, to deliver fair services throughout the cell regardless of whether the user is in a crowded area or deserted area in the cell.

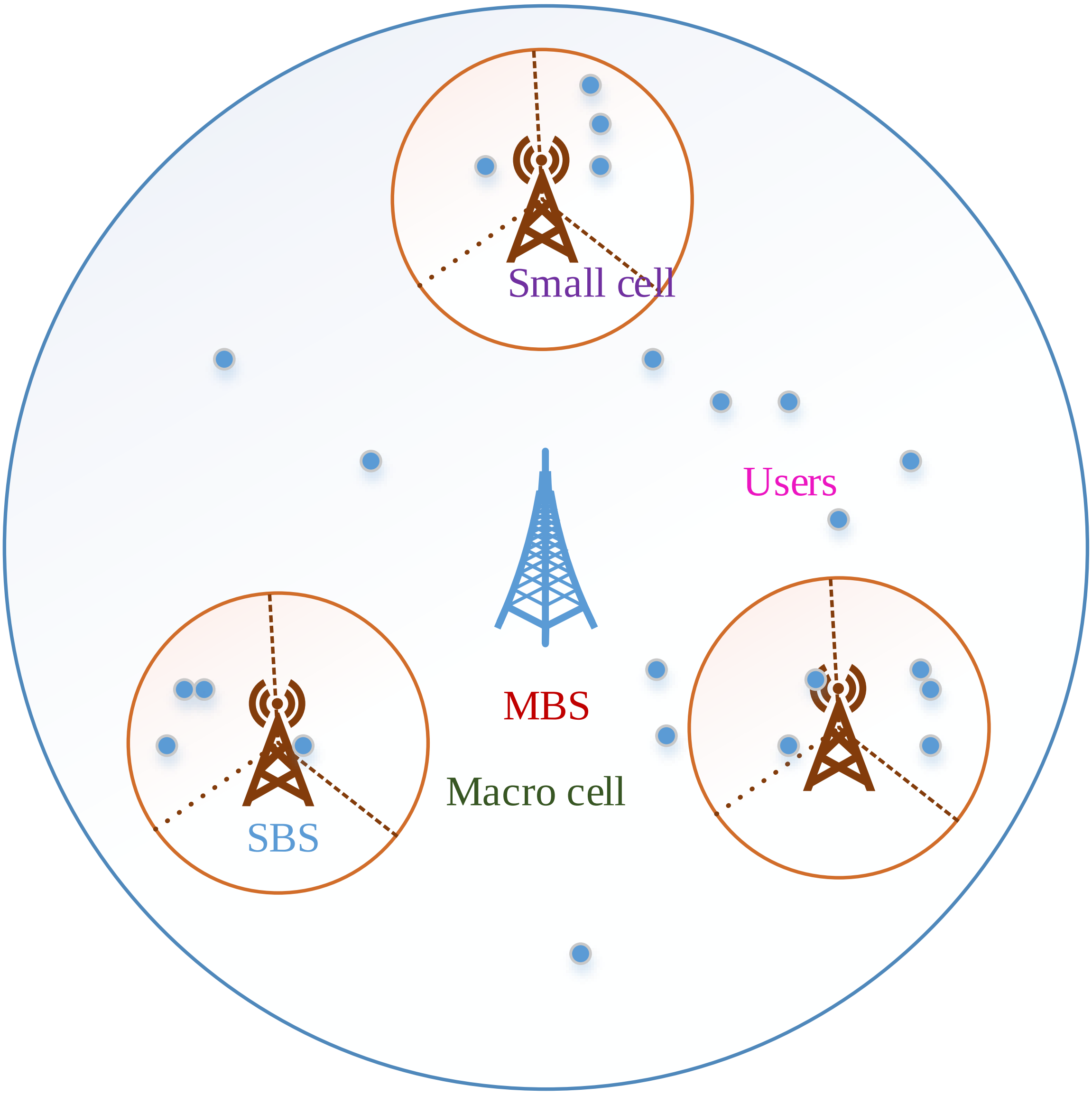

Fig. 6.1. Proposed 6G hybrid system model.

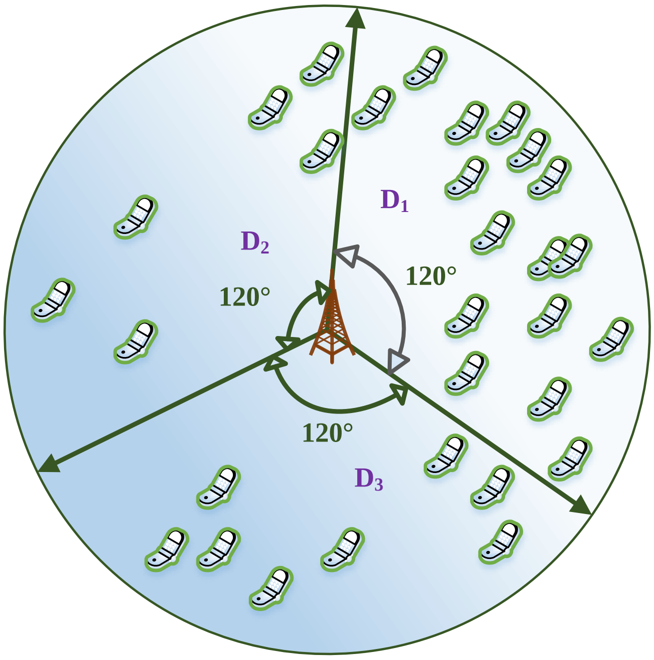

Fig. 6.2. Traditional sectorization approach.

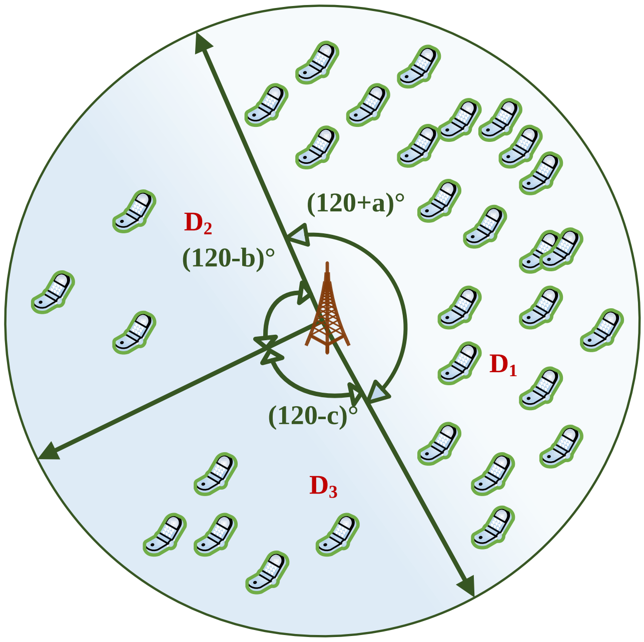

Fig. 6.3. Dynamic sectorization approach.

TABLE 6.1: NOTATIONS

N_T	Transmitting antennas at each BS
Ɓ	Set of BSs
Ų	Set of Users
Ş	Set of small cell sectors
$Æ_{D_{b,n}}$	Angle of sector $D_{b,n}$
$Ú_{D_{b,n}}$	Number of users in the sector $D_{b,n}$
$Ƥ_b$	Total transmit power of b^{th} BS
Ñ	Total number of users in each cell
$u_{b,n,l}^i$	i^{th} user in l^{th}cluster in sector $D_{b,n}$of b^{th} BS
$M_{b,n,l}$	Number of users in l^{th}cluster in $D_{b,n}$ sector of b^{th} BS
$a_{b,n,l}^i$	Power allocation coefficient of $u_{b,n,l}^i$
$z_{b,n,l}$	The set of user signals in l^{th}cluster in $D_{b,n}$ sector of b^{th} BS

$v_{b,n,l}^{i}$	Additive white Gaussian noise at $u_{b,n,l}^{i}$
$h_{b,n,l}^{i}$	Downlink channel of $u_{b,n,l}^{i}$
$y_{b,n,l}^{i}$	Received signal at $u_{b,n,l}^{i}$
$\text{q}_{b,\text{n},w,f}$	Transmit power of cellular user $u_{b,n}^{w}$ for f^{th} D2D pair
ξ	Amplifier inefficiency
$SINR_{b,n,l}^{i}$	SINR of $u_{b,n,l}^{i}$
$R_{b,n,l}^{i}$	Achievable rate at $u_{b,n,l}^{i}$
Ƥ_{b+1}	Total power consumption of MBS
$\text{p}_{b,n}$	Total power consumption of $D_{b,n}$ sector of b^{th} BS

To assure fair services to all the users the proposed 6G system with dynamic sectorization alters sector angles according to the user density and assets greater transmission power for the compactly inhabited areas in the cell, and smaller transmit power for low-density areas of the cells. Fig. 6.2 and Fig 6.3 show traditional and dynamic sectorization approaches. It can be seen from the Fig. 6.3 that the angle and area of sectors D_2 and D_3 is reduced and D_1 is increased concerning Fig 6.2. In the dynamic sectorization the sector angle is calculated as

$$\text{Æ}_{D_{b,n}} = \frac{360*\text{Ú}_{D_{b,n}}}{\text{Ñ}} \tag{6.1}$$

Subsequently, with new sector angles the sector area and the number of users inside each sector change. Now, the transmit power earmarked for $D_{b,n}$ is given by

$$\text{p}_{D_{b,n}} = \frac{\text{p}_{b}*\text{Ú}_{D_{b,n}}}{\text{Ñ}} \tag{6.2}$$

In the dynamic sectorization, the transmit power earmarked for each user in $D_{b,n}$ is

$$p_{D_{b,n}} = \frac{\text{p}_{D_{b,n}}}{\text{Ú}_{D_{b,n}}} \tag{6.3}$$

By putting the value of $\text{p}_{D_{b,n}}$ from equation (2), equation (3) becomes

$$p_{D_{b,n}} = \frac{\text{p}_{b}}{\text{Ñ}} \tag{6.4}$$

The equation (4) proves that in contrast with traditional approaches the dynamic sectorization earmarks the same transmit power for each user unrelatedly density variations in the small cell, and proficiently exploits the SBS energy without enhancing the complexity.

The i^{th} cellular user in l^{th}cluster in sector D_n of b^{th} BS is represented as $u_{b,n,l}^{i} \in U_b$. Let l^{th}cluster in $D_{b,n}$ sector of b^{th} BS contain $M_{b,n,l}$ users. Then the signal transmitted by b^{th} BS through NOMA is given as

$$x_{b,n,l} = \sum_{i=1}^{M_{b,n,l}} \sqrt{a_{b,n,l}^{i}\text{p}_{b,\text{n},l}}\, z_{b,n,l}^{i} \tag{6.5}$$

here $a_{b,n,l}^{i}$ denotes the power allocation coefficient, $z_{b,n,l} = \{z_{b,n,l}^{1}, z_{b,n,l}^{2}, \dots, z_{b,n,l}^{M_{b,n,l}}\}$ represent set of signals, and $\mathrm{p}_{b,n,l}$ represents the transmit power for l^{th}cluster in $D_{b,n}$ sector of b^{th} BS.

Remark 6.2*: For each cluster,* $\sum_{i=1}^{L} \mathrm{p}_{b,n,l} \leq \mathrm{p}_{b}$ *is the condition put on* $\mathrm{p}_{b,n,l}$.

Then, the received signal at $u_{b,n,l}^{i}$ is given by

$$y_{b,n,l}^{i} = h_{b,n,l}^{i} w_{b,n,l} \sqrt{a_{b,n,l}^{i} \mathrm{p}_{b,n,l}} z_{b,n,l}^{i} + I_{b,n,l,i}^{1} + I_{b,n,l,i}^{2} + I_{b,n,l,i}^{3} + v_{b,n,l}^{i} \quad (6.6)$$

$$I_{b,n,l,i}^{1} = h_{b,n,l}^{i} \sum_{j=1, j \neq l}^{L} w_{b,n,j} x_{b,n,j} \quad (6.7)$$

$$I_{b,n,l,i}^{3} = h_{b,n,l}^{i} w_{b,n,l} \sum_{j=1}^{M_{b,n,l}} \sqrt{a_{b,n,l}^{j} \mathrm{p}_{b,n,l}}\, z_{b,n,l}^{j} \quad (6.8)$$

where, $v_{b,n,l}^{i} \sim CN(0, \sigma_l^2)$ is the additive white gaussian noise (AWGN) with zero mean and variance σ_l^2, $w_{b,n,l}$ denotes the precoding vector. $I_{b,n,l,i}^{1}$ and $I_{b,n,l,i}^{3}$ respectively signifies the inter-cluster interference and intra-cluster interference at $u_{b,n,l}^{i}$. As THz performed better at short distances in the proposed system the SBS employs the THz band for communications and the macro cell employs the RF band for communication. The inter-cell interference between the macro cell and small cells in the proposed system is mitigated due to the employment of different channels. Moreover, the small cells are placed in such a way that the interference amongst them is also alleviated.

The cellular users forward the signals to the D2D pairs, by clustering them through the proposed AAB scheme. Let there be W cellular users that act as relays. Consequently, the total number of D2D clusters turns out to be W. The set of D2D pairs is signified by $\text{Đ} = \{d_1, d_2, \dots, d_f, \dots d_F\}$ where, d_f is f^{th} D2D pair. Let the total number of D2D pairs in the cluster of w^{th}cluster of $D_{b,n}$ sector of b^{th} BS be $F_{b,n,w}$. The signal forwarded by the $u_{b,n,l}^{w}$ cellular user for d_f be expressed as

$$x_{b,n,w,f} = \sum_{i=1}^{F_{b,n,w}} \sqrt{a_{b,n,w}^{f} \mathrm{q}_{b,n,w,f}}\, z_{b,n,w}^{f} \quad (6.9)$$

Then, the received signal at $u_{b,n,l}^{i}$ is given by

$$y_{b,n,w,f} = h_{b,n,w,f} w_{b,n,w,f} \sqrt{a_{b,n,w}^{f} \mathrm{q}_{b,n,w,f}} z_{b,n,w}^{f} + I_{b,n,w,f}^{1} + I_{b,n,w,f}^{2} + \eta_{b,n,w,f} \quad (6.10)$$

$$I_{b,n,w,f}^{1} = h_{b,n,w,f} \sum_{i=1, i \neq w}^{\mathrm{W}} w_{b,n,i,f} x_{b,n,i,f} \quad (6.11)$$

$$I_{b,n,w,f}^{2} = h_{b,n,w,f} w_{b,n,w,f} \sum_{j=1}^{F_{b,n,w}} \sqrt{a_{b,n,w}^{j} \mathrm{q}_{b,n,w,f}} z_{b,n,w}^{j} \quad (6.12)$$

where $h_{b,n,w,f}$ signifies the THz channel and $w_{b,n,w,f}$ is the denotes vector of d_f. $\mathrm{q}_{b,n,w,f}$ is the transmit power of $u_{b,n}^{w}$ for d_f, $\eta_{b,n,w,f} \sim CN(0, \sigma_f^2)$ is the AWGN with variance σ_f^2. $I_{b,n,w,f}^{1}$ and $I_{b,n,w,f}^{2}$ respectively signifies inter-cluster and intra-cluster interference.

The RF channel with Gaussian distribution of $h \sim CN(0, \dagger)$ [105] with zero mean and $\dagger$ variance. Channel gain for RF channel is expressed as

$$h_{b,n,l}^{i} = 10^{-(V(d)/10)} \tag{6.13}$$

The RF channel path loss [105], at d (km) from the transmitter, is given as

$$V(d)[dB] = 148.1 + 37.6\, log_{10}(d) \tag{6.14}$$

where $\gamma(f, d)$denotes path loss at d distance away from the BS at frequency f,ω represents the antenna gain, φ signifies the angle of departure. ß(φ) represents the array steering vector, and it is calculated as

$$ß(\varphi) = \frac{1}{\sqrt{N_T}}\left[1, \dots, e^{j\pi[n sin\varphi]}, \dots, e^{j\pi[(N_T-1)\sin\varphi]}\right]' \tag{6.15}$$

The THz channel path loss at frequency f and traveled distance d is calculated as

$$\gamma(f, d)[dB] = 20\, log_{10}\left(\frac{4\pi}{\lambda_c}\right) + 10 g(f) d\, log_{10} e \tag{6.16}$$

here, λ_c is the wavelength of f and $g(f)$ is the frequency-dependent medium absorption coefficient. In the THz channels, the atmospheric attenuation in water vapor molecules is considerably greater than in air molecules. In this paper, simply the influence of water molecules is considered for uncomplicatedness. The parameters of $g(f)$ are given in [105].

The SINR of $u_{b,n,l}^{i}$ is calculated as

$$SINR_{b,n,l}^{i} = \frac{a_{b,n,l}^{i} P_{b,n,l} ||h_{b,n,l}^{i} w_{b,n,l}||^2}{\sum_{j=1, j\neq l}^{L} P_{b,n,j} ||h_{b,n,l}^{i} w_{b,n,j}||^2 + \sum_{j=1}^{M_{b,n,l}} a_{b,n,l}^{j} P_{b,n,l} \left||h_{b,n,l}^{i} w_{b,n,l}|\right|^2 + \sigma_l^2} \tag{6.17}$$

If the bandwidth of the channel is represented as Б, then from the capacity model in [105], the rate at $u_{b,n,l}^{i}$ is calculated as

$$R_{b,n,l}^{i} = \frac{Б}{L} log_2(1 + SINR_{b,n,l}^{i}) \tag{6.18}$$

The total power consumption of b^{th} BS in $D_{b,n}$ sector [105] can be expressed as

$$P_{b,n} = P_{b,n}^{cir} + \xi\left(\sum_{l=1}^{L} P_{b,n,l}\right) \tag{6.19}$$

here, ξ is the power amplifier, the circuit power of $D_{b,n}$ sector of b^{th} BS is represented as $P_{b,n}^{cir}$. Let power consumption of MBS be P_{b+1}. The energy efficiency is expressed as the ratio of the sum rate and to the total power consumption and can be calculated BS as

$$EE_{system} = \sum_{b=1}^{B} \frac{\sum_{l=1}^{L} \sum_{i=1}^{M_{b,n,l}} R_{b,n,l}^{i}}{\sum_{n=1}^{N} p_{b,n}} \quad (6.20)$$

6.3 Proposed Antenna Angle Bound (AAB) Clustering

In the literature, the antenna beamwidth of the user devices has not been considered, and they were simply presumed to be omnidirectional. Such considerations enhance the interference between the users. In the proposed system the cellular users employ NOMA and the proposed AAB clustering technique to put the D2D pairs into clusters. The AAB clustering technique considers directional antennas, this greatly reduces the inter-user interference. The AAB clustering technique employs antenna beamwidth signified as ϖ^T. Fig. 6.4 shows the proposed small cell with AAB clustering. Algorithm 6.1 shows pseudocode for AAB. The condition put on the cellular users for AAB is it can serve almost two users. The remaining D2D pairs will be served by other cellular users.

The beam direction of $u_{b,n}^{w}$ is given as

$$\alpha_w = |\varpi^w \pm \Theta| \quad (6.21)$$

where, ϖ^w signifies the relay coordinate angle and Θ is an arbitrary constant angle provided

$$\Theta \leq \frac{|180° - \varpi^T|}{2} \quad (6.22)$$

Equation (6.22) limits the direction of $u_{b,n}^{w}$ relay beam towards D2D pairs. Let the coordinate angle of j^{th} D2D pair be denoted as ϖ_j.

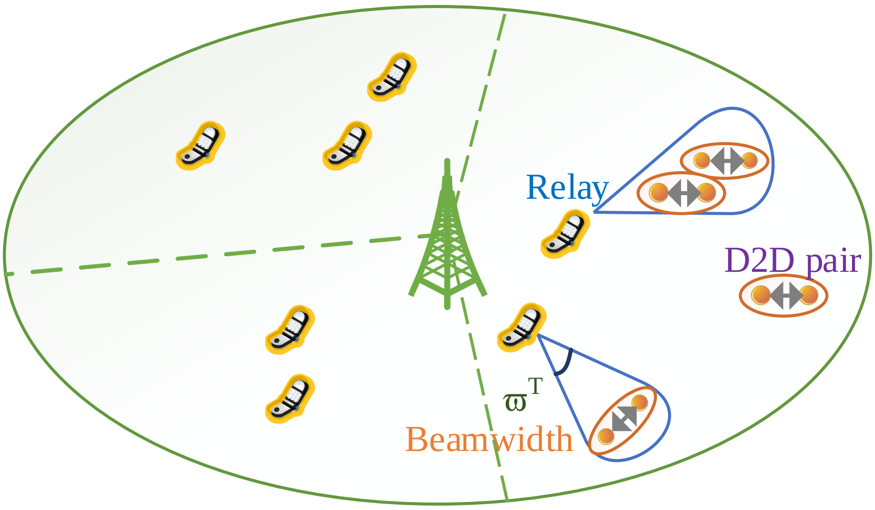

Fig. 6.4. Proposed Small cell with Antenna angle bound (AAB) clustering.

Remark 6.3: *All the angles are taken in degrees, as positive angles, and the SBS BS is considered at (0,0). The direction of the beams of the cellular users is randomly chosen as either* $\varpi^w + \Theta$ *or* $\varpi^w - \Theta$. $¥_j$ *and* $¥_j$ *denotes the coordinate angle of the D2D pair.*

Algorithm 1 for Antenna Angle Bound Clustering

for i= 1: total number of Relay

for j = 1: total number of D2D pairs

With the help of coordinate points of users,

Calculate $\varpi_{i,j}$: the angle between the i^{th} relay beam direction and j^{th} D2D

$$\varpi_{i,j} = |\alpha_i - \varpi_j| \quad (6.23)$$

if $0 \leq |\varpi_{i,j}| \leq \frac{\varpi^T}{2}$

then

The j^{th} D2D pair can be clustered by i^{th} relay

end

end

end

6.4 Simulation Results

In this section, the numerical results of the achieved sum rates, power consumption, and energy efficiency are presented to show the effectiveness of the proposed hybrid system for the 6G model with the proposed AAB clustering technique. The proposed hybrid 6G system employs THz mMIMO NOMA at SBS and RF mMIMO NOMA at MBS. In the simulation results, we have named the proposed hybrid 6G system model with AAB as 'Proposed THz'. We have compared 'Proposed THz' with 'Proposed mmWave' and 'mmWave Basic'. The 'Proposed mmWave' represents the proposed hybrid 6G system model with SBS employing mmWave channel instead of THz channel, the 'mmWave Basic' represents the traditional system model with mmWave mMIMO NOMA at SBS, RF mMIMO NOMA at MBS, and conventional clustering approaches.

TABLE 6.2: Simulation Parameters

Parameters	Value
THz carrier frequency	0.34 THz
RF carrier frequency	2 GHz
Bandwidth at BS employing THz channel	10 GHz
Bandwidth at BS employing RF channel	10 MHz
Radius of MBS	500 m
Radius of SBS	40 m
Threshold distance for D2D pair formation	20 m
Noise Power	-174 dBm/Hz

SBS transmitter power	5 W
MBS transmission power	42.7 dBm
Amplifier inefficiency	1/0.388
Relay antenna beam width in azimuth plane, ¥^{T} [126]	90°

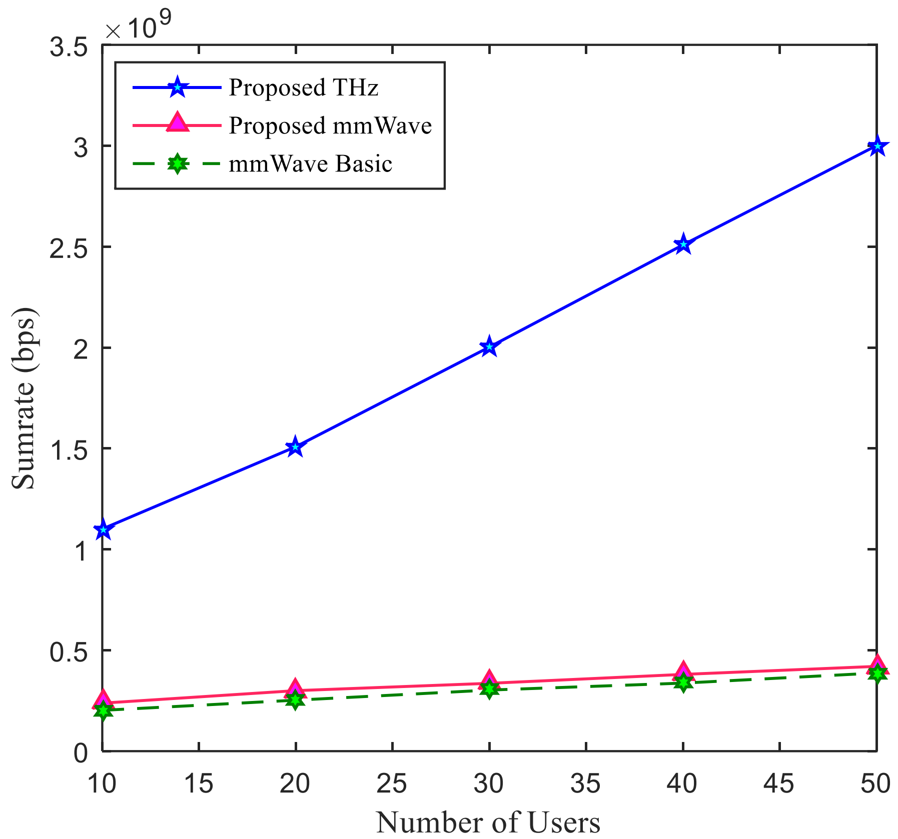

Fig. 6.5: Sum data rate versus the number of users.

The comparison of the sum rate versus the number of users in the system is shown in Fig. 6.5. The number of users is varied from 10 to 50. From Fig. 6.5 it can be observed that the sum rate rises with growth in the number of users. Moreover, the sum rate of the 'Proposed THz' is greater than the 'Proposed mmWave' and 'mmWave Basic', this is due to the higher bandwidth of the THz channel consequently, it can deliver high rates. Additionally, it can be observed that the sum rate of the 'Proposed THz' and 'Proposed mmWave' is greater than the 'mmWave Basic'. This is due to the employment of the proposed AAB clustering technique. The AAB clustering technique mitigates the interference by employing directional antennas.

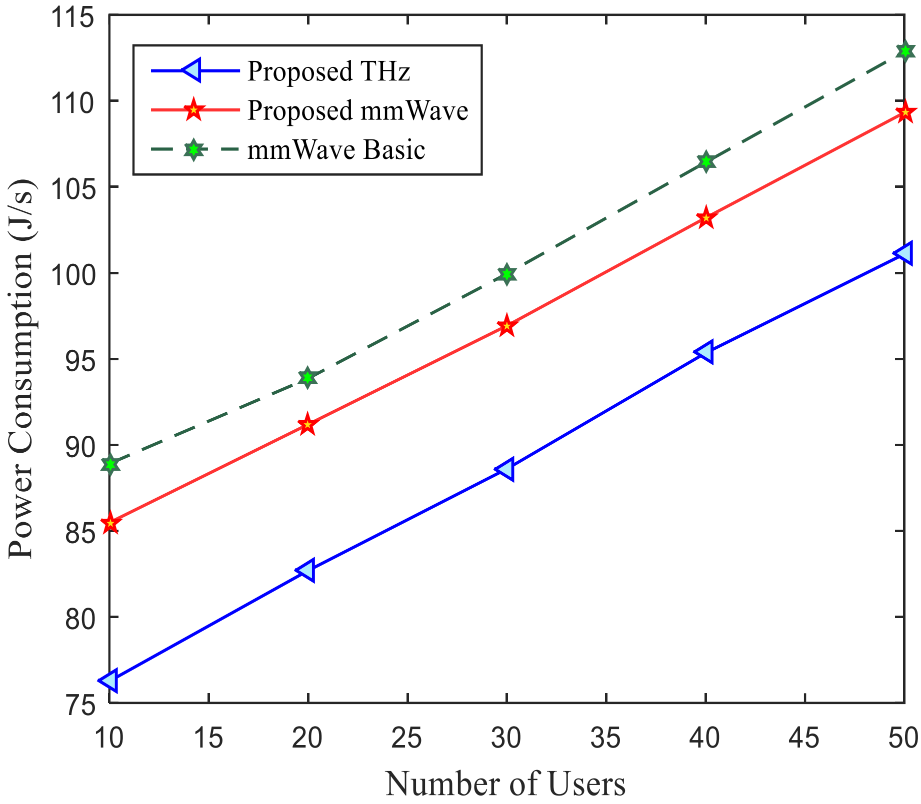

Fig. 6.6: Power consumption versus the number of users.

Fig. 6.6 displays the power consumption evaluation versus the number of users. The number of users is increased from 10 to 50. It can be noticed from Fig. 6.6 that the power consumption rises with the number of users. This is due to more power consumption due to more users. Further, the power consumption of the 'Proposed THz' and 'Proposed mmWave' is less than 'mmWave Basic', with the power consumption of the 'Proposed THz' being the least. This is due to the employment of relaying techniques. The relays help in offloading the transmission power of the BSs. Moreover, due to the employment of the proposed AAB clustering technique, all the transmit power of the relay is directed in one direction, saving it from getting dissipated in all directions as in the conventional techniques.

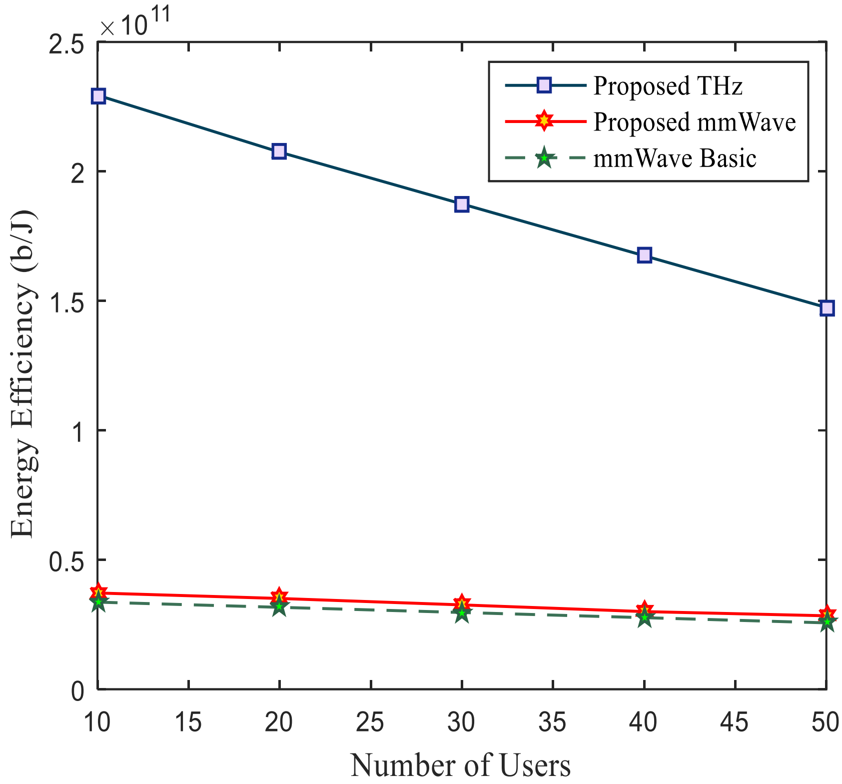

Fig. 6.7: The energy efficiency versus the number of users.

Fig. 6.7 displays energy efficiency against different numbers of users. it can be observed from Fig. .6.7 that as the number of users rises the energy efficiency also rises. Moreover, it can be perceived that the ‘Proposed THz’ is more energy-efficient than the ‘Proposed mmWave’ and ‘mmWave Basic’. The energy efficiency is calculated as the fraction of the achieved data rate and power consumption. From Fig. 6.5 and Fig. 6.6 it can be seen that the sum rate and power consumption of the ‘Proposed THz’ are maximum and minimum respectively. Therefore, the energy efficiency of the ‘Proposed THz’ is highest in comparison with the ‘Proposed mmWave’ and ‘mmWave Basic’ systems.

CHAPTER 7

IMPLEMENTATION OF AN ENERGY EFFICIENT MOBILE SMALL-CELL FOR BEYOND 5G NETWORKS USING NOMA TECHNOLOGY

In this chapter, an energy efficient mobile small-cell for beyond 5G networks using NOMA technology is implemented. This chapter integrated the advantage of wide THz bandwidth, spectrum efficiency of mMIMO and NOMA, and on-demand services of mobile BSs to form a green 2-tier 6G HetNet. This chapter propose a track selection scheme (TSS) for flying BS conferring to real-time parameters the flying BS chooses an optimal path to decrease the flying time, and power consumption of flying BS, and improvement in the energy efficiency of the 6G HetNet. The simulations examine the performance of the proposed TSS in comparison with the traditional approaches of flying BS deployment and path designs with the employment of mmWave channels.

7.1 Introduction

Year on year, the wireless traffic has increased with an increase in the number of wireless devices. The main reason behind this is a shift in user demands from connection-centric communications, for example, text messages and phone calls, to data-streaming communication, for example, connected cars, high-definition video streaming, and smart gaming. A high density of users in small areas such as movies and stadiums large data transmission load on the macro-cell base stations (MBS) [127]. It is challenging to provide fair broadband wireless services by the MBS in such high-density areas. Also, the wall penetration loss in indoor scenarios such as offices, movie theatres, etc., results in high signal attenuation. This has led to the rise of the deployment of mobile base stations (BS)s. This is a very efficacious key to delivering energy-efficient services to the users. The mobile BSs can be set up as flying BSs to deliver on-demand services to remotely located users. For example, blind zones of the wireless communication coverage in ocean communication are common due to a lack of infrastructure. This issue can be effectively addressed by the deployment of the flying BSs. The flying BSs can offer attention to such blind zones with onshore BSs [128]. Some research has been carried out in the past few years in the direction of developing remotely operated flying BSs to serve terrestrial or aerial devices. Flying BSs provide a much broader coverage range than terrestrial static BSs. Additionally, the Flying BSs are very cost-efficient and manually operable. This makes them appropriate for numerous mission-critical applications [129], [130]. The employment of flying BSs can offer better coverage and high-quality service to users with poor channel conditions.

The total energy of the flying BS is limited. Thus, to improve the performance of the cellular users in beyond 5G systems and reduce communication energy, a collaboration of NOMA and mobile BSs is considered a promising technology. In this, the energy efficiency and spectral efficiency can be significantly enhanced in downlink communication. The code division multiple access (CDMA) enhances spectrum efficiency but causes multiple access interference. The orthogonal frequency division multiplexing (OFDM) technology places the subchannels orthogonally to eliminate multiple access interference. However, OFDM allocates a single subchannel to each user. This creates the problem of resource scarcity. To solve the problem of resource scarcity, NOMA is employed. In NOMA, the number of users is divided into groups. The channel gain of a group of users is arranged in decreasing order. In power division NOMA each user functions in the same time/frequency block where they are differentiated by their power levels. The power division NOMA allocates power to the signals of the user in the same order as their channel gains. Thereafter, NOMA superimposes signals for a group of users. Then, NOMA allocates a single resource block to a group of users and transmits the superimposed signal to the group of users. In this way, using the same resource block signals are transmitted to a group of users. The multiple access interference in the NOMA is eliminated for the user with lower allocated power through successive interference cancellation (SIC). The user with higher allocated power faces interference with the signals of the users with lower allocated power. The SIC successively cancels interference caused by the signal of higher allocated power. First, the signal with the highest allocated power is detected, and then it is reconstructed. The reconstructed signal is then subtracted from the superimposed signal eliminating the interference caused by the signal with the highest power. NOMA enhances spectral efficiency as it can serve a group of users using the same time/frequency block. Consequently, it also improves system throughput [131].

The limitations of existing wireless networks such as capacity restrictions and spectrum scarcity can be solved by the employment of higher frequency bands. The THz communication technology has the potential to realize the demands of envisioned 6G communication systems. As THz band can provide 10-100 GHz bandwidth, feeble interference in the absence of full legacy regulation, combine 1000s antennas of sub-millimeter size, and symbol duration in pico-second range. Moreover, to achieve the target 6G ultra-broadband communications researcher are exploring of THz channel [132]. However, the THz band has been minimally explored bands in the whole spectrum. Lately, high data traffic owing to plentiful ground-breaking applications for ultra-high-definition data put the burden on flying BSs by the adoption of lower sub-6 GHz frequency bands. Hence, the employment of millimeter-wave (mmWave) channel and terahertz (THz) channel, at flying BSs in 6G networks can provide a huge spectrum and directional transmission. The integration of THz NOMA and flying BS technology can fulfill the provisional demands of ultra-high-definition data in small geographical areas such as movie theatres, offices, stadiums, disaster-affected areas, etc. Moreover, it can offer robust control and real-time communication services [133].

7.2 System Model

This chapter implement a downlink two-tier HetNet, consisting of a macro-cell and a flying BS. Fig. 7.1 shows the considered downlink 6G HetNet. The flying BS travel to serve areas with high user density. The MBS is equipped with N_S antennas and transmit superimposed messages through NOMA. Total G users are randomly distributed with Poisson distribution under the coverage of MBS. We consider the flying BS flying at an altitude H and s m/s speed of flying.

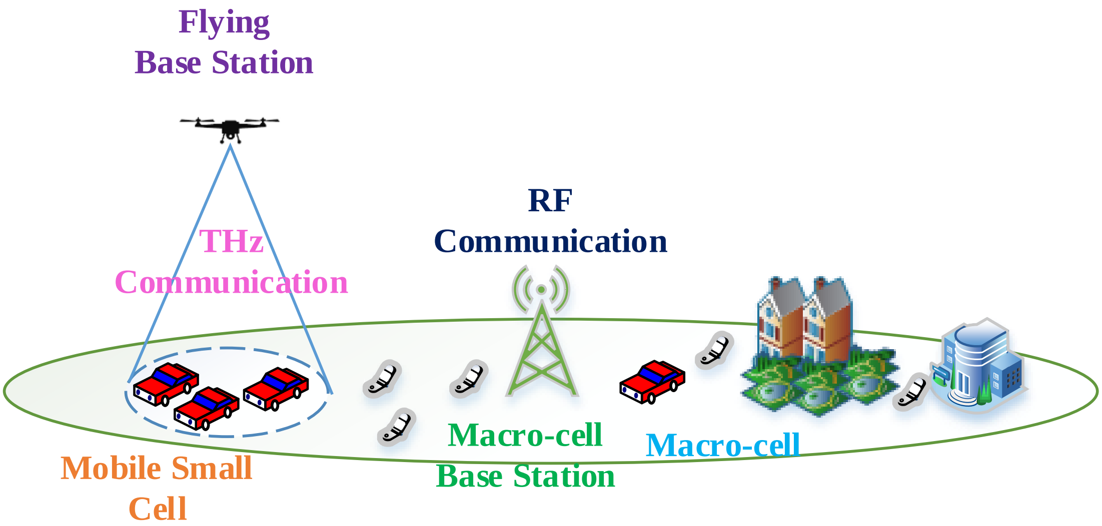

Fig. 7.1. Considered Downlink 6G HetNet

The flying BS is equipped with a directional antenna, and so its beam projects a circle of radius R on the ground. The trajectory projected on the ground of the mobile cell BS concerning time t is represented as e(t)$\in C^{2\times1}$. The set of all users is represented as $U = \{u_S, u_M\}$ where, u_S and u_M represents a set of users inside flying BS and macro-cell respectively. If there are N users inside the mobile small-cell then the number of users inside the macrocell can be given as $K = G - N$.

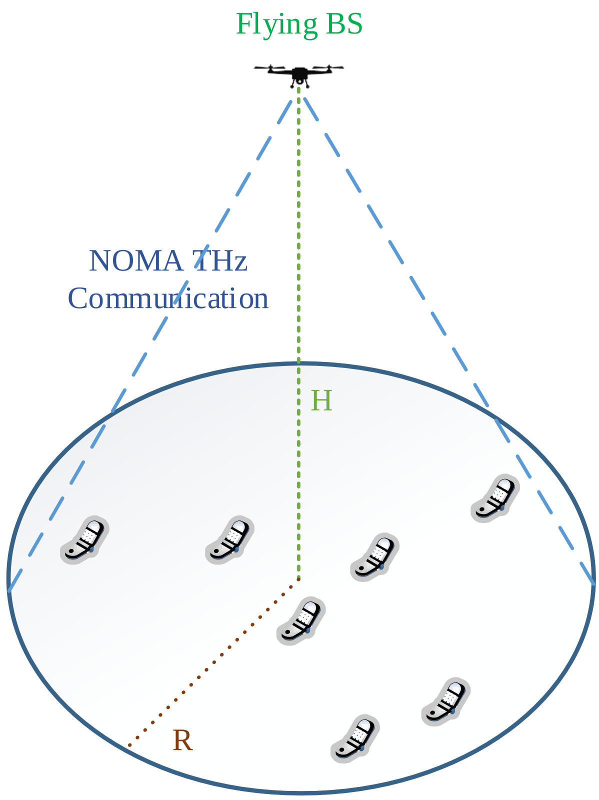

Fig. 7.2. Flying BS enabled communication system.

The sets of users inside macro-cell and flying BS coverage are respectively represented as $u_S = \{s_1, s_2, \dots, s_n, \dots, s_N\}$ and $u_M = \{m_1, m_2, \dots, m_k, \dots m_K\}$ where, s_n denotes is n^{th} a user inside macro-cell and m_k denotes k^{th} a user inside a mobile small-cell. The locations of the users $s_n \in u_S$ and $m_k \in u_M$ are denoted by p_n^s and p_k^m respectively, and their estimated sojourn time is denoted by $t_s^{s_n p_n^s}$ and $t_s^{m_k p_k^m}$ respectively. Sojourn time portrays the probable period that a user is located in a particular cell, and can be calculated from an enhanced random waypoint mobility model's cumulative distribution/probability density function, taking the speed of the user, distance traveled, and time is taken to travel the distance as inputs in the given distributions [134]. It is presumed that perfect channel state information (CSI) for all users is present at all BSs. The notations used in the paper are shown in Table 7.1.

TABLE 7.1: NOTATIONS

N_s	No. of antennas on MBS
N_m	No. of antennas on Flying BS
G	Total number of users
K	Number of users in MBS
N	The capacity of mobile small-cell
U	Set of all users
u_M	Sets of users inside macro-cell
u_S	Sets of users inside mobile small-cell
H	The altitude of flying BS
$e(t)$	The trajectory of flying BS projected on the ground
R	Radius of mobile small cell
p_k^m	Location of m_k user
p_n^s	Location of s_n user
B^{RF}	RF Bandwidth
N_m	Number of antennas at the flying BS
N_s	Number of antennas at MBS
$Ᵽ_{M,c}$	The transmit power of cluster c of flying BS
$Ᵽ_{S,c}$	The transmit power of cluster c of MBS
$Ᵽ_{M_{max}}$	The maximum transmit power of flying BS
$Ᵽ_{S_{max}}$	The maximum transmit power of MBS
$h_{M,c}^k$	Downlink channel of m_k user in c^{th}cluster of mobile small cell
$h_{S,c}^n$	Downlink channel of s_n user in c^{th}cluster of macro cell
a^k	the power allocation coefficient of m_k
a^n	the power allocation coefficient of s_n
$y_{M,c}^k$	Received signal at m_k user in c^{th}cluster in mobile small cell
$y_{S,c}^n$	Received signal at $s_n$user in c^{th}cluster in macro cell
ξ	Drain efficiency of the power amplifier of MBS
ξ_M	Drain efficiency of the power amplifier of flying BS
$Ᵽ_S^{cir}$	Circuit power of MBS
$Ᵽ_M^{cir}$	Circuit power of flying BS
$\eta_{M,c}^k$	Additive white gaussian noise at m_k
$R_{M,c}^k$	Achievable rate at m_k user of c^{th} cluster in mobile small cell
$R_{S,c}^n$	Achievable rate at s_n user of c^{th} cluster of MBS

In the considered system model, the MBS employs mMIMO NOMA technology for communication. MBS has a large coverage area and employs Rayleigh fading channel at downlink as it can form strong long-distance communication links. Flying BS dynamically moves and serves the users via NOMA technology. Fig. 2 shows a flying BS-enabled communication system. The flying BS has a coverage radius R on the ground and flies at an altitude H. To deliver high-speed and short-distance services flying BS employs a THz channel at the downlink. The use of different frequency bands at flying and MBS BS transmitters mitigate cross-tier interference. MBS and flying BS both use NOMA for downlink communication. NOMA uses superimposition coding to simultaneously serve q users clustered in a group with the same resource block. Upon receiving the signal, the users decode the message using successive interference cancellation (SIC). It is assumed that there are C clusters inside each cell.

The superimposed signal transmitted by the MBS for c^{th} cluster with q users is given as

$$x_{S,c} = \sum_{n=1}^{q} \sqrt{a_{S,c}^{n} \mathrm{P}_{S,c}}\, z_{S,c}^{n} \tag{7.1}$$

here, $z_{M,c}^{n}$ denotes the modulated signal of s_n, $a_{S,c}^{n}$ signifies the power allocation coefficient of s_n, and $\mathrm{P}_{S,c}$ represents transmit power for c^{th} cluster and is limited by $\sum_{c=1}^{C} \mathrm{P}_{S,c} \leq \mathrm{P}_{S_{max}}$ where, $\mathrm{P}_{S_{max}}$ is the maximum transmit power of MBS.

Then, the received signal by the user s_n over the $1 \times C \times u_S$ channel matrix H where, $\mathrm{H} = \{h_{S,c}^{1}, \ldots, h_{S,c}^{q}\}$ is given by

$$y_{S,c}^{n} = h_{S,c}^{n} w_{S,c} \sqrt{a_{S,c}^{n} \mathrm{P}_{S,c}}\, z_{M,c}^{n} + I_{S,c,n}^{1} + I_{S,c,n}^{2} + \eta_{S,c}^{n} \tag{7.2}$$

$$I_{S,c,n}^{1} = h_{S,c}^{n} \sum_{j=1, j\neq c}^{C} w_{S,j} x_{S,j} \tag{7.3}$$

$$I_{S,c,n}^{2} = h_{S,c}^{n} w_{S,c} \sum_{j=1}^{q} \sqrt{a_{S,c}^{j} \mathrm{P}_{S,c}}\, z_{S,c}^{j} \tag{7.4}$$

$\eta_{S,c}^{n} \sim CN(0, \sigma_c^2)$ is the additive white gaussian noise (AWGN) with zero mean and variance σ_c^2, $w_{S,j}$ is the precoding vector, $I_{S,c,n}^{1}$ and $I_{S,c,n}^{2}$ denotes inter-cluster interference and intra-cluster respectively. For the RF channel model, the Rayleigh fading channel is considered with Gaussian distribution of $h \sim CN(0, \beta)$ [19] with zero mean and β variance. The large-scale fading is characterized by β encompassing penetration losses, path loss, shadowing losses, and antenna gains in NLoS path. Channel gain for RF is given by

$$h_{S,c}^{n} = 10^{-(L(d)^{RF}/10)} \tag{7.5}$$

The path loss for RF channel [19], at traveled distance d^{RF} (km), is given as follows:

$$L(d)^{RF}[dB] = 148.1 + 37.6\ log_{10}d^{RF} \tag{7.6}$$

The signal to interference and noise ratio (SINR) of the s_n in cluster c of MBS is given by

$$SINR_{S,c}^{n} = \frac{a_{S,c}^{n}\mathbb{P}_{S,c}||h_{S,c}^{n}w_{S,c}||^2}{\sigma_c^2+\sum_{j=1,j\neq c}^{C}\mathbb{P}_{S,j}||h_{S,c}^{n}w_{S,j}||^2+\sum_{j=1}^{q}a_{S,c}^{j}\mathbb{P}_{S,c}\left||h_{S,c}^{n}w_{S,c}|\right|^2} \tag{7.7}$$

Through the capacity model in [20], the rate of s_n in the cluster c is calculated as

$$R_{S,c}^{n} = \frac{B^{RF}}{C}log_2(1+SINR_{S,c}^{n}) \tag{7.8}$$

where B^{RF} is the RF bandwidth employed at the MBS.

The flying BS moves dynamically to serve users in the macro cell. The flying BS finds its target location l_i' according to TSS. Then flying BS employs NOMA to send the downlink signal to the users. The superimposed signal transmitted by the flying BS for c^{th} cluster with q users is given as

$$x_{M,c} = \sum_{k=1}^{q}\sqrt{a_{M,c}^{k}\mathbb{P}_{M,c}}\ z_{M,c}^{k} \tag{7.9}$$

here, $z_{M,c}^{k}$ denotes the modulated signal of m_k, $a_{M,c}^{k}$ signifies the power allocation coefficient of m_k, and $\mathbb{P}_{M,c}$ represents transmit power for c^{th} cluster and is limited by $\sum_{c=1}^{C}\mathbb{P}_{M,c} \leq \mathbb{P}_{M_{max}}$ where, $\mathbb{P}_{M_{max}}$ is transmit power of MBS.

Then, the received signal by the user m_k over the $1\times C\times u_M$ channel matrix $\hat{H}$, where $\hat{H} = \{h_{M,c}^{1}, \ldots, h_{M,c}^{q}\}$ is given by

$$y_{M,c}^{k} = h_{M,c}^{k}w_{M,c}\sqrt{a_{M,c}^{k}\mathbb{P}_{M,c}}z_{M,c}^{k} + I_{M,c,k}^{1} + I_{M,c,k}^{2} + \eta_{M,c}^{k} \tag{7.10}$$

$$I_{M,c,k}^{1} = h_{M,c}^{k}\sum_{j=1,j\neq c}^{C}w_{M,j}x_{M,j} \tag{7.11}$$

$$I_{M,c,k}^{2} = h_{M,c}^{k}w_{M,c}\sum_{j=1}^{q}\sqrt{a_{M,c}^{j}\mathbb{P}_{M,c}}\ z_{M,c}^{j} \tag{7.12}$$

$\eta_{M,c}^{k} \sim CN(0,\sigma_m^2)$ is the AWGN with zero mean and variance σ_m^2, $w_{M,j}$ is the precoding vector, $I_{M,c,k}^{1}$ and $I_{M,c,k}^{2}$ denotes inter-cluster interference and intra-cluster respectively. The flying BS uses the THz channel model [105], and the channel gain $h_{M,c}^{k}$ is given as

$$h_{M,c}^{k} = \sqrt{N_m}\left(\sqrt{\frac{1}{L(d)}}\omega\alpha\left(\phi_{M,c,g}^{k}\right)\right) \tag{7.13}$$

here $L(d)$ represents path loss at d distance from the flying BS, ω signifies the antenna gain, ϕ is the angle of departure, $\alpha\left(\phi_{M,c,g}^{k}\right)$ represents array steering vector which is given by

$$\alpha\left(\phi_{M,c,g}^{k}\right) = \frac{1}{\sqrt{N_m}}\left[1, \dots, e^{j\pi[n sin\phi]}, \dots, e^{j\pi[(N_m-1)\sin\phi]}\right]' \quad (7.14)$$

The path loss due to spreading and molecular absorption cannot be ignored. The path loss of the THz signal is given as

$$L(d)[dB] = 20\ log_{10}\left(\frac{4\pi}{\lambda}\right) + 10r(f)d\ log_{10}e \quad (7.15)$$

here, λ represents the wavelength of the carrier frequency f, and $r(f)$ is the frequency-dependent medium absorption coefficient as given in [105]. Let B represent the utilized bandwidth of THz channel.
The SINR of the user m_k in cluster c of flying BSis given by

$$SINR_{M,c}^{k} = \frac{a_{M,c}^{k} \mathrm{P}_{M,c}||h_{M,c}^{k} w_{M,c}||^2}{\sigma_c^2 + \sum_{j=1,j\neq c}^{C} \mathrm{P}_{M,j}||h_{M,c}^{k} w_{M,j}||^2 + \sum_{j=1}^{q} a_{M,c}^{j} \mathrm{P}_{M,c}\left||h_{M,c}^{k} w_{M,c}|\right|^2} (7.16)$$

Thus, the rate of user m_k in the cluster, c is given by

$$R_{M,c}^{k} = \frac{B}{C} log_2(1 + SINR_{M,c}^{k}) \quad (7.17)$$

The total power consumption of MBS [105] can be expressed as

$$\mathrm{P}_S = \mathrm{P}_S^{cir} + \xi\left(\sum_{c=1}^{C} \mathrm{P}_{S,c}\right) \quad (7.18)$$

where P_S^{cir} is the circuit power of MBS, ξ is the drain efficiency of the power amplifier of MBS. P_S^{cir} can be expressed as

$$\mathrm{P}_S^{cir} = \mathrm{P}_b + N_R \mathrm{P}_R + N_s \mathrm{P}_P + N_s \mathrm{P}_A \quad (7.19)$$

where N_R is the number of RF chains, P_b, P_R, P_P, and P_A is respective power utilization of baseband and at each RF chain, phase shifter, and amplifier. The energy efficiency of the MBS is the ratio of the profit brought by the long-term utility of capacity to the total power consumption and can be expressed as

$$\mathrm{EE}_{MBS} = \frac{\sum_{c=1}^{C}\sum_{i=1}^{q} R_{S,c}^{n}}{\mathrm{P}_S^{cir} + \xi\left(\sum_{c=1}^{C} \mathrm{P}_{S,c}\right)} \quad (7.20)$$

The power expenditure of flying BS can be given as

$$\mathrm{P}_M = \mathrm{P}_M^{cir} + \xi_M\left(\sum_{c=1}^{C} \mathrm{P}_{M,c}\right) \quad (7.21)$$

where, P_M^{cir} is the circuit power of flying BS, ξ_M is the drain efficiency of the power amplifier.

The energy efficiency of the flying BS can be expressed as

$$\text{EE}_{SBS} = \frac{\sum_{c=1}^{C}\sum_{i=1}^{q} R_{M,c}^{k}}{\text{P}_M} \tag{7.22}$$

The energy efficiency of the system can be expressed as

$$\text{EE}_{Sys} = \text{EE}_{SBS} + \text{EE}_{MBS} \tag{7.23}$$

7.3 Proposed Track Selection Scheme (TSS)

The total flying BS target locations present for period T are assumed to be W and are defined in set £ = $\{ł_1, ł_2, \dots, ł_i, \dots ł_W\}$. The flying BS requires a time $t^{l,ł_i}$ to move from location l to l_i' to serve a set of users $u_M^{l_i'}$ at $ł_i$. The capacity of a mobile small cell is defined as N. The total number of users at $ł_i$ in the set $u_M^{ł_i}$ is $M^{ł_i}$ provided $N \geq M^{ł_i}, \forall ł_i \in$ £. Each user ${m_k}^{ł_i}$ in the considered set $u_M^{ł_i}$ is located at p_k^m, and has sojourn time $t_s^{{m_k}^{ł_i}}$. If user ${m_k}^{ł_i} \in u_M^{ł_i}$ is covered by flying BS, then the time is taken to serve the user ${m_k}^{ł_i}$ is $t_{m_k}{}^{l,ł_i}$ = max $\{0, t_s^{{m_k}^{ł_i}} - t^{l,ł_i}\}$. The dynamic movement of the flying BS causes superfluous overhead, to alleviate this overhead the flying BS is deployed once every period T provided $T \geq t_s^{{m_k}^{ł_i}}, \forall {m_k}^{ł_i} \in u_M^{ł_i}$. To design a green 6G HetNet, TSS optimizes the path of flying BS by selecting to order of target location to be served, period T. This order of target locations is selected according to three parameters. First, travel time, second, user density, and third request in the queue. The request of each user $ɥ^{{m_k}^{ł_i}}$ is defined in a queue set Q. Algorithm 7.1 explains TSS. Algorithm 1 initially defines Ł as an empty set to store the target locations. The algorithm first sorts the target locations according to travel time, and if the travel time of two target locations is the same, it checks user density and selects the next location with higher user density. If user densities of the two target locations are also the same then the algorithm checks the request in the queue and selects the target location with smaller queue requests. The computational complexity of Algorithm 1 is O (W^2).

Algorithm 7.1 for TSS

Input: £, $u_M^{ł_i}$, $t_s^{{m_k}^{ł_i}}$, $t^{l,ł_i}$, Q, $M^{ł_i}$, T, N

Output: $ł_i, \forall ł_i \in$ £

1. Ł← ∅
2. **for** $i = 0$ to W

sort locations $ł_i$ according to travel time $t^{l,ł_i}$

Ł← ł $[i]$

for $(j = i + 1; i < W; j + +)$

if (ł $[i]$== ł$[j]$)

check user densities

if M$^{ł}[i] \geq$ M$^{ł}[j]$

a = ł $[i]$

ł $[i]$ = ł $[j]$

ł $[j] = a$

elseif M$^{ł}[i]$ == M$^{ł}[j]$

check queue requests

if Ч$^{ł}[i] \leq$ Ч$^{ł}[j]$

a = ł $[j]$

ł $[j]$ = ł $[i]$

ł $[i] = a$

end if

end for

end for

7.4 Simulation results

In this section, the efficiency of the proposed TSS in the flying BS system model deployed in a two-tier HetNet is presented through simulation and is compared with other traditional schemes in terms of flying latency, power consumption, and energy efficiency. Table 7.2 shows considered simulation parameters. In the considered downlink 2-tier HetNet, the MBS is in the cell center, and flying BS is in the coverage of MBS. The users are randomly moving throughout the cell, within the scope of their allied BS. The considered system model uses the mMIMO RF NOMA technology at MBS and THz NOMA technology at the flying BS. We labeled the proposed 2-tier flying BS HetNet with TSS as 'Proposed THz' and compared it with two network models. First, uses the mMIMO RF NOMA technology at MBS and mmWave channel, NOMA, and proposed TSS technology at the flying BS, and is labeled as 'Proposed mmWave'. Second, uses the mMIMO RF NOMA technology at MBS and mmWave NOMA at the flying BS, and is labeled as 'Basic'.

Table 7.3: Simulation Parameters

Parameters	**Value**
Radius of macrocell	2 km
THz carrier frequency	0.34 THz [105]
RF carrier frequency	2 GHz
Bandwidth at BS employing THz channel, B	10 GHz [105]
Bandwidth at BS employing RF channel, B^{RF}	10 MHz
Altitude of mobile small cell, H	100 m [135]
Radius of mobile small cell, R	300 m [135]

Speed of mobile small cell, s	50 m/s [135]
Number of antennas at the flying BS, N_m	1
Number of antennas at MBS, N_s	100 [135]
Noise Power in macro cell, σ_c^2	-174 dBm/Hz
Noise Power in mobile small cell, σ_m^2	-109 dBm
Maximum transmitter power of MBS, $\text{Ᵽ}_{S_{max}}$	43 dBm
Maximum transmitter power of Flying BS, $\text{Ᵽ}_{M_{max}}$	10 dBm
The circuit power of flying BS, Ᵽ_M^{cir}	-10 dBm/s
Baseband power consumption Ᵽ_b	200 mW
RF chain power consumption, Ᵽ_R	160 mW
Phase shifter power consumption, Ᵽ_P	40 mW
Amplifier power consumption, Ᵽ_A	20 mW
Drain efficiency of MBS amplifier and flying BS amplifier, ξ and ξ_m	1/0.38 [135], [136]
The deployment interval, T	500 s

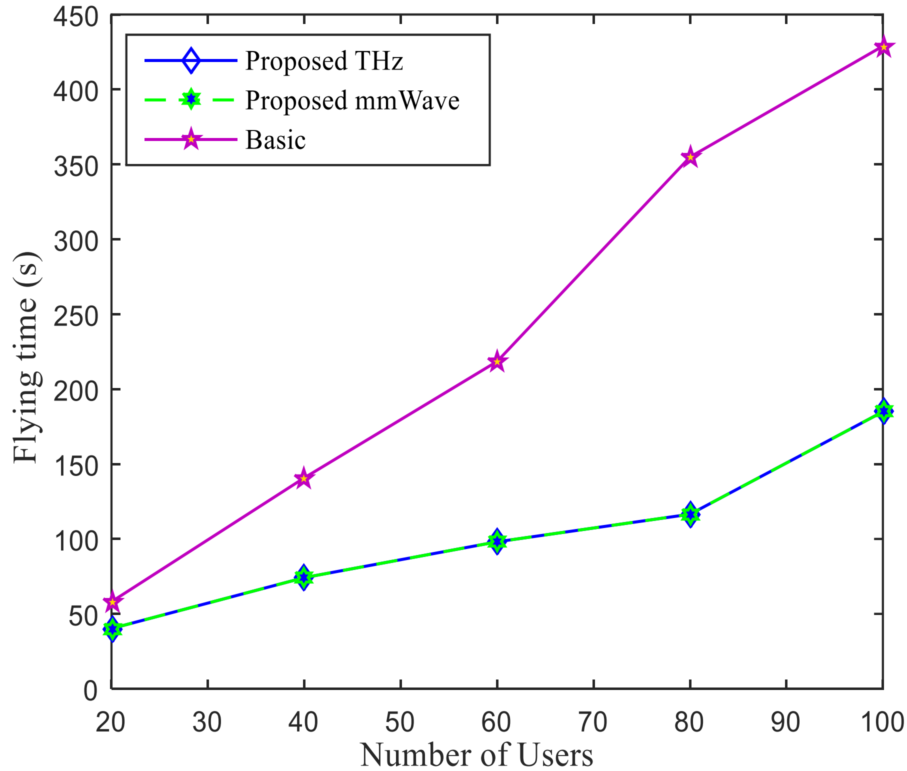

Fig. 7.3. Flying latency v/s Number of users.

Fig. 7.3 shows the comparison of flying latency of the ‘Proposed THz’ with ‘Proposed mmWave’ and ‘Basic’. The number of users is varied from 20 to 100. It can be observed from the figure that as the number of users rises the flying latency also rises. The flying latency of the ‘Proposed THz’ and ‘Proposed mmWave’ is less than ‘Basic’. This is due to the proposed TSS selecting the path of flying BS first according to the required travel time and saving flying latency. The flying latency of the ‘Proposed THz’ and ‘Proposed mmWave’ is the same. This is because the channel does not have any effect on flying latency.

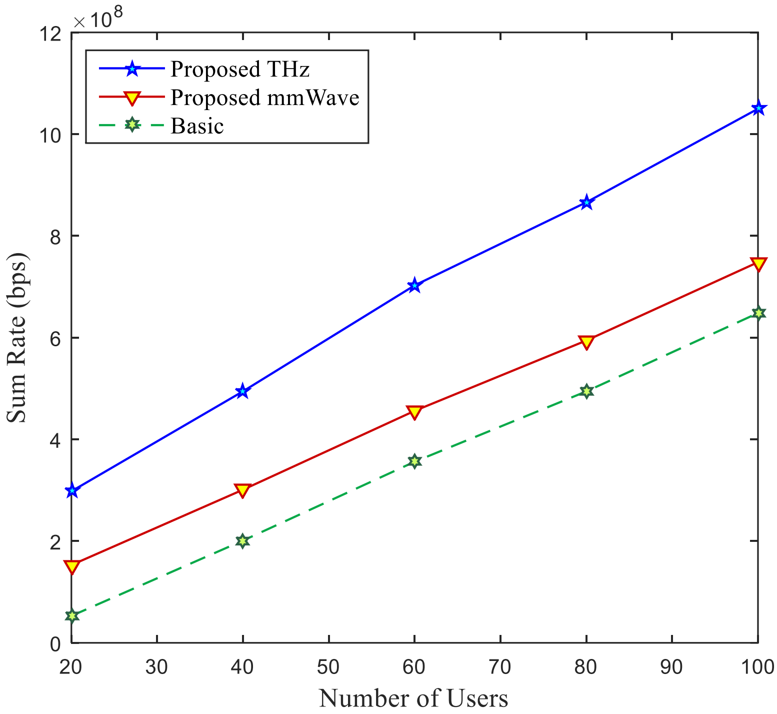

Fig. 7.4. Sum Rate v/s Number of users.

Fig. 7.4 shows the comparison of total power consumption of flying BS of the ‘Proposed THz’ with ‘Proposed mmWave’ and ‘Basic’. The number of users is varied from 20 to 100. It can be observed from the figure that as the number of users rises the sum rate also rises. From Fig. 7.4 it can be observed that the sum rate of the ‘Proposed THz’ is more than the ‘Proposed mmWave’ and ‘Basic’. This is due to huge bandwidth provided by THz communication channel when compared with mmWave and RF channel used in ‘Basic’. The massive bandwidth available in THz channel aids in improving the sum rate of the ‘Proposed THz’. Similarly, the mmWave channel provide larger bandwidth than the RF channel, therefore the sum rate of the ‘Proposed mmWave’ is greater than the ‘Basic’.

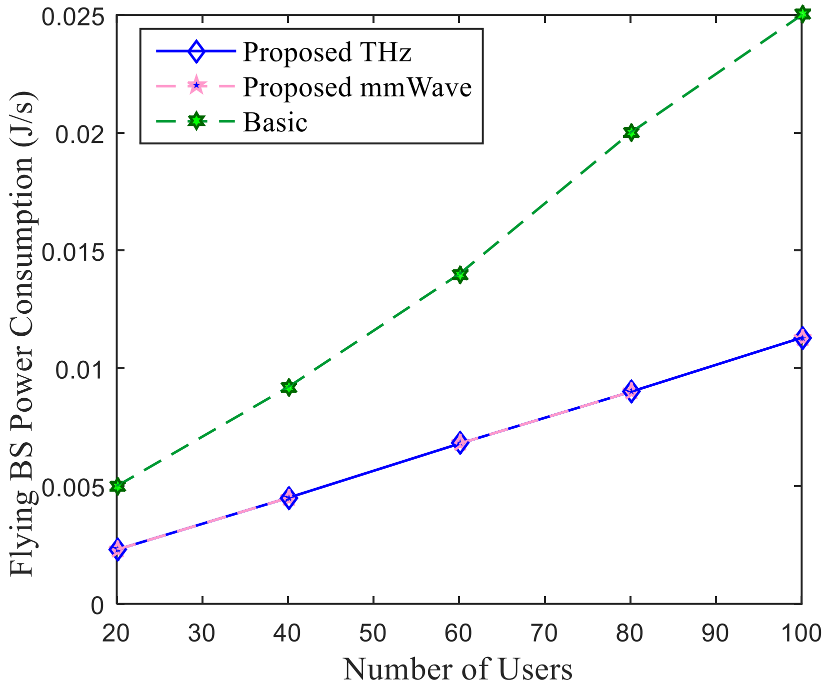

Fig. 7.5. Flying BS power consumption v/s number of users.

Fig. 7.5 shows the comparison of total power consumption of flying BS of the ‘Proposed THz’ with ‘Proposed mmWave’ and ‘Basic’. The number of users is varied from 20 to 100. It can be observed from the figure that as the number of users rises the flying BS power consumption also rises. The flying BS power consumption of the ‘Proposed THz’ and ‘Proposed mmWave’ is the same because the channel does not have any effect on the flying BS power consumption. Moreover, the power consumption of the ‘Proposed THz’ and ‘Proposed mmWave’ is less than ‘Basic’. This is due to the proposed TSS selecting the path of flying BS first according to the required travel time. The travel time is defined as the ratio of travel distance and speed of flying BS. Less power is consumed to travel shorter distances. TSS efficiently plans the path of flying BS to save flying circuit power consumption.

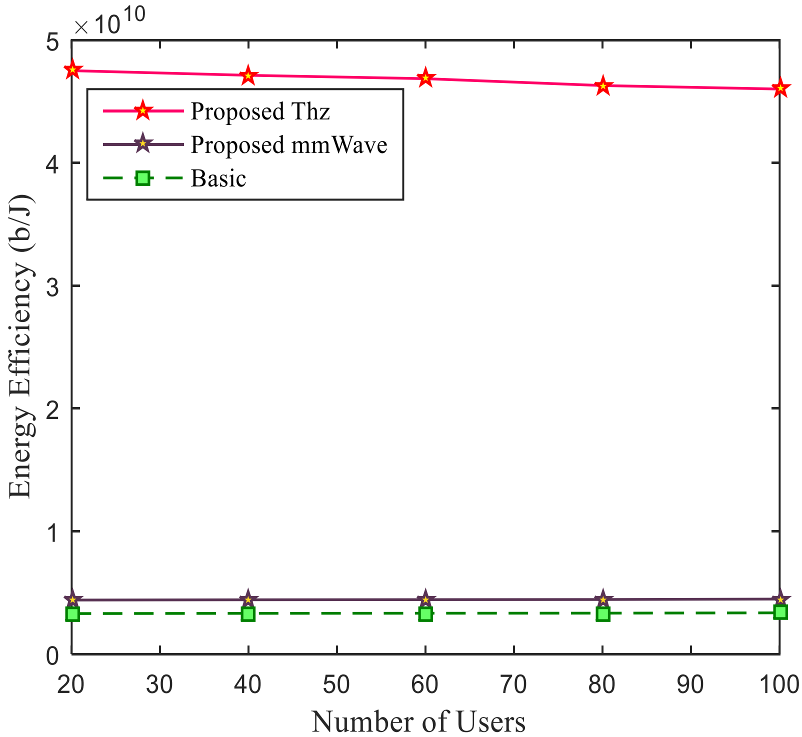

Fig. 7.6. Energy efficiency v/s number of users

Fig. 7.6 shows the comparison of energy efficiency of the 2-tier HetNet for the 'Proposed THz' with 'Proposed mmWave' and 'Basic'. The number of users is varied from 20 to 100. It can be observed from the figure that as the number of users rises the energy efficiency reduces. The energy efficiency of the 'Proposed THz' is more than 'Proposed mmWave' and 'Basic'. This is due to both the THz channel and proposed TSS. As energy efficiency of the system is defined as ratio of rate and power consumed. From Fig. 7.5 it can be seen that the power consumption of the 'Proposed THz' and 'Proposed mmWave' is less than 'Basic'. Moreover, the achieved rates of THz channel are better than mmWave channel due to its larger bandwidth. This enhances the energy efficiency of the 'Proposed THz'.

CHAPTER 8

ENERGY EFFICIENCY CLUSTERING IN A MOBILE SMALL-CELL USING NOMA D2D TECHNIQUE IN BEYOND 5G NETWORKS

In this chapter, energy efficient clustering in a mobile small-cell using NOMA D2D technique in beyond 5G networks is designed. we put forward a mobile BS-based 6G HetNet that integrates THz communication, mMIMO, NOMA, and D2D technologies. This chapter propose a joint power allocation and clustering scheme to enhance the performance of the proposed 6G mobile small cell system. As ML provides more accurate outcome prediction. This chapter first propose an energy-efficient mobile small cell system model. Then, a novel fuzzy logic system that exploits channel gains to design optimum power allocation in NOMA is proposed. Further, this chapter propose a clustering scheme that effectively integrates user device antenna parameters, NOMA, and D2D communication to reduce interference and enhance the energy efficiency of MSBS. The MSBS moves over the macro-cell and uses NOMA to provide services to the users, while these users form clusters and relay this information to D2D user pairs via the same resources at the same time. Simulation results demonstrate that the proposed schemes for mobile small cell-based 6G HetNet can realize enhanced system performance, compared with the state-of-the-art methods in terms of sum rate, power consumption, and energy efficiency.

8.1 Introduction

In the upcoming wireless communication generation beyond 5G (B5G) and 6G networks, a massive number of additional users and communication devices will be connected to the network. Leads to high latency, signal interference, low data rates, and mammoth data traffic demanding ultra-high-definition data services at hot-spot areas such as stadiums, disaster areas, concerts, movie theatres, and offices. An additional huge expense will be required for installing new BSs at such locations for temporary communication services. New technologies are emerging to address these issues and develop a 6G wireless network. Mobile small cells are one of these incipient technologies. The mobile small cell technology is a very effective technology to bring energy-efficient user services. Moreover, the terrestrial BSs single-handedly face many issues such as low quality of service in areas with high user density. Further, there are areas where signals cannot reach and this is common in ocean communication or hilly terrains are common due to lack of infrastructure is another issue. Additionally, terrestrial BSs are inoperable in the disaster area. The MSBS can effectively offload the terrestrial BS seamlessly and can provide an impeccable connection between transmitter and receiver. These issues can be effectively addressed by the deployment of the mobile small cell BSs (MSBS)s [137]. This embarks more heterogeneous and denser wireless networks. MSBSs have the potential to efficiently deliver on-demand services to remotely located users, blind zones, and densely located users. Especially, in rural scenarios, the MSBS can deliver wireless facilities to the areas with deprived network services such as cultivation areas, inaccessible zones, industry sweatshops, construction areas, etc, [138]. Few works has been carried out in the past few years in the direction of developing remotely operated flying BSs to serve the terrestrial or aerial devices. Unmanned aerial vehicles (UAV)s when deployed as MSBSs, provide a much broader coverage range than terrestrial BSs. MSBSs can deliver better communication services due to their ability to form close-range line-of-sight (LoS) wireless connections. Additionally, the MSBSs are very cost-efficient and fully manually operable. This makes them appropriate for numerous mission-critical applications [139], [140].

In designing wireless systems, proficient information of procedures like detection, coding, modulation, etc., are required by mathematical and statistical tools. However, practical conditions like time disparities due to high user mobility, hardware deficiencies, latency, etc. can lead to signal distortions. To address these issues in 6G, machine learning (ML) is seen as prime technology as it can aid in enhancing system performance even with deficient system characteristic knowledge. ML can be used to execute tasks that comprise manipulation, reasoning, learning, planning, perception, and problem-solving in an intelligent manner. Hence, ML will equip 6G with intelligent system control. The device-to-device (D2D) communications are considered for aiding energy efficiency, fairness, latency, and throughput enhancements [141]-[143]. The device-to-device D2D communications allow high data rate applications and services like connected cars, high-definition video sharing, and vicinity-aware social networking. Mobile small cells thus refute the requirement for installing and maintaining supplementary network infrastructure by the network operators. The total energy consumption of the MSBSs is a critical performance parameter as it has limited battery life. Consequently, the greatest challenge in MSBS deployment is considered energy consumption minimization. Thus, to improve the performance of the cellular users in the 6G system and reduce communication energy consumption, a collaboration of ML, NOMA, THz, D2D communications, and mobile small cells are considered capable technologies.

8.2 System Model

We study a downlink 6G wireless communication network, containing a macro-cell and mobile small-cell. The mobile. the small cell can move to serve high-density locations in macro-cell. The MBS employs mMIMO NOMA and has N_B antennas. Total U users are considered in the system and their distribution is considered as stochastic. The mobile small cell BS (MSBS) is considered to be flying at a height Ƕ and moving with speed ś. N_t directional antennas are fabricated on MSBS to project a circular beam on land with a radius Ř. It is presumed that perfect channel state information (CSI) for all users is present at all BSs. The set of all users is represented as $\bar{U} = \{u_b, u_m\}$ where, u_b and u_m represents set of users in macro-cell and mobile small cell respectively. It is presumed that perfect channel state information (CSI) for all users is present at all BSs. The sets of users inside macro-cell and mobile small-cell are respectively represented as $u_b = \{b_1, b_2, \dots, b_n, \dots, b_N\}$ and $u_m = \{d_1, d_2, \dots, d_k, \dots d_K\}$ where, b_n symbolizes is n^{th} user in macro-cell and n_k symbolizes k^{th} a user inside a mobile small-cell. The user locations $b_n \in u_b$ and $d_k \in u_m$ are represented by

p_n^b and p_k^d respectively, and their estimated sojourn time is represented by t_n^b and t_k^d respectively. The probable period of a user to be present in a particular place is depicted by Sojourn time. It can be calculated from an enhanced random waypoint mobility model's cumulative distribution/probability density function, taking the speed of the user, distance traveled, and time is taken to travel the distance as inputs in the given distributions [144]. Fig. 8.1 shows the considered downlink 6G HetNet model. The notations used in the paper are shown in Table 8.1.

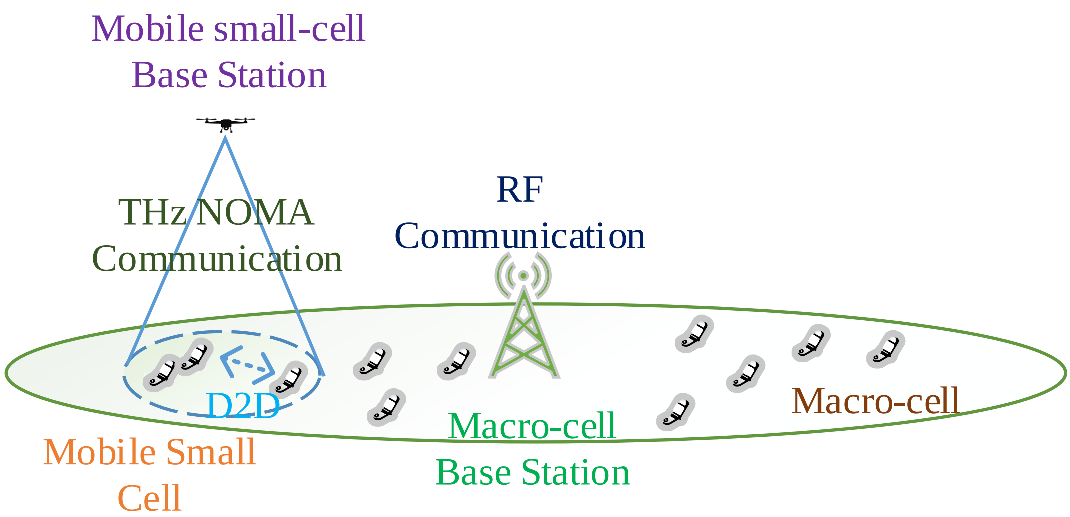

Fig. 8.1. Considered Downlink 6G HetNet model.

In the network model under study, the MBS employs Rayleigh fading channel and MSBS uses THz NOMA technology for signal transmission. This employment of different spectrum bands alleviates cross-tier interference in the network. Total C clusters are assumed inside each cell where each cluster contains g users. The MBS transmits superimposed signal for b_n and is given by

$$x_{b,c} = \sum_{n=1}^{g} \sqrt{a_{b,c}^{n} \mathbb{P}_{b,c}}\, z_{b,c}^{n} \tag{8.1}$$

here, $z_{b,c}^n$ denotes the modulated signal of b_n, $a_{b,c}^n$ signifies the coefficient of power allocation, and $\mathbb{P}_{b,c}$ signifies transmit power for c^{th} cluster and is limited by $\sum_{c=1}^{C} \mathbb{P}_{b,c} \leq \mathbb{P}_{b_{max}}$ where, $\mathbb{P}_{b_{max}}$ is maximum MBS transmit power.

Then, the user b_n receives the transmitted signal over the channel matrix H where $H = \{h_{b,c}^1, \dots, h_{b,c}^g\}$ is given by

$$y_{b,c}^{n} = h_{b,c}^{n} w_{b,c} \sqrt{a_{b,c}^{n} \mathbb{P}_{b,c}}\, z_{b,c}^{n} + I_{b,c,n}^{1} + I_{b,c,n}^{2} + \eta_{b,c}^{n} \tag{8.2}$$

$$I_{b,c,n}^{1} = h_{b,c}^{n} \sum_{j=1, j\neq c}^{C} w_{b,j} x_{b,j} \tag{8.3}$$

$$I_{b,c,n}^{2} = h_{b,c}^{n} w_{b,c} \sum_{j=1}^{g} \sqrt{a_{b,c}^{j} \mathbb{P}_{b,c}}\, z_{b,c}^{j} \tag{8.4}$$

TABLE 8.1: NOTATIONS

N_B	No. of MBS antennas
U	Number of users in macro cell
Ū	Set of all users
u_b	Sets of users inside macro-cell
u_m	Sets of users inside small-cell
Ƕ	Height of mobile small cell
ś	Speed of mobile small cell
Ř	Mobile small cell radius
p_k^d	Location of d_k user
p_n^b	Location of b_n user
ß	Channel Bandwidth employed at MBS
N_t	Number of antennas at the MSBS
$Ᵽ_{d,c}$	The transmit power of cluster c of MSBS
$Ᵽ_{b,c}$	The transmit power of cluster c of MBS
$Ᵽ_{b_{max}}$	The maximum MBS transmit power
$Ᵽ_{d_{max}}$	The maximum of MSBS transmit power
$Ꝗ_{k_{max}}$	The maximum of transmit power of d_k
$h_{d,c}^k$	Downlink channel of d_k user in c^{th}cluster of mobile small cell
$h_{b,c}^n$	Downlink channel of b_n user in c^{th}cluster of macro cell
$a_{d,c}^k$	the power allocation coefficient of d_k
$a_{b,c}^n$	the power allocation coefficient of b_n
s	Received signal at d_k in mobile small cell
$y_{b,c}^n$	Received signal at b_n in macro cell
ῥ	Inefficiency of the power amplifier of MBS
$ῥ_M$	Inefficiency of the power amplifier of MSBS
$Ᵽ_b^{cir}$	MBS circuit power
$Ᵽ_d^{cir}$	MSBS circuit power
$\eta_{b,c}^n$	Additive white gaussian noise at b_n
$\eta_{d,c}^n$	Additive white gaussian noise at d_k
$R_{b,c}^n$	Data rate at b_n
$R_{d,c}^k$	Data rate at d_k

$\eta_{b,c}^n \sim CN(0, \sigma_n^2)$, denotes the additive white gaussian noise (AWGN) with zero mean and variance σ_n^2, $w_{b,c}$ is the precoding vector, $I_{b,c,n}^1$ signifies inter-cluster interference and $I_{b,c,n}^2$ signifies intra-cluster interference. The channel $h_{b,c}^n$ is considered with Gaussian distribution of $h \sim CN(0, \gamma)$ [20] with zero mean and γ variance. The $h_{b,c}^n$ is given by

$$h_{b,c}^n = 10^{-(L(r)^{RF}/10)} \tag{8.5}$$

The path loss of considered channel [18], at a distance r^{RF} (km), is given as follows:

$$L(r)^{RF}[dB] = 148.1 + 37.6\ log_{10} r^{RF} \tag{8.6}$$

The signal to interference and noise ratio (SINR) at b_n is given by

$$SINR_{b,c}^{n} = \frac{a_{b,c}^{n}\text{Ᵽ}_{b,c}||h_{b,c}^{n}w_{b,c}||^2}{\sigma_n^2+\sum_{j=1,j\neq c}^{C}\text{Ᵽ}_{b,j}||h_{b,c}^{n}w_{b,j}||^2+\sum_{j=1}^{g}a_{b,c}^{j}\text{Ᵽ}_{b,c}\left||h_{b,c}^{n}w_{b,c}|\right|^2} \quad (8.7)$$

The rate of user b_n through the capacity model in [19], which is given by

$$R_{b,c}^{n} = \frac{ß}{C}log_2(1 + SINR_{b,c}^{n}) \quad (8.8)$$

where ß is the channel bandwidth employed at the MBS.

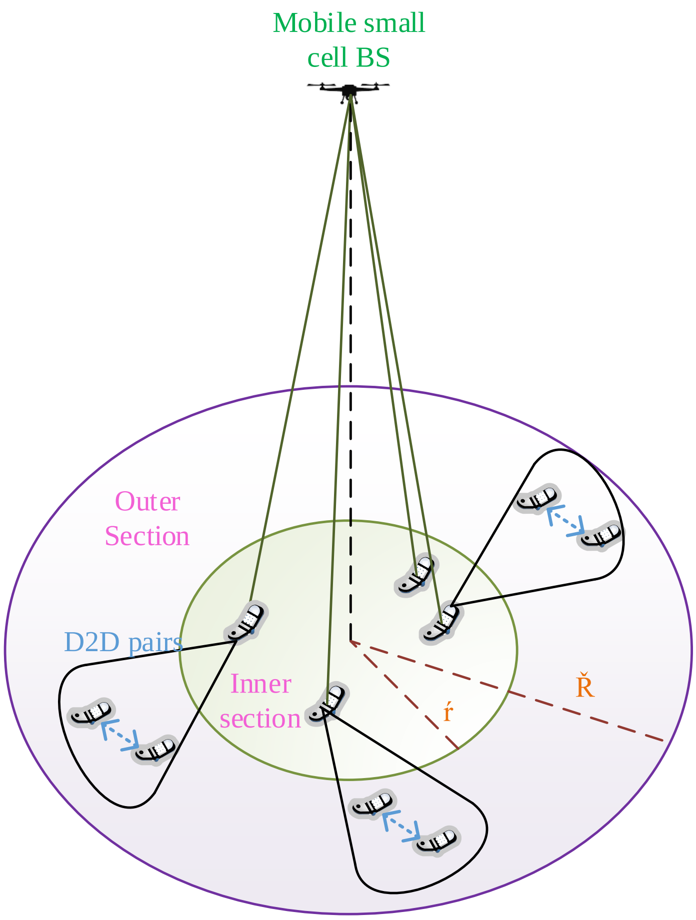

Fig. 8.2. Proposed MSBS communication system model.

Fig. 8.2 shows the proposed MSBS communication system model. The mobile small cell finds its target location l_u' with maximum user density. Each user m_k in the considered set u_M is located at p_k^m, and has sojourn time t_k^m. The dynamic movements of the mobile small cell cause superfluous overhead, to alleviate this overhead the mobile small cell is deployed once every period T provided $T \geq t_k^m$, $\forall m_k \in u_M$. To save power and improve the energy efficiency of the networks, the mobile small cell is divided into two sections; inner and outer. The users inside the outer section form D2D pairs with each other. The set of D2D pairs is represented by $Đ = \{p_1, p_2, \dots, p_s, \dots p_S\}$ where, p_s symbolizes is s^{th} D2D pair. The MSBS sends the multicast signals to the users inside the inner section through NOMA. The MSBS employs the proposed fuzzy logic-based power allocation scheme when transmitting signals to the inner section users through NOMA. The users inside the inner section receive the signals and form clusters through the proposed clustering scheme. Thereafter, these users relay the signals to the D2D pairs.

The users in the inner section are divided into E clusters having g users in each cluster, then the superimposed signal transmitted by MSBS for d_k in e^{th} cluster is given as

$$x_{d,e} = \sum_{k=1}^{g} \sqrt{a_{d,e}^{k} \text{Ᵽ}_{d,e}}\, z_{d,e}^{k} \tag{8.9}$$

here $z_{d,e}^{k}$ denotes the modulated signal of d_k, $a_{d,e}^{k}$ signifies the power allocation coefficient of d_k, and $\text{Ᵽ}_{d,c}$ represents transmit power for e^{th} cluster in MSBS and is limited by $\sum_{e=1}^{E} \text{Ᵽ}_{d,e} \leq \text{Ᵽ}_{d_{max}}$ where, $\text{Ᵽ}_{d_{max}}$ is the maximum transmit power of MSBS. Then, the received signal by the user d_k over the channel matrix Ƕ where Ƕ $=\{h_{d,e}^{1}, \dots, h_{d,e}^{g}\}$ is given by

$$y_{d,e}^{k} = h_{d,e}^{k} w_{d,e} \sqrt{a_{d,e}^{k} \text{Ᵽ}_{d,e}} z_{d,e}^{k} + I_{d,e,k}^{1} + I_{d,e,k}^{2} + \eta_{d,e}^{k} \tag{8.10}$$

$$I_{d,e,k}^{1} = h_{d,e}^{k} \sum_{j=1, j\neq e}^{E} w_{d,j} x_{d,j} \tag{8.11}$$

$$I_{d,e,k}^{2} = h_{d,e}^{k} w_{d,e} \sum_{j=1}^{g} \sqrt{a_{d,e}^{j} \text{Ᵽ}_{d,e}}\, z_{d,e}^{j} \tag{8.12}$$

$\eta_{d,e}^{k} \sim CN(0, \sigma_d^2)$ is the AWGN with variance σ_d^2, $w_{M,j}$ is the precoding vector, $I_{d,e,k}^{1}$ and $I_{d,e,k}^{2}$ denotes inter-cluster interference and intra-cluster respectively.

THz channel model [105], and the channel gain $h_{M,c}^{k}$ is given as

$$h_{d,e}^{k} = \sqrt{N_t}(\sqrt{\frac{1}{P(d)}}\, \omega \alpha \left(\phi_{M,e,g}^{k}\right)) \tag{8.13}$$

here $L(d)$ represents path loss at d distance from the flying BS, ω signifies the antenna gain, ϕ is the angle of departure, $\alpha\left(\phi_{M,e,g}^{k}\right)$ represents array steering vector which is given by

$$\alpha\left(\phi_{M,e,g}^{k}\right) = \frac{1}{\sqrt{N_m}} \left[1, \dots, e^{j\pi[n sin\phi]}, \dots, e^{j\pi[(N_m-1)\sin\phi]}\right]' \tag{8.14}$$

The path loss due to spreading and molecular absorption cannot be ignored. The path loss of THz signal is given as

$$P(r)[dB] = 20\, log_{10}\left(\frac{4\pi}{\lambda}\right) + 10\, b(f) r\, log_{10} e \tag{8.15}$$

here, λ represents the wavelength of the carrier frequency f, and $b(f)$ is the frequency-dependent medium absorption coefficient as given in [105].

The SINR of the user m_k in cluster e of the mobile small cell is given by

$$SINR_{d,e}^{k} = \frac{a_{d,e}^{k} P_{d,e} ||h_{d,e}^{k} w_{d,e}||^2}{\sigma_d^2 + \sum_{j=1, j\neq e}^{E} P_{d,j} ||h_{d,e}^{k} w_{d,j}||^2 + \sum_{j=1}^{g} a_{d,e}^{j} P_{d,e} \left|\left|h_{d,e}^{k} w_{d,e}\right|\right|^2} \quad (8.16)$$

Thus, the achieved rate of user d_k is given by

$$R_{d,e}^{k} = \frac{B}{E} log_2(1 + SINR_{d,e}^{k}) \quad (8.17)$$

where B is the THz bandwidth employed at the MSBS.

The users in the inner section form clusters of D2D pairs in the outer section, through the proposed clustering scheme. Let there be M relays in the inner section forming one cluster each in the outer section. The total number of clusters becomes M. Let the total number of D2D pairs in each cluster be S. Let the cluster formed by the user d_k be m. Then the signal is forwarded by d_k to D2D pair p_s, and it can be expressed as

$$y_{s,k} = h_{s,k} w_{s,k} \sqrt{a_{s,k} q_{s,k}} z_{s,k} + I_{s,k}^{1} + I_{s,k}^{2} + \eta_{s,k} \quad (8.18)$$

$$I_{s,k}^{1} = h_{s,k} \sum_{i=1, i\neq m}^{M} w_{i,k} x_{i,k} \quad (8.19)$$

$$I_{s,k}^{2} = h_{s,k} w_{s,k} \sum_{j=1}^{S} \sqrt{a_{j,k} P_{j,k}} z_{j,k} \quad (8.20)$$

here $h_{s,k}$ denotes the channel between p_s and d_k. The power of the user d_k used in transmitting the signal to p_s is denoted by $q_{s,k}$ and is limited by $\sum_{s=1}^{S} q_{s,k} \leq q_{k_{max}}$ where $q_{k_{max}}$ is the maximum transmit power of d_k. $\eta_{s,k} \sim CN(0, \sigma_s^2)$ is the AWGN with variance σ_s^2, $w_{s,k}$ is the precoding vector, $I_{s,k}^{1}$ and $I_{s,k}^{2}$ denotes inter-cluster interference and intra-cluster respectively.

Therefore, the SINR at p_s is expressed as

$$SINR_{s,k} = \frac{a_{s,k} q_{s,k} ||h_{s,k} w_{s,k}||^2}{\sigma_d^2 + \sum_{j=1, j\neq e}^{M} q_{s,k} ||h_{s,k} w_{i,k}||^2 + \sum_{j=1}^{S} a_{d,e}^{j} q_{s,k} \left|\left|h_{s,k} w_{s,k}\right|\right|^2} \quad (8.21)$$

Thus, the achieved rate of user p_s is given by

$$R_{s,k} = B\, log_2(1 + SINR_{s,k}) \quad (8.22)$$

The total power consumption is defined as the summation of power consumption in transmission and circuit power consumption [20]. The power consumption at MBS can be expressed as

$$P_b = P_b^{cir} + \varrho(\sum_{c=1}^{Ce} P_{b,c}) \quad (8.23)$$

where the MBS circuit power consumption is denoted by P_b^{cir} the MBS power amplifier's inefficiency is represented by ϱ. The total power consumption of MSBS can be expressed as

$$\mathbb{P}_d = \mathbb{P}_d^{cir} + \varrho_d \left(\sum_{c=1}^{C} \mathbb{P}_{d,e}\right) \tag{8.24}$$

The total power consumption of d_k consumed in transmitting the signal to the D2D pair p_s can be expressed as

$$\mathbb{q}_k = \mathbb{q}_k^{cir} + \varrho_s \left(\sum_{s=1}^{S} \mathbb{q}_{s,k}\right) \tag{8.25}$$

where, $\mathbb{q}_k^{cir}$ is the circuit power of the user d_k, ϱ_s is the inefficiency of the power amplifier. Hence, the system power consumption can be given as

$$\mathbb{P}_{system} = \mathbb{P}_b + \mathbb{P}_d + \sum_{m=1}^{M} \mathbb{q}_k \tag{8.26}$$

To design a green 6G system energy efficiency is an important performance parameter. The total energy efficiency is expressed as the ratio of sum rate and power consumption. The energy efficiency of the MSBS can be expressed as

$$\mathrm{EE}_{MSBS} = \frac{\sum_{e=1}^{E} \sum_{i=1}^{g} R_{d,e}^{k}}{\mathbb{P}_d} \tag{8.27}$$

8.3 Proposed Fuzzy based power allocation

The MSBS employs the proposed fuzzy logic-based power allocation scheme when transmitting signals to the inner section users through NOMA. Fuzzy logic employs fuzzy sets to understand the data and apiece set embodies terms like ‘small’, ‘big’ etc. The fuzzy sets employ membership functions to show the constancy of a component. The degree of membership is defined between 0 to 1, where 0 specifies a non-membership and 1 directs a full membership. In this paper, we use triangular functions as their computational complexities are comparatively less than the other fuzzy membership functions. Such system comprises of a fuzzifier, defuzzifier, and intellegence block. The output of our fuzzy logic system is the power allocation coefficient. The computational complexity of the fuzzy logic system is based on the number of input rules.

It is assumed that the perfect knowledge of CSI is present at the transmitter. The transmitter transmits the signals to the users employing NOMA. For simplicity, two numbers of users are assumed in the system. NOMA allocates power between 0 and 1, to the users. The power allocation coefficient in NOMA depends on the channel gain [145]. A lower power allocation coefficient is allocated to the user with higher channel gain and vice versa. The objective is to allocate optimum power to all the users. For this, in the proposed method the channel gains of both the users are determined. Then the difference between these channel gains is given as input of the fuzzy system. Fig. 8.3 shows the input fuzzy variable namely channel gain difference. The fuzzified input of difference between the channel gains into the fuzzy system is divided into three membership functions. That is ‘Low’, ‘Average’, and ‘High’. The rule base consists of three rules. Rendering to the association among channel gain differences, the power allocation coefficients are estimated by the fuzzy logic system based on the information on user channel gains.

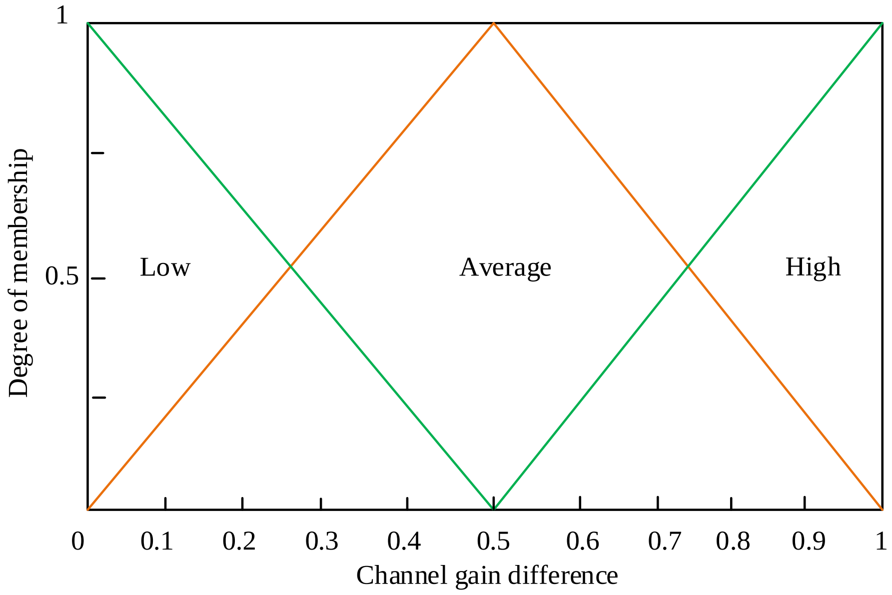

Fig. 8.3. The membership of the channel gain difference.

Remark 8.1: The number of input variables influences the fuzzy logic system sensitivity. The numbers of fuzzy rules inputs influence the computational complexity of the fuzzy logic system. Therefore, number of fuzzy membership functions cannot be extensively raised in this chapter.

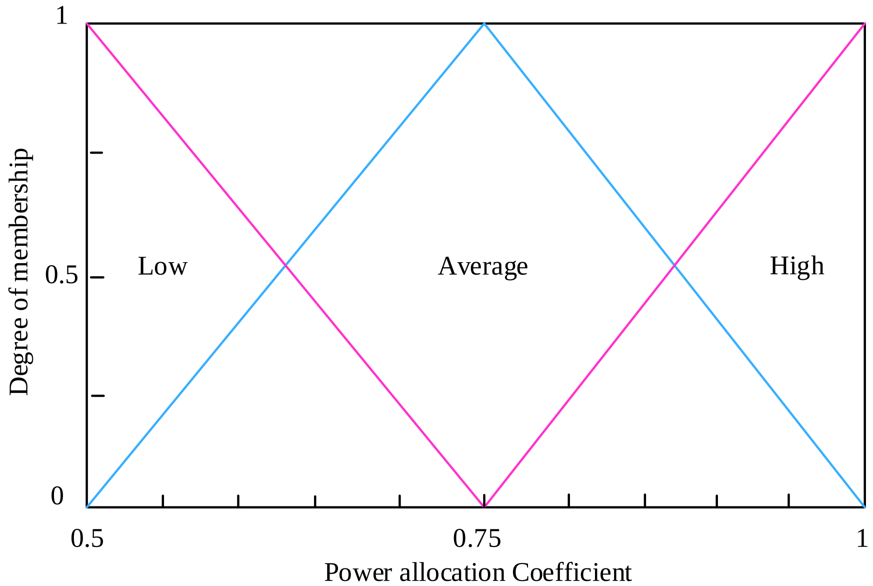

Fig. 8.4. The membership of power allocation coefficient.

The universe set is represented as ψ which contains a fuzzy set R. δ_R is a membership function such that $\delta_R: \psi \rightarrow [0,1]$. $\delta_R(o)$ represents the grade of membership to R provided $o \subseteq \psi$.

In the fuzzy logic system, the fields of the input variable are designated according to the scenario. This paper employs Min-Max inference method. The Centroid Defuzzification method is employed in the fuzzy logic system, as the objective is to attain an accurate value of the power allocation coefficient. This method calculates the solution balance point and the fuzzy region weighted mean. The value of the crisp output field ʕ is expressed as

$$\varsigma = \frac{\sum_{i=0}^{r} W_i\, \delta_{\mathrm{R}}(\psi_i)}{\sum_{i=0}^{r} \delta_{\mathrm{R}}(\psi_i)} \qquad (8.28)$$

here r is the number of inference rules in the fuzzy engine and W_i is the value of weight matching to i^{th} rule, and $\delta_{\mathrm{R}}(\psi_i)$ is the value of the anticipated truth for that field. Fig. 8.4 is the output fuzzy variable (power allocation coefficient), which consists of three membership functions.

8.4 Proposed energy efficient clustering

The users inside the inner section act as a relay to forward the signals to the D2D pair through the proposed energy-efficient clustering scheme. Fig. 8.5 shows the proposed clustering scheme.

The D2D pairs are chosen by the relay based on the relay beamwidth. In the literature, the relays are simply assumed to be omnidirectional. However, such methods increase the interference due to omnidirectionality. In the proposed energy-efficient clustering scheme, the width and direction of the signal beam are signified by $¥^T$ degrees and ϖ degrees respectively. The beam direction of i^{th} relay is given as

$$\varpi_i = |¥_i \pm \chi| \qquad (8.29)$$

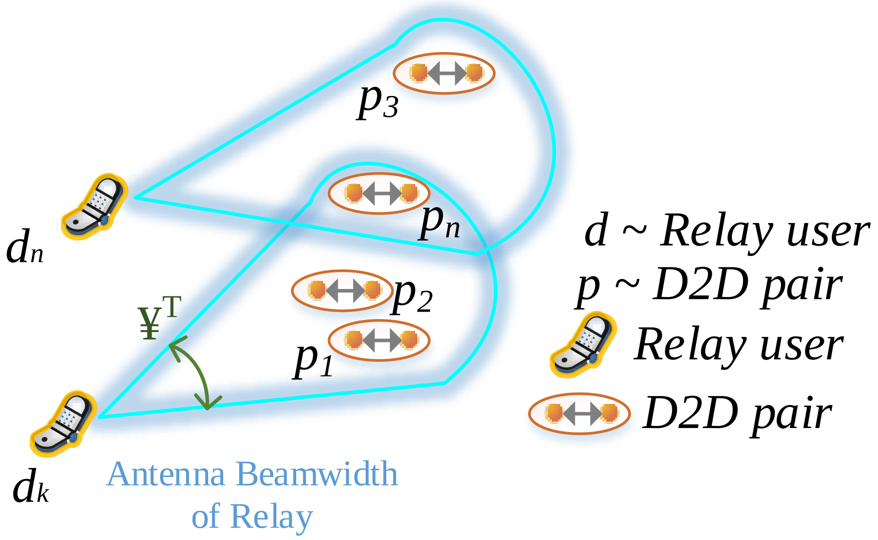

Fig. 8.5. Proposed clustering scheme.

where, $¥_i$ and χ respectively represents the coordinate angle and beam scanning of the relay. To guarantee that the relay directs its signal beam towards the outer section users we put fowwoing condition on it

$$\chi \leq \frac{|180° - ¥^T|}{2} \qquad (8.30)$$

8.4 Simulation results

In this section, the proficiency of proposed schemes is shown via simulation results in comparison with other conventional methods in terms of sum rate, power consumption, and energy efficiency. Table 8.2 shows the considered parameters used in the simulation. In the considered 6G HetNet, the MBS is in the center of the macro-cell, and MSBS moves in the coverage of MBS. The users are assumed to be arbitrarily moving in the macro-cell. In the considered 6G HetNet the MBS employs mMIMO NOMA RF and MSBS employs THz NOMA. We have labeled the considered 6G HetNet with proposed schemes as ‘Proposed THz’. The results are compared with ‘Proposed mmWave’ and ‘Basic’. In the ‘Proposed mmWave’ system the MBS employs mMIMO NOMA RF and MSBS employs mmWave NOMA and the proposed schemes. Whereas, in the ‘Basic’ system the MBS employs mMIMO NOMA RF and MSBS employs mmWave NOMA.

TABLE 8.2: SIMULATION PARAMETERS

Parameters	**Value**
Radius of macrocell	2 km
THz carrier frequency	0.34 THz
RF carrier frequency	2 GHz
Bandwidth at BS employing THz channel, B	10 GHz
Bandwidth at BS employing RF channel, ß	10 MHz
Altitude of mobile small cell, Ƕ	100 m
Radius of mobile small cell, Ř	300 m
Speed of mobile small cell, ś	50 m/s
Number of antennas at the flying BS, N_t	1
Number of antennas at MBS, N_B	100
Macro cell noise power, σ_n^2	-174 dBm/Hz
Mobile small cell noise power, σ_d^2	-109 dBm
Maximum transmitter power of MBS, $Ᵽ_{S_{max}}$	43 dBm
Maximum transmitter power of Flying BS, $Ᵽ_{M_{max}}$	10 dBm
The circuit power of flying BS, $Ᵽ_d^{cir}$	-10 dBm/s
The circuit power of MBS, $Ᵽ_b^{cir}$	20 dBm
Drain efficiency of MBS amplifier and flying BS amplifier, ϱ and $ϱ_d$	1/0.38
The deployment interval, T	500 s

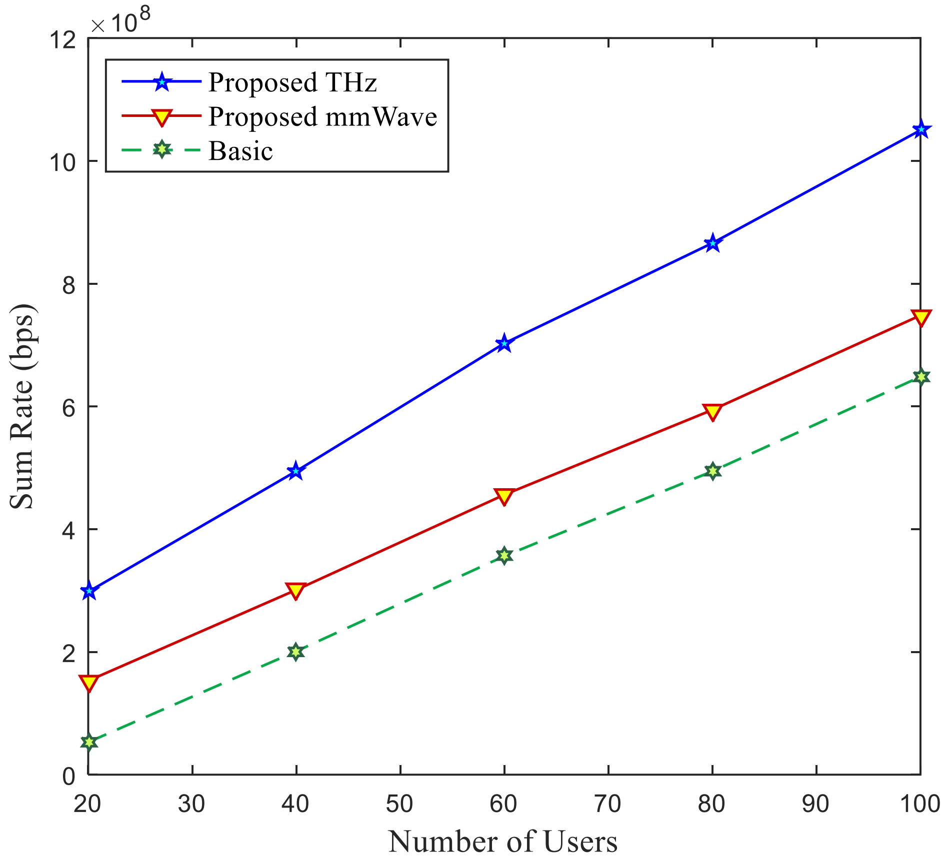

Fig. 8.6. Sum Rate v/s Number of users.

Fig. 8.6 shows the comparison of the sum rate of the 'Proposed. Proposed THz' with 'Proposed mmWave' and 'Basic'. The number of users is varied from 20 to 100. From Fig. 8.6 it can be seen that as the number of users increase the sum rate also increases. Further, the sum rate of the 'Proposed THz' is more than 'Proposed mmWave' and 'Basic'. This is due to the proposed fuzzy logic-based optimum power allocation. As the achieved rate depends on the power allocation coefficients. Moreover, the employment of the THz channel. The bandwidth of the THz channel is more than mmWave, therefore, the achieved rates are also higher in the THz band than in the mmWave band. Moreover, the proposed clustering technique reduces interference due to its directional characteristics. This enhances the SINR and hence, the rates.

Fig. 8.7 shows the comparison of power consumption of the system of the 'Proposed THz' and compares it with the power consumption of 'Proposed mmWave' and 'Basic'. The number of users is varied from 20 to 100. From Fig. 8.7 it can be seen that as the number of users increases the power consumption also increases. Further, the power consumption of the 'Proposed THz' is less than 'Proposed mmWave' and 'Basic'. This is because of the proposed mobile small cell model, power allocation, and clustering schemes. The load of MSB is reduced due to the employment of MSBS further, the users in the inner section of the mobile small cell relay the signals to the users of the outer section. This reduces the load and power consumption of MSBS.

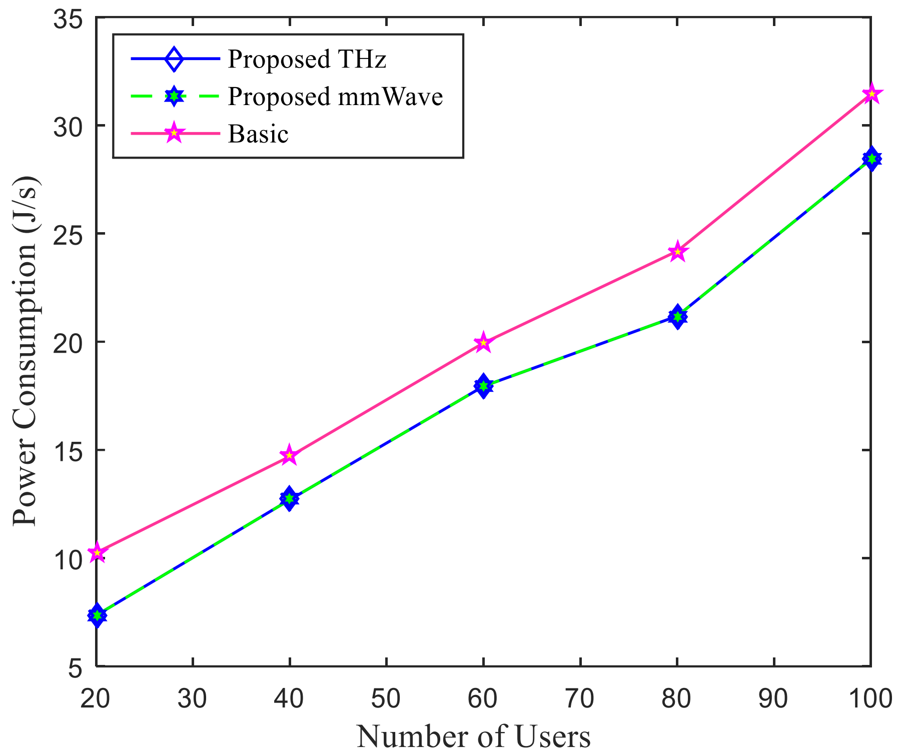

Fig. 8.7. Power consumption v/s number of users.

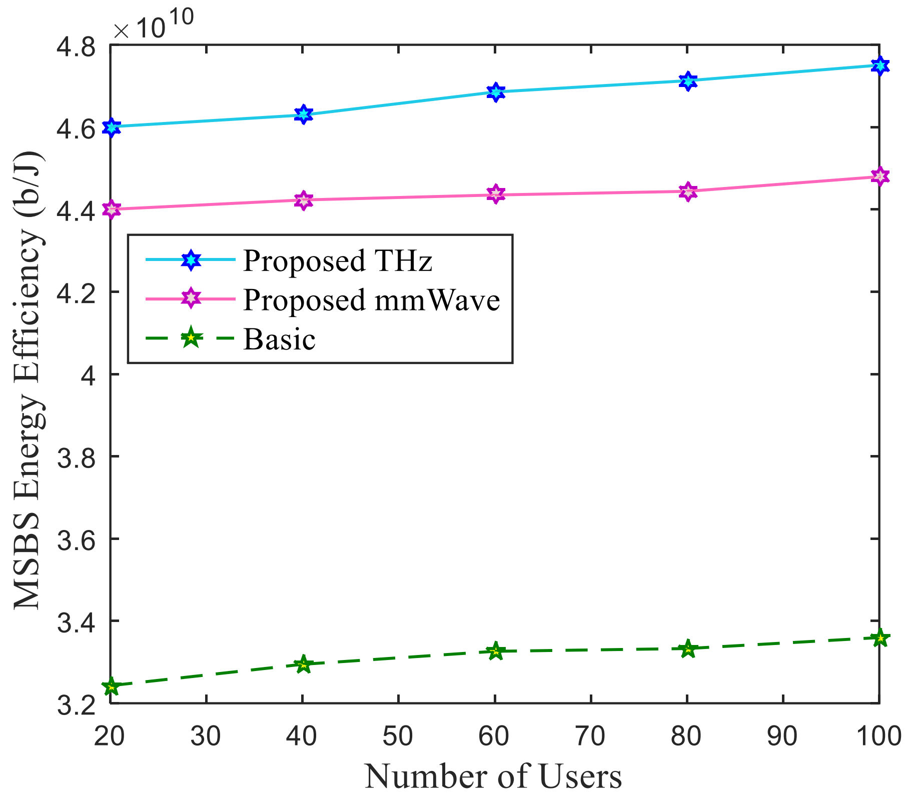

Fig. 8.8. MSBS energy efficiency v/s number of users

Fig. 8.8 shows the comparison of energy efficiency of the 'Proposed THz' with 'Proposed mmWave' and 'Basic'. The number of users is varied from 20 to 100, and energy efficiency also upsurges with number of users. It can be seen from Fig. 8.8 that the energy efficiency of the 'Proposed THz' is higher than the less than 'Proposed mmWave' and 'Basic'. This is due to the proposed mobile small cell model. Energy efficiency is defined as the ratio of sum rate and power consumption. From Fig. 8.6 it can be seen that the proposed clustering scheme enhances the sum rate of the system. Moreover. the users in the inner section of the mobile small cell relay the signals to the users of the outer section. This reduces the load and power consumption of MSBS hence, the energy efficiency rises.

CONCLUSION

The crucial background of the research work carried out in the thesis has been described in the **first chapter**. It commences with the overview showing 5G trends and B5G/6G driving force, following motivation behind picking the topic of research challenges to be faced while transitioning from 5G to B5G/6G, research gaps in the current works and culminates with the objectives and organization of thesis. While **second chapter** has shown the detailed literature review in the five phases related to the work of the thesis. While the important conclusions drawn from the proposed work are described below:

1. In **chapter 3**, puts light on the what is lacking in previous architectures and why there is a requirement of new architecture for B5G/6G. The B5G/6G is envisioned as a platform for connecting everything; people, things, and even intelligence. The first source of induction for the need for the development of B5G/6G is to keep addressing the world's insatiable demands and insistence on better service experiences. Moreover, a unified platform needs to be designed to enable new industries and new services that 5G will be unable to achieve. The prime engine of continuous research is envisioning to raise the bars to attain, ultra-fast wireless speed, high mobility, full coverage, increased bandwidth, connectivity, and greater security while reducing the energy consumption and achieving ultra-low round-trip latency, to such a level that is unachievable with 5G. This chapter further proposes a general 6G wireless network architecture as shown in Fig. 3.2 which may provide a good platform for future 6G standardization network.
2. In **chapter 4**, a hybrid system model for B5G/6G is proposed using millimeter-wave, massive-MIMO and NOMA with D2D enabled small-cell communication network. Combining the advantages of THz communications, mmWave communication, RF communications, mMIMO, and NOMA in a two-tier 6G HetNet, this chapter further propose a novel application specific channel selection (ASCS) scheme. In the proposed ASCS scheme, conferring to the application demand of the small cell users the SBS switches downlink frequency channel dynamically. This aids in the efficient utilization of the spectrum. Additionally, to decrease the transmission load and energy cost at the BS due to the huge bandwidth of mmWave/THz-wave each BS is enabled with caches. This chapter also comprises of a pseudo code that will be helpful for developing the ASCS scheme. The efficiency of the proposed scheme is showed by the simulation results.
3. In **chapter 5**, the energy efficiency of a hybrid millimeter-wave massive-MIMO NOMA with D2D enabled beyond 5G network is optimized using a novel battery efficient NOMA technique. Further this chapter propose modified cooperative NOMA (MCN) and THz blockage alleviation (TBA) methods. The TBA method aids in ensuring the end-to-end signal communication in presence of obstructions in the path. The TBA method uses device-to-device (D2D) communication to redirect the signal to evade hindrances in the propagation path. TBA method also aids in reducing the interference and hence, improving the SINR and achievable rates. The MCN helps in reducing the power consumption and efficiently utilizing the system's energy. The MCN integrates cooperative relaying technique with NOMA. This supports in reducing the

transmission power at the BS and outstretch the signals to the users at the edge of the cell, which have poor channel qualities or cannot build direct links with the BS. Aiming efficient use of user power and interference mitigation, this chapter design two procedures in MCN to forward signal to the end-user based on the power levels of the users. Further, the proposed methods are analyzed in terms of key performance parameters.

4. In **chapter 6**, an efficient user clustering approach in hybrid millimeter-wave massive-MIMO NOMA with D2D enabled beyond 5G small-cell network using antenna angle bound clustering technique is implemented. This chapter first, design a 6G hybrid system model employing THz communication, mMIMO, cooperative NOMA, and device-to-device (D2D) communication with macrocells and small cells. Thereafter, this chapter propose Antenna Angle Bound (AAB) clustering technique to enhance the sum rate of the proposed 6G hybrid system model. The proposed ABB clustering technique employs antenna parameters such as beam angle and beamwidth to form clusters and mitigate interference. This chapter analyze simulation results to validate the superior performance of the proposed 6G hybrid system model in assessment with traditional models.
5. In **chapter 7**, an energy efficient mobile small-cell for beyond 5G networks using NOMA technology is implemented. This chapter integrated the advantage of wide THz bandwidth, spectrum efficiency of mMIMO and NOMA, and on-demand services of mobile BSs to form a green 2-tier 6G HetNet. This chapter propose a track selection scheme (TSS) for flying BS conferring to real-time parameters the flying BS chooses an optimal path to decrease the flying time, and power consumption of flying BS, and improvement in the energy efficiency of the 6G HetNet. The simulations examine the performance of the proposed TSS in comparison with the traditional approaches of flying BS deployment and path designs with the employment of mmWave channels.
6. In **chapter 8**, In this chapter, energy efficient clustering in a mobile small-cell using NOMA D2D technique in beyond 5G networks is designed. we put forward a mobile BS-based 6G HetNet that integrates THz communication, mMIMO, NOMA, and D2D technologies. This chapter propose a joint power allocation and clustering scheme to enhance the performance of the proposed 6G mobile small cell system. As ML provides more accurate outcome prediction. This chapter first propose an energy-efficient mobile small cell system model. Then, a novel fuzzy logic system that exploits channel gains to design optimum power allocation in NOMA is proposed. Further, this chapter propose a clustering scheme that effectively integrates user device antenna parameters, NOMA, and D2D communication to reduce interference and enhance the energy efficiency of MSBS. The MSBS moves over the macro-cell and uses NOMA to provide services to the users, while these users form clusters and relay this information to D2D user pairs via the same resources at the same time. Simulation results demonstrate that the proposed schemes for mobile small cell-based 6G HetNet can realize enhanced system performance, compared with the state-of-the-art methods in terms of sum rate, power consumption, and energy efficiency.

FUTURE SCOPE

As the technology developments for 5G will keep driving the potentials and expectations of the mobile networks, new and unanticipated services, use cases, and applications are expected to develop.

The B5G/6G needs to increase the chipset density, which poses a challenge to the semiconductor industry. With miniaturized chips, the manufacturing complexity increases, making devices and chipsets more cost-effective and feasible. The utilization of EHF bands and THz bands in B5G/6G will require a miniaturized design of transmitter and receiver components. For instance, Qualcomm and other companies expended years to make components for mmWave technology, from meter scale to fingertip-sized antennas and modems. For the THz band, this issue might pose further challenges, for example, the antenna for combined technology of mmWave and THz bands may need to be reinvented since antenna size may vary in proportion of micrometers and nanometers. Optoelectronic integrated modules may benefit from the advancement of antenna techniques. Intelligent B5G/6G services will be AI-oriented, which depends on the computing power and storage of the devices. Therefore, new hardware designs need to be energy efficient and long battery lifetime, which is challenging. Further, resource management is complex due to the device capability. To run AI algorithms, the AI technologies in B5G/6G will need high computational power. Hence, network equipment will be more power-hungry than ever. The user equipment will need to break the physical limits to operate with intelligence, higher diversities, and multiplexing gains at wider bandwidths. Traditional Silicon (Si), Gallium Arsenide (GaAs) transceiver components produce excessive heat and are not energy efficient. The amplifiers around 300 GHz band are extremely difficult to realize with CMOS integrated circuits. This intends that the present hardware technologies are incapable of supporting high computational ultra-fast applications of B5G/6G. Hence, new materials-based designs of hardware technologies are needed for emerging B5G/6G systems.

Although, the THz bands are susceptible to molecular absorption and blockage the propagation modeling becomes challenging. Moreover, the lack of understanding of the exact channel characteristics makes the situation more challenging. Additionally, the circuity and antenna size miniaturize, which makes fabrication difficult. Therefore, powerful synchronization schemes, low-density channel codes, energy efficient modulation schemes, ultra-massive MIMO system, nano-antennas, robust beamforming, noise modeling, and less complex low-power hardware circuits require further research to address the challenges in THz communications.

The modulator's performance is a determining factor for direct THz modulation. Hence, good performance of amplitude modulator in terms of speed and depth and phase modulator in terms of linear and large-scale phase shifts is vital to design considerations, at THz bands. Advanced materials are promising for the design of THz modulators, such as Graphene and GaN-HEMT. Low-Temperature Co-Fired Ceramic (LTCC) technology, technologies metal-coated 3D printing, and cutting-edge technology is some recently developed low-cost, compact, and lightweight solution in packaging technology in THz band. Electro-optic sampling can provide and cutting-edge technology are some recently developed low-cost, compact, and lightweight solutions in packaging technology in the THz band. Electro-optic sampling can provide a potential solution for THz measurements. However, so far it has not been extended to 1.5 THz for resolution improvements. Moreover, for THz measurements, there is a great requirement of robust atmospheric accountability to the International Systems of Units (SI).

Instead of being a promising multiple access technology, NOMA has several practical challenges. The hardware complexity, processing complexity, and computation complexity of the SIC scheme limit the NOMA scheme. In fading environments with time-varying interference, adaptive coding and modulation implementations are nontrivial.

Moreover, due to the possible allied error propagation in coding and decoding techniques, the performance of the whole system can deteriorate. For example, if the signals of the preceding users are not appropriately decoded, the decoding errors get amassed for the residual users. The SIC is performed in presence of the inter-user interference, which is naturally persuaded in NOMA. The SIC is effective if this self-interference is not efficiently mitigated. Therefore, well-designed self-interference techniques are needed for efficient induced inter-user interference in NOMA. For instance, with perfect CSI, resource allocation techniques give improved performance than with limited feedback CSI. However, severe communication overheads are induced in optimal or near-optimal CSI, while adding complexity. Consequently, reducing overheads and complexity is pivotal and resource allocation schemes relying on partial CSI must be investigated to reduce the overheads.

With an increase in the number of users, the power allocation and clustering, become immensely complex. The problem proliferates as the topology and schedule of the users become dynamic. The ML or DL-based MIMO NOMA systems can help to address this problem through the learning-based mechanism of beamforming, power allocation, and clustering techniques. The ML/DL algorithms try to learn the data patterns for making near-optimal decisions although, their effective operation in the dynamic environment of NOMA is challenging and not yet fully explored.

BIBLIOGRAPHY

[1] M. Agiwal, A. Roy and N. Saxena, "Next Generation 5G Wireless Networks: A Comprehensive Survey," in IEEE Communications Surveys & Tutorials, vol. 18, no. 3, pp. 1617-1655, thirdquarter 2016.

[2] CISCO, “Cisco Annual Internet Report (2018–2023) White Paper," White paper, Mar. 2020 [Online]Available:www.cisco.com/c/en/us/solutions/collateral/executiveperspectives/annual-internet-report/white-paper-c11-741490.html.

[3] S. K. Sharma and X. Wang, “Distributed caching enabled peak traffic reduction in ultra-dense IoT networks,” IEEE Commun. Lett., vol. 22, no. 6, pp. 1252–1255, Jun. 2018.

[4] B. Zong, C. Fan, X. Wang, X. Duan, B. Wang and J. Wang, "6G Technologies: Key Drivers, Core Requirements, System Architectures, and Enabling Technologies," in IEEE Vehicular Technology Magazine, vol. 14, no. 3, pp. 18-27, Sept. 2019.

[5] I. F. Akyildiz, A. Kak and S. Nie, "6G and Beyond: The Future of Wireless Communications Systems," in IEEE Access, vol. 8, pp. 133995- 134030, 2020.

[6] Y. Chen, P. Zhu, G. He, X. Yan, H. Baligh and J. Wu, "From Connected People, Connected Things, to Connected Intelligence," 2020 2nd 6G Wireless Summit (6G SUMMIT), Levi, Finland, 2020, pp. 1-7, doi: 10.1109/6GSUMMIT49458.2020.9083770.

[7] K. Chang, K. Chu, H. Wang, Y. Lin and J. Pan, "Energy Saving Technology of 5G Base Station Based on Internet of Things Collaborative Control," in IEEE Access, vol. 8, pp. 32935-32946, 2020.

[8] M. Abedi and M. J. Emadi, "Cooperative Power Management in Energy Harvesting Communication Systems in Presence of a Helper," in IEEE Transactions on Green Communications and Networking, vol. 3, no. 1, pp. 147-158, March 2019.

[9] H. Wang, Z. Zhao, X. Cheng, J. Ying, J. Qu and G. Xu, "Base Station Sleeping Strategy for On-Grid Energy Saving in Cellular Networks With Hybrid Energy Supplies in IoT Environment," in IEEE Access, vol. 6, pp. 45578-45589, 2018.

[10] L. Tang, W. Wang, Y. Wang and Q. Chen, "An Energy-Saving Algorithm With Joint User Association, Clustering, and On/Off Strategies in Dense Heterogeneous Networks," in IEEE Access, vol. 5, pp. 12988-13000, 2017.

[11] L. Li, N. Deng and W. Zhou, "Environment-Aware Dynamic Management for Energy Saving in MIMO-Based C-RAN," in IEEE Access, vol. 7, pp. 77514-77523, 2019.

[12] H. Farooq, A. Asghar and A. Imran, "Mobility Prediction-Based Autonomous Proactive Energy Saving (AURORA) Framework for Emerging Ultra-Dense Networks," in IEEE Transactions on Green Communications and Networking, vol. 2, no. 4, pp. 958-971, Dec. 2018.

[13] P. Uthansakul, P. Anchuen, M. Uthansakul and A. Ahmad Khan, "Estimating and Synthesizing QoE Based on QoS Measurement for Improving Multimedia Services on Cellular Networks Using ANN

Method," in IEEE Transactions on Network and Service Management, vol. 17, no. 1, pp. 389-402, March 2020.

[14] X. He, H. Lu, H. Huang, Y. Mao, K. Wang and S. Guo, "QoE-based Cooperative Task Offloading with Deep Reinforcement Learning in Mobile Edge Networks," in IEEE Wireless Communications, Early Access, Apr. 2020.

[15] S. Yang, C. Xu, L. Zhong, J. Shen and G. Muntean, "A QoE-Driven Multicast Strategy With Segment Routing—A Novel Multimedia Traffic Engineering Paradigm," in IEEE Transactions on Broadcasting, vol. 66, no. 1, pp. 34-46, March 2020.

[16] H. Zhang, W. Quan, H. Chao and C. Qiao, "Smart identifier network: A collaborative architecture for the future internet," in IEEE Network, vol. 30, no. 3, pp. 46-51, May-June 2016.

[17] S. K. Sharma, I. Woungang, A. Anpalagan and S. Chatzinotas, "Toward Tactile Internet in Beyond 5G Era: Recent Advances, Current Issues, and Future Directions," in IEEE Access, vol. 8, pp. 56948-56991, 2020.

[18] X. Wei, Q. Duan and L. Zhou, "A QoE-Driven Tactile Internet Architecture for Smart City," in IEEE Network, vol. 34, no. 1, pp. 130- 136, January/February 2020.

[19] P. Mekikis et al., "NFV-Enabled Experimental Platform for 5G Tactile Internet Support in Industrial Environments," in IEEE Transactions on Industrial Informatics, vol. 16, no. 3, pp. 1895-1903, March 2020.

[20] V. Gokhale, K. Kroep, V. S. Rao, J. Verburg and R. Yechangunja, "TIXT: An Extensible Testbed for Tactile Internet Communication," in IEEE Internet of Things Magazine, vol. 3, no. 1, pp. 32-37, March 2020.

[21] A. S. Cacciapuoti et al., "Beyond 5G: THz-Based Medium Access Protocol for Mobile Heterogeneous Networks," IEEE Commun. Mag., vol. 56, no. 6, June 2018, pp. 110–15.

[22] S. Sekander et al., "Multi-Tier Drone Architecture for 5G/ B5G Cellular Networks: Challenges, Trends, and Prospects," IEEE Commun. Mag., vol. 56, no. 3, Mar. 2018, pp. 96–103.

[23] Ü. Şenol, A. Yazar and H. Arslan, "Communications Scenarisos and a New Mixed Numerology Set for Flying Base Stations in 5G and Beyond," 2018 IEEE International Black Sea Conference on Communications and Networking (BlackSeaCom), Batumi, 2018, pp. 1-5.

[24] R. Li, Z. Zhao, Z. Xuan, G. Ding, C. Yan, Z. Wang, and H. Zhang, "Intelligent 5G: When cellular networks meet artificial intelligence," IEEE Wireless Commun., vol. 24, no. 5, pp. 175–183, Oct. 2017.

[25] D. F. P. Rojas, F. Nazmetdinov and A. Mitschele-Thiel, "Zero-touch coordination framework for Self-Organizing Functions in 5G," 2020 IEEE Wireless Communications and Networking Conference (WCNC), Seoul, Korea (South), 2020, pp. 1-8.

[26] C. Benzaid and T. Taleb, "AI-Driven Zero Touch Network and Service Management in 5G and Beyond: Challenges and Research Directions," in IEEE Network, vol. 34, no. 2, pp. 186-194, March/April 2020.

[27] C. Liaskos, S. Nie, A. Tsioliaridou, A. Pitsillides, S. Ioannidis, and I. Akyildiz, "A new wireless

communication paradigm through software controlled metasurfaces,” IEEE Commun. Mag., vol. 56, no. 9, pp. 162– 169, Sep. 2018.

[28] Jane, J. Betty, and E. N. Ganesh. "Big Data and Internet of Things for Smart Data Analytics Using Machine Learning Techniques." International conference on Computer Networks, Big data and IoT. Springer, Cham, 2019.

[29] Rai, Shubham, and Rejo Mathew. "Adaptive Object Tracking Using Algorithms Employing Machine Learning." International conference on Computer Networks, Big data and IoT. Springer, Cham, 2019.

[30] A. Singh, M. Andrello, N. Thawdar, and J. M. Jornet, “Design and operation of a Graphene-based Plasmonic nano-antenna array for communication in the Terahertz band,” IEEE J. Sel. Areas Commun. (to appear), 2020.

[31] F. Khan, Z. Pi, and S. Rajagopal, “Millimeter-wave mobile broadband with large scale spatial processing for 5G mobile communication,” in Proc. 50th Annu. Allerton Conf. Commun. Control Comput. (Allerton), 2012, pp. 1517–1523.

[32] X. Lin et al., “5G New Radio: Unveiling the Essentials of the Next Generation Wireless Access Technology,” IEEE Communications Standards Magazine, vol. 3, no. 3, pp. 30–37, Sep. 2019.

[33] E. Dahlman, S. Parkvall, and J. Skold, 5G NR: The Next Generation Wireless Access Technology. Elsevier Science, 2018.

[34] H. Wymeersch and G. Seco-Granados, "Adaptive Detection Probability for mmWave 5G SLAM," 2020 2nd 6G Wireless Summit (6G SUMMIT), Levi, Finland, 2020, pp. 1-5.

[35] D. Marasinghe, N. Jayaweera, N. Rajatheva and M. Latva-Aho, "Hierarchical User Clustering for mmWave-NOMA Systems," 2020 2nd 6G Wireless Summit (6G SUMMIT), Levi, Finland, 2020, pp. 1-5.

[36] P. Skrimponis et al., "Power Consumption Analysis for Mobile MmWave and Sub-THz Receivers," 2020 2nd 6G Wireless Summit (6G SUMMIT), Levi, Finland, 2020, pp. 1-5.

[37] J. N. Murdock and T. S. Rappaport, “Consumption factor: A figure of merit for power consumption and energy efficiency in broadband wireless communications,” in Proc. IEEE Global Commun. Conf. (GLOBECOM) Workshops, Dec. 2011, pp. 1393–1398.

[38] M. Youssef, J. Farah, C. A. Nour and C. Douillard, "Resource Allocation in NOMA Systems for Centralized and Distributed Antennas With Mixed Traffic Using Matching Theory," in *IEEE Transactions on Communications*, vol. 68, no. 1, pp. 414-428, Jan. 2020.

[39] Z. Ding, "Robust Beamforming Design for OTFS-NOMA," in *IEEE Open Journal of the Communications Society*, vol. 1, pp. 33-40, 2020.

[40] X. Li *et al.*, "A Unified Framework for HS-UAV NOMA Networks: Performance Analysis and Location Optimization," in *IEEE Access*, vol. 8, pp. 13329-13340, 2020.

[41] F. Kara and H. Kaya, "Error Probability Analysis of NOMA-Based Diamond Relaying Network," in *IEEE Transactions on Vehicular Technology*, vol. 69, no. 2, pp. 2280-2285, Feb. 2020.

[42] V. Aswathi and A. V. Babu, "Ensuring equal outage performance for down-link secondary users in full/half duplex cognitive NOMA systems," in *IET Communications*, vol. 14, no. 1, pp. 63-75, 3 1 2020.

[43] E. M. Almohimmah and M. T. Alresheedi, "Error Analysis of NOMA-Based VLC Systems With Higher Order Modulation Schemes," in *IEEE Access*, vol. 8, pp. 2792-2803, 2020.

[44] S. Dhanasekaran and T. R. Sushma, "Performance Analysis of Cell-Center Users in NOMA Based-Spectrum Sharing Protocol," in *IEEE Communications Letters*, vol. 24, no. 1, pp. 52-56, Jan. 2020.

[45] L. P. Qian, B. Shi, Y. Wu, B. Sun and D. H. K. Tsang, "NOMA-Enabled Mobile Edge Computing for Internet of Things via Joint Communication and Computation Resource Allocations," in *IEEE Internet of Things Journal*, vol. 7, no. 1, pp. 718-733, Jan. 2020.

[46] K. N. Doan, M. Vaezi, W. Shin, H. V. Poor, H. Shin and T. Q. S. Quek, "Power Allocation in Cache-Aided NOMA Systems: Optimization and Deep Reinforcement Learning Approaches," in *IEEE Transactions on Communications*, vol. 68, no. 1, pp. 630-644, Jan. 2020.

[47] J. Ding, J. Cai and C. Yi, "An Improved Coalition Game Approach for MIMO-NOMA Clustering Integrating Beamforming and Power Allocation," in *IEEE Transactions on Vehicular Technology*, vol. 68, no. 2, pp. 1672-1687, Feb. 2019.

[48] L. Liu, Y. Chi, C. Yuen, Y. L. Guan and Y. Li, "Capacity-Achieving MIMO-NOMA: Iterative LMMSE Detection," in *IEEE Transactions on Signal Processing*, vol. 67, no. 7, pp. 1758-1773, 1 April1, 2019.

[49] D. Tong, Y. Ding, Y. Liu and Y. Wang, "A MIMO-NOMA Framework With Complex-Valued Power Coefficients," in *IEEE Transactions on Vehicular Technology*, vol. 68, no. 3, pp. 2244-2259, March 2019.

[50] K. He, Y. Li, Y. Zhang, K. Zhang and C. Yin, "A Novel Tensor CS-Based NOMA MIMO System for the Downlink of Massive Mission-Critical MTC in 5G and Beyond," in *IEEE Access*, vol. 7, pp. 97624-97640, 2019.

[51] S. Park, A. Q. Truong and T. H. Nguyen, "Power Control for Sum Spectral Efficiency Optimization in MIMO-NOMA Systems With Linear Beamforming," in *IEEE Access*, vol. 7, pp. 10593-10605, 2019.

[52] A. Nasser, O. Muta, M. Elsabrouty and H. Gacanin, "Interference Mitigation and Power Allocation Scheme for Downlink MIMO–NOMA HetNet," in *IEEE Transactions on Vehicular Technology*, vol. 68, no. 7, pp. 6805-6816, July 2019.

[53] Z. Ding and H. V. Poor, "Design of Massive-MIMO-NOMA With Limited Feedback," in *IEEE Signal Processing Letters*, vol. 23, no. 5, pp. 629-633, May 2016.

[54] Y. Li and G. A. Aruma Baduge, "Underlay Spectrum-Sharing Massive MIMO NOMA," in *IEEE Communications Letters*, vol. 23, no. 1, pp. 116-119, Jan. 2019.

[55] X. Liu, Y. Liu, X. Wang and H. Lin, "Highly Efficient 3-D Resource Allocation Techniques in 5G for NOMA-Enabled Massive MIMO and Relaying Systems," in *IEEE Journal on Selected Areas in Communications*, vol. 35, no. 12, pp. 2785-2797, Dec. 2017.

[56] M. Zeng, N. Nguyen, O. A. Dobre and H. V. Poor, "Securing Downlink Massive MIMO-NOMA Networks With Artificial Noise," in *IEEE Journal of Selected Topics in Signal Processing*, vol. 13, no. 3, pp. 685-699, June 2019.

[57] D. Zhang, Y. Liu, Z. Ding, Z. Zhou, A. Nallanathan and T. Sato, "Performance Analysis of Non-Regenerative Massive-MIMO-NOMA Relay Systems for 5G," in *IEEE Transactions on Communications*, vol. 65, no. 11, pp. 4777-4790, Nov. 2017.

[58] K. Senel, H. V. Cheng, E. Björnson and E. G. Larsson, "What Role can NOMA Play in Massive MIMO?," in *IEEE Journal of Selected Topics in Signal Processing*, vol. 13, no. 3, pp. 597-611, June 2019.

[59] D. Kudathanthirige and G. A. A. Baduge, "NOMA-Aided Multicell Downlink Massive MIMO," in *IEEE Journal of Selected Topics in Signal Processing*, vol. 13, no. 3, pp. 612-627, June 2019.

[60] X. Chen, F. Gong, G. Li, H. Zhang and P. Song, "User Pairing and Pair Scheduling in Massive MIMO-NOMA Systems," in *IEEE Communications Letters*, vol. 22, no. 4, pp. 788-791, April 2018.

[61] E. P. Simon, J. Farah and P. Laly, "Performance Evaluation of Massive MIMO With Beamforming and Nonorthogonal Multiple Access Based on Practical Channel Measurements," in *IEEE Antennas and Wireless Propagation Letters*, vol. 18, no. 6, pp. 1263-1267, June 2019.

[62] W. A. Al-Hussaibi and F. H. Ali, "Efficient User Clustering, Receive Antenna Selection, and Power Allocation Algorithms for Massive MIMO-NOMA Systems," in *IEEE Access*, vol. 7, pp. 31865-31882, 2019.

[63] L. Zhu, Z. Xiao, X. Xia and D. Oliver Wu, "Millimeter-Wave Communications With Non-Orthogonal Multiple Access for B5G/6G," in *IEEE Access*, vol. 7, pp. 116123-116132, 2019.

[64] Z. Wei, L. Zhao, J. Guo, D. W. K. Ng and J. Yuan, "Multi-Beam NOMA for Hybrid mmWave Systems," in *IEEE Transactions on Communications*, vol. 67, no. 2, pp. 1705-1719, Feb. 2019.

[65] N. Rupasinghe, Y. Yapıcı, İ. Güvenç, M. Ghosh and Y. Kakishima, "Angle Feedback for NOMA Transmission in mmWave Drone Networks," in *IEEE Journal of Selected Topics in Signal Processing*, vol. 13, no. 3, pp. 628-643, June 2019.

[66] L. Zhu, J. Zhang, Z. Xiao, X. Cao, D. O. Wu and X. Xia, "Millimeter-Wave NOMA With User Grouping, Power Allocation and Hybrid Beamforming," in *IEEE Transactions on Wireless Communications*, vol. 18, no. 11, pp. 5065-5079, Nov. 2019.

[67] Y. Song, W. Yang, Z. Xiang, B. Wang and Y. Cai, "Secure Transmission in mmWave NOMA Networks With Cognitive Power Allocation," in *IEEE Access*, vol. 7, pp. 76104-76119, 2019.

[68] D. Fan, F. Gao, G. Wang, Z. Zhong and A. Nallanathan, "Channel Estimation and Transmission Strategy for Hybrid mmWave NOMA Systems," in *IEEE Journal of Selected Topics in Signal Processing*, vol. 13, no. 3, pp. 584-596, June 2019.

[69] K. Belbase, C. Tellambura and H. Jiang, "Coverage Analysis of Cooperative NOMA in Millimeter Wave Networks," in *IEEE Communications Letters*, vol. 23, no. 12, pp. 2154-2158, Dec. 2019.

[70] J. Li, X. Jing, Y. Zhang and J. Mu, "Performance Analysis of Agile-Beam NOMA in Millimeter Wave Networks," in *IEEE Access*, vol. 8, pp. 6638-6649, 2020.

[71] Z. Wei, D. W. K. Ng and J. Yuan, "NOMA for Hybrid mmWave Communication Systems With Beamwidth Control," in *IEEE Journal of Selected Topics in Signal Processing*, vol. 13, no. 3, pp. 567-583, June 2019.

[72] M. Zeng, W. Hao, O. A. Dobre and H. V. Poor, "Energy-Efficient Power Allocation in Uplink mmWave Massive MIMO With NOMA," in *IEEE Transactions on Vehicular Technology*, vol. 68, no. 3, pp. 3000-3004, March 2019.

[73] X. Hu, C. Zhong, X. Chen, W. Xu and Z. Zhang, "Cluster Grouping and Power Control For Angle-Domain MmWave MIMO NOMA Systems," in *IEEE Journal of Selected Topics in Signal Processing*, vol. 13, no. 5, pp. 1167-1180, Sept. 2019.

[74] N. Wang, L. Jiao, A. Alipour-Fanid, M. Dabaghchian and K. Zeng, "Pilot Contamination Attack Detection for NOMA in 5G mm-Wave Massive MIMO Networks," in *IEEE Transactions on Information Forensics and Security*, vol. 15, pp. 1363-1378, 2020.

[75] P. Liu, Y. Li, W. Cheng, W. Zhang and X. Gao, "Energy-Efficient Power Allocation for Millimeter Wave Beamspace MIMO-NOMA Systems," in *IEEE Access*, vol. 7, pp. 114582-114592, 2019.

[76] V. Mandawaria, E. Sharma and R. Budhiraja, "WSEE Maximization of mmWave NOMA Systems," in *IEEE Communications Letters*, vol. 23, no. 8, pp. 1413-1417, Aug. 2019.

[77] B. Wang, L. Dai, Z. Wang, N. Ge and S. Zhou, "Spectrum and Energy-Efficient Beamspace MIMO-NOMA for Millimeter-Wave Communications Using Lens Antenna Array," in IEEE Journal on Selected Areas in Communications, vol. 35, no. 10, pp. 2370-2382, Oct. 2017.

[78] W. Hao, M. Zeng, Z. Chu and S. Yang, "Energy-Efficient Power Allocation in Millimeter Wave Massive MIMO With Non-Orthogonal Multiple Access," in IEEE Wireless Communications Letters, vol. 6, no. 6, pp. 782-785, Dec. 2017.

[79] L. Dai, B. Wang, M. Peng and S. Chen, "Hybrid Precoding-Based Millimeter-Wave Massive MIMO-NOMA With Simultaneous Wireless Information and Power Transfer," in IEEE Journal on Selected Areas in Communications, vol. 37, no. 1, pp. 131-141, Jan. 2019.

[80] D. Zhang, Z. Zhou, C. Xu, Y. Zhang, J. Rodriguez and T. Sato, "Capacity Analysis of NOMA With mmWave Massive MIMO Systems," in IEEE Journal on Selected Areas in Communications, vol. 35, no. 7, pp. 1606-1618, July 2017.

[81] Z. Ding, L. Dai, R. Schober and H. Vincent Poor, "NOMA Meets Finite Resolution Analog Beamforming in Massive MIMO and Millimeter-Wave Networks," in IEEE Communications Letters, vol. 21, no. 8, pp. 1879-1882, Aug. 2017.

[82] W. Shao, S. Zhang, H. Li, N. Zhao and O. A. Dobre, "Angle-Domain NOMA over Multicell Millimeter Wave Massive MIMO Networks," in IEEE Transactions on Communications.

[83] Q. Liu, T. Lv, and Z. Lin, "Energy-Efficient Transmission Design in Cooperative Relaying Systems Using NOMA," in IEEE Communications Letters, vol. 22, no. 3, pp. 594-597, March 2018.

[84] H. Zhang et al., "Energy-Efficient Dynamic Resource Optimization in NOMA System," in IEEE Transactions on Wireless Communications, vol. 17, no. 9, pp. 5671-5683, Sept. 2018.

[85] W. A. Al-Hussaibi and F. H. Ali, "Efficient User Clustering, Receive Antenna Selection, and Power Allocation Algorithms for Massive MIMO-NOMA Systems," in IEEE Access, vol. 7, pp. 31865-31882, 2019.

[86] J. Ding, J. Cai and C. Yi, "An Improved Coalition Game Approach for MIMO-NOMA Clustering Integrating Beamforming and Power Allocation," in IEEE Transactions on Vehicular Technology, vol. 68, no. 2, pp. 1672-1687, Feb. 2019.

[87] W. A. Al-Hussaibi, "Optimal cluster formation and power control for high connectivity wireless MIMO-NOMA applications," in Electronics Letters, vol. 55, no. 20, pp. 1110-1112, 3 10 2019.

[88] K. Wang, W. Liang, Y. Yuan, Y. Liu, Z. Ma and Z. Ding, "User Clustering and Power Allocation for Hybrid Non-Orthogonal Multiple Access Systems," in IEEE Transactions on Vehicular Technology, vol. 68, no. 12, pp. 12052-12065, Dec. 2019.

[89] S. Chou, Y. Yu and A. Pang, "Mobile Small Cell Deployment for Service Time Maximization Over Next-Generation Cellular Networks," in IEEE Transactions on Vehicular Technology, vol. 66, no. 6, pp. 5398-5408, June 2017.

[90] L. P. Qian, Y. Wu, H. Zhou and X. Shen, "Dynamic Cell Association for Non-Orthogonal Multiple-Access V2S Networks," in IEEE Journal on Selected Areas in Communications, vol. 35, no. 10, pp. 2342-2356, Oct. 2017.

[91] S. Cai, Y. Che, L. Duan, J. Wang, S. Zhou and R. Zhang, "Green 5G Heterogeneous Networks Through Dynamic Small-Cell Operation," in IEEE Journal on Selected Areas in Communications, vol. 34, no. 5, pp. 1103-1115, May 2016.

[92] L. P. Qian, Y. Wu, H. Zhou and X. Shen, "Joint Uplink Base Station Association and Power Control for Small-Cell Networks With Non-Orthogonal Multiple Access," in IEEE Transactions on Wireless Communications, vol. 16, no. 9, pp. 5567-5582, Sept. 2017.

[93] L. P. Qian, Y. Wu, H. Zhou and X. Shen, "Non-Orthogonal Multiple Access Vehicular Small Cell Networks: Architecture and Solution," in IEEE Network, vol. 31, no. 4, pp. 15-21, July-August 2017.

[94] Y. Tsai and H. Wei, "Quality-Balanced User Clustering Schemes for Non-Orthogonal Multiple Access Systems," in IEEE Communications Letters, vol. 22, no. 1, pp. 113-116, Jan. 2018.

[95] Q. Zhang, L. Zhang, Y.-C. Liang, and P. Y. Kam, “Backscatter-NOMA: A symbiotic system of cellular and Internet-of-Things networks,” IEEE Access, vol. 7, pp. 20000-20013, Feb. 2019.

[96] Y. Dai, D. Xu, S. Maharjan, Z. Chen, Q. He, and Y. Zhang, “Blockchain and Deep Reinforcement Learning Empowered Intelligent 5G Beyond,” IEEE Network, vol. 33, no. 3, pp. 10–17, 2019.

[97] K. Zhang, Y. Zhu, S. Maharjan, and Y. Zhang, “Edge Intelligence and Blockchain Empowered 5G Beyond for the Industrial Internet of Things,” IEEE Network, vol. 33, no. 5, pp. 12–19, 2019.

[98] K. Lei, M. Du, J. Huang and T. Jin, "Groupchain: Towards a Scalable Public Blockchain in Fog Computing of IoT Services Computing," in IEEE Transactions on Services Computing, vol. 13, no. 2, pp. 252-262, 1 March-April 2020.

[99] Z. Yang, C. Pan, W. Xu and M. Chen, "Compressive Sensing-Based User Clustering for Downlink NOMA Systems With Decoding Power," in IEEE Signal Processing Letters, vol. 25, no. 5, pp. 660-664, May 2018.

[100] A. W. Ahmad and N. Mehmood Bahadar, "Exploiting Heterogeneous Networks model for Cluster Formation and Power Allocation in Uplink NOMA," 2019 21st International Conference on Advanced Communication Technology (ICACT), PyeongChang Kwangwoon_Do, Korea (South), 2019, pp. 129-133.

[101] M. S. Ali, H. Tabassum and E. Hossain, "Dynamic User Clustering and Power Allocation for Uplink and Downlink Non-Orthogonal Multiple Access (NOMA) Systems," in IEEE Access, vol. 4, pp. 6325-6343, 2016.

[102] I. F. Akyildiz, A. Kak and S. Nie, "6G and Beyond: The Future of Wireless Communications Systems," in IEEE Access, vol. 8, pp. 133995-134030, 2020.

[103] 3GPP TS 38.104, “NR: Base station (BS) radio transmission and reception,” 3GPP, Valbonne, Technical Report, Rel. 15, Mar. 2018.

[104] S. Rommel, T. R. Raddo and I. T. Monroy, "Data Center Connectivity by 6G Wireless Systems," 2018 Photonics in Switching and Computing (PSC), 2018, pp. 1-3.

[105] H. Zhang, H. Zhang, W. liu, K. long, J. Dong and V. C. M. Leung, "Energy Efficient User Clustering and Hybrid Precoding for Terahertz MIMO-NOMA Systems," ICC 2020 - 2020 IEEE International Conference on Communications (ICC), 2020, pp. 1-5.

[106] C. Han and I. F. Akyildiz, “Distance-aware bandwidth-adaptive resource allocation for wireless systems in the terahertz band,” IEEE Trans. Terahertz Sci. Technol., vol. 6, no. 4, pp. 541-553, Jul. 2016.

[107] J. M. Jornet and I. F. Akyildiz, “Channel modeling and capacity analysis for electromagnetic wireless nanonetworks in the terahertz band,” IEEE Trans. Wireless Commun., vol. 10, no. 10, pp. 3211-3221, Oct. 2011.

[108] L. Dai, B. Wang, M. Peng and S. Chen, “Hybrid precoding-based millimeter-wave massive MIMO-NOMA with simultaneous wireless information and power transfer,” IEEE J. Sel. Areas Commun., vol. 37, no. 1, pp. 131-141, Jan. 2019.

[109] Jain, Preksha, and Akhil Gupta. "Adaptive NOMA towards 5G green wireless network." Transactions on Emerging Telecommunications Technologies, vol. 31, no. 3, pp. e3887, Mar. 2020.

[110] M. Katz, P. Pirinen and H. Posti, "Towards 6G: Getting Ready for the Next Decade," 2019 16th International Symposium on Wireless Communication Systems (ISWCS), 2019, pp. 714-718.

[111] T. S. Rappaport et al., "Wireless Communications and Applications Above 100 GHz: Opportunities and Challenges for 6G and Beyond," in IEEE Access, vol. 7, pp. 78729-78757, 2019.

[112] P. Jain and A. Gupta, "Energy-Efficient Adaptive Sectorization for 5G Green Wireless Communication Systems," in IEEE Systems Journal, vol. 14, no. 2, pp. 2382-2391, June 2020.

[113] E. Björnson, E. G. Larsson and M. Debbah, "Massive MIMO for Maximal Spectral Efficiency: How Many Users and Pilots Should Be Allocated?," in IEEE Transactions on Wireless Communications, vol. 15, no. 2, pp. 1293-1308, Feb. 2016.

[114] D. A. Basnayaka and H. Haas, "Spatial modulation for massive MIMO," in Proc. IEEE Int. Conf. Commun., June 2015, pp. 1945– 1950.

[115] W. Saad, M. Bennis and M. Chen, "A Vision of 6G Wireless Systems: Applications, Trends, Technologies, and Open Research Problems," in IEEE Network, vol. 34, no. 3, pp. 134-142, May/June 2020.

[116] A. Ghosh, A. Maeder, M. Baker, and D. Chandramouli, ‘‘5G evolution: A view on 5G cellular technology beyond 3GPP release 15,’’ IEEE Access, vol. 7, pp. 127639–127651, 2019.

[117] H. Zhang, H. Zhang, W. liu, K. long, J. Dong and V. C. M. Leung, "Energy Efficient User Clustering and Hybrid Precoding for Terahertz MIMO-NOMA Systems," ICC 2020 - 2020 IEEE International Conference on Communications (ICC), 2020, pp. 1-5.

[118] H. Zhang, H. Zhang, W. liu, K. long, J. Dong and V. C. M. Leung, "Energy Efficient User Clustering and Hybrid Precoding for Terahertz MIMO-NOMA Systems," ICC 2020 - 2020 IEEE International Conference on Communications (ICC), 2020, pp. 1-5.

[119] J. Zhang, L. Dai, X. Zhang, E. Bjornson and Z. Wang, "Achievable ¨ rate of rician large-scale MIMO channels with transceiver hardware Impairments," IEEE Trans. Veh. Technol., vol. 65, no. 10, pp. 8800-8806, Oct. 2016.

[120] Y. Jin, J. Zhang, S. Jin and B. Ai, "Channel Estimation for Cell-Free mmWave Massive MIMO Through Deep Learning," IEEE Trans. Veh. Technol., 2019.

[121] J. Zhang, L. Dai, S. Sun and Z. Wang, "On the spectral efficiency of massive MIMO systems with low-resolution ADCs," IEEE Commun. Lett., vol. 20, no. 5, pp. 842-845, May 2016.

[122] Y. Saito, Y. Kishiyama, A. Benjebbour, T. Nakamura, A. Li, and K. Higuchi, "Non-orthogonal multiple access (NOMA) for cellular future radio access," in Proc. IEEE Veh. Technol. Conf., Dresden, Germany, Jun. 2013, pp. 1–5.

[123] Z. Zhang, H. Sun, and R. Q. Hu, "Downlink and uplink non-orthogonal multiple access in a dense wireless network," IEEE J. Sel. Areas Commun., vol. 35, no. 12, pp. 2771–2784, Dec. 2017.

[124] Z. Ding et al., "Application of non-orthogonal multiple access in LTE and 5G networks," IEEE Commun. Mag., vol. 55, no. 2, pp. 185–191, Feb. 2017.

[125] Z. Wei, L. Zhao, J. Guo, D. W. K. Ng and J. Yuan, "Multi-beam NOMA for hybrid mmWave systems," IEEE Trans. Commun., vol. 67, no. 2, pp. 1705-1719, Feb. 2019.

[126] W. -Y. Li, W. Chung, H. Tsuji and A. Miura, "Novel internal high gain loop handset phone antenna design for satellite and terrestrial integrated mobile communications system applications," *2015 International Symposium on Antennas and Propagation (ISAP)*, 2015, pp. 1-4.

[127] Zeng, Yong, et al., eds. UAV Communications for 5G and Beyond. John Wiley & Sons, 2020.

[128] R. Tang, W. Feng, Y. Chen and N. Ge, "NOMA-based UAV communications for maritime coverage enhancement," in China Communications, vol. 18, no. 4, pp. 230-243, April 2021.

[129] Y. Zeng, R. Zhang, et al., "Wireless communications with unmanned aerial vehicles: Opportunities and challenges," IEEE Communications Magazine, vol. 54, no. 5, 2016, pp. 36–42.

[130] C. Liu, W. Feng, et al., "Cell-free satellite-UAV networks for 6G wide-area Internet of Things," IEEE Journal on Selected Areas in Communications, early access, 2020.

[131] Y. Zeng, J. Lyu and R. Zhang, "Cellular-Connected UAV: Potential, Challenges, and Promising Technologies," in IEEE Wireless Communications, vol. 26, no. 1, pp. 120-127, February 2019.

[132] H. J. Song and T. Nagatsuma, "Present and Future of Terahertz Communications," IEEE Trans. Terahertz Science and Technology, vol. 1, no. 1, Sept. 2011, pp. 256–63.

[133] K. -T. Feng et al., "3D On-Demand Flying Mobile Communication for Millimeter-Wave Heterogeneous Networks," in IEEE Network, vol. 34, no. 5, pp. 198-204, September/October 2020.

[134] X. Lin, R. K. Ganti, P. J. Fleming, and J. G. Andrews, "Towards understanding the fundamentals of mobility in cellular networks," IEEE Trans. Wireless Commun., vol. 12, no. 4, pp. 1686–1698, Apr. 2013.

[135] B. Wang *et al.*, "Graph-Based File Dispatching Protocol With D2D-Enhanced UAV-NOMA Communications in Large-Scale Networks," in *IEEE Internet of Things Journal*, vol. 7, no. 9, pp. 8615-8630, Sept. 2020.

[136] A. Masaracchia, L. D. Nguyen, T. Q. Duong, C. Yin, O. A. Dobre and E. Garcia-Palacios, "Energy-Efficient and Throughput Fair Resource Allocation for TS-NOMA UAV-Assisted Communications," in *IEEE Transactions on Communications*, vol. 68, no. 11, pp. 7156-7169, Nov. 2020.

[137] R. Tang, W. Feng, Y. Chen and N. Ge, "NOMA-based UAV communications for maritime coverage enhancement," in China Communications, vol. 18, no. 4, pp. 230-243, April 2021.

[138] J. Lee and V. Friderikos, "Interference-aware path planning optimization for multiple UAVs in beyond 5G networks," in Journal of Communications and Networks, vol. 24, no. 2, pp. 125-138, April 2022.

[139] Y. Zeng, R. Zhang, et al., "Wireless communications with unmanned aerial vehicles: Opportunities and challenges," IEEE Communications Magazine, vol. 54, no. 5, 2016, pp. 36–42.

[140] C. Liu, W. Feng, et al., "Cell-free satellite-UAV networks for 6G wide-area Internet of Things," IEEE Journal on Selected Areas in Communications, early access, 2020.

[141] U. Saleem, Y. Liu, S. Jangsher, X. Tao and Y. Li, "Latency Minimization for D2D-Enabled Partial Computation Offloading in Mobile Edge Computing," in IEEE Transactions on Vehicular Technology, vol. 69, no. 4, pp. 4472-4486, April 2020.

[142] J. Yan, Z. Kuang, F. Yang and X. Deng, "Mode Selection and Resource Allocation Algorithm in Energy-Harvesting D2D Heterogeneous Network," in IEEE Access, vol. 7, pp. 179929-179941, 2019

[143] A. Y. Awan, M. Ali, M. Naeem, F. Qamar and M. N. Sial, "Joint Network Admission Control, Mode Assignment, and Power Allocation in Energy Harvesting Aided D2D Communication," in IEEE Transactions on Industrial Informatics, vol. 16, no. 3, pp. 1914-1923, March 2020.

[144] X. Lin, R. K. Ganti, P. J. Fleming, and J. G. Andrews, “Towards understanding the fundamentals of mobility in cellular networks,” IEEE Trans. Wireless Commun., vol. 12, no. 4, pp. 1686–1698, Apr. 2013.

[145] Liaqat, Mahrukh, et al. "Power-domain non orthogonal multiple access (PD-NOMA) in cooperative networks: an overview." Wireless Networks (2018): 1-23.

INDEX

LIST OF PUBLICATIONS

Sr. no.	Title of paper	Name of journal / conference	Published/Accepted/Communicated	Impact Factor/ SJR	Indexing
1.	A Vision Towards Integrated 6G Communication Networks: Promising Technologies, Architecture and Use-Cases	Physical Communication	Revision	2.379/ 0.61/ Q2	SCI
2.	Performance Evaluation of Cooperative OMA and NOMA Systems in 6G Deployment Scenarios	Sensors	Published	3.576/ 0.8/ Q1	SCI
3.	Underwater Service Specific Channel Selection Scheme with mmWave and THz bands	IEEE Internet of Things Magazine	Communicated	-	-
4.	Dynamic and Efficient Spectrum Utilization for 6G with THz, mmWave, and RF band	IEEE Transactions on Vehicular Technology	Revision	6.239/ 2.52/ Q1	SCI
5.	Massive MIMO NOMA Double mode Model towards Green 5G Networks	Microprocessors and Microsystems	Accepted	1.525/ 0.54/ Q2	SCI
6.	Customized NOMA and Sector Model for Battery Efficient Beyond 5G Green Networks	IEEE Network	Published	10.294/ 5.05/ Q1	SCI
7.	Adaptive NOMA towards 5G green wireless network	Transactions on Emerging Telecommunications Technologies	Published	3.310/ 0.71/ Q2	SCI
8.	Hybrid Green 6G HetNet with THz Blockage Alleviation and Modified Cooperative NOMA	IEEE System Journal	Communicated	4.802/ 1.36/ Q1	SCI

9.	Efficient Clustering for NOMA with THz mMIMO D2D Inspired 6G System Model	IEEE TNSM	Communicated	4.758/ 1.62/ Q1	SCI
10.	Energy Efficient Track Selection Scheme (TSS) for Flying BS in 2-tier 6G HetNet	IEEE Internet of Things Journal	Communicated	10.238/ 3.85/ Q1	SCI
11.	Green 6G Mobile Small Cell Model with ML-based Optimum Power Allocation and Efficient Clustering	IEEE Transactions on Fuzzy systems	Communicated	12.253/ 4.08/ Q1	SCI

LIST OF PATENTS

Sr. no.	Title	Patent	Published/Accepted/Communicated
1.	Dynamic and Efficient Spectrum Utilization for 6G with THz, mmWave, and RF band	Indian Patent	Published
2.	Hybrid Green 6G HetNet with THz Blockage Alleviation and Modified Cooperative NOMA	Indian Patent	Published
3.	A method to provide energy efficient network services through battery-efficient NOMA and adaptive sectorization	Indian Patent	Published

LIST OF CONFERENCES

Sr. no.	Title of paper	Name of journal / conference	Published date	Indexing
1	Efficient 5G Massive MIMO Millimeter Wave 2-tier Network	IEEE 7th I2CT 2022	18 July 2022	Scopus
2	Performance analysis of massive MIMO millimeter wave NOMA HetNet	4th IEEE International Conference on ESCI	22 April 2022	Scopus

AISSMS
INSTITUTE OF INFORMATION TECHNOLOGY
ADDING VALUE TO ENGINEERING
An Autonomous Institute Affiliated to Savitribai Phule Pune University
Approved by AICTE, New Delhi and Recognised by Govt. of Maharashtra
Accredited by NAAC with 'A+' Grade

4th IEEE INTERNATIONAL CONFERENCE

on

Emerging Smart Computing & Informatics (IEEE ESCI-2022)

9th – 11th March 2022

Technically Co-Sponsored by IEEE

Organized by

All India Shri Shivaji Memorial Society's

INSTITUTE OF INFORMATION TECHNOLOGY

Kennedy Road, Near RTO, Pune– 411001, Maharashtra, India

Certificate

This is to certify that Dr./Prof./Mr./Ms. Preksha Jain Affiliation School of Electronics and Electrical Engineering, Lovely Professional University, Punjab has participated in 4th IEEE International Conference on Emerging Smart Computing and Informatics (IEEE ESCI-2022) during 9th - 11th March 2022.

He/She presented a technical paper titled Performance Analysis of Massive MIMO Millimeter Wave NOMA HetNet.

Dr. V. K. Bairagi	**Dr. S. V. Limkar**	**Dr. P. B. Mane**
Technical Programme Chair	Organizing Chair	General Chair

Academic Partners

Muscat College

SIRG Scientific Innovation Research Group

7^{th} International Conference for Convergence in Technology (I2CT)

IEEE BOMBAY SECTION

7^{th} – 9^{th} April 2022

This is to certify

Dr./Prof./Mr./Ms. Preksha Jain

has presented paper entitled ***Efficient 5G Massive MIMO Millimeter Wave 2-tier Network*** in 7^{th} International Conference for Convergence in Technology (I2CT) during 7^{th} to 9^{th} April 2022.

General Chair -I2CT

Dr. Chanakya Kumar Jha